



UNIVERSITÀ DEGLI STUDI DI TRIESTE
e
UNIVERSITÀ CA' FOSCARI DI VENEZIA
XXXII CICLO DEL DOTTORATO DI RICERCA IN
CHIMICA

PHOTOINDUCED ENERGY AND ELECTRON
TRANSFER PROCESSES AT LIQUID-LIQUID
INTERFACES

Settore scientifico-disciplinare: **CHIM/06**

DOTTORANDO

GUSTAVO CORREIA RIBEIRO

COORDINATORE

PROF. ENZO ALESSIO

SUPERVISORE DI TESI

PROF. PAOLO TECILLA

ANNO ACCADEMICO 2019/2020



This work was realized with financial support of project (G.A No: 722591) funded by the Marie Skłodowska-Curie Actions of the European H2020 programme, **PHOTOTRAIN** is an Innovative Training Network (ITN).

Abstract

The photoinduced electron transfer chemistry is an essential process to trigger chemical reactions. In this context, the selection of effective photoactive catalysts, reagents and reaction environment is crucial for the successful transfer of an electron from a donor to an acceptor via excitation with light starting a radical based chemical reaction. Several examples demonstrate that photoredox catalysis can be successfully applied in organic synthesis.

However, some issues limit the applicability and practical implementation of photocatalytic processes in organic synthesis. In particular, the common use of high cost metal catalysts (i.e. ruthenium/ iridium complexes) and the difficulty of the separation of the complex reaction mixture to recover the product and recycle the catalyst obstacle the scale up of these processes. Finally, the charge-charge recombination is a common problem that limit the overall efficiency of the process.

Most of these limitations could be addressed in a system in which the different components are confined in different phases and the reaction takes place at the interphase. The focus of this project is the study of photoinduced energy and electron transfer processes at liquid-liquid interfaces and for this investigation we choose to use complex emulsion and the micellar/water interphase as models for static liquid/liquid interfaces.

Complex emulsions include multiple components emulsion with several interfaces in droplets and Janus droplets. Among these emulsions we choose to investigate a complex hexane/perfluorohexane/water emulsion stabilized by a surfactant that ensure a great contact area between two immiscible organic solvents (hexane and perfluorohexane). Also chosen was a micellar water-surfactant solution using different surfactants depending on the solubility of the components of the electron transfer reaction chosen.

Moving from previous research and analysing the properties of different fluorescent dyes we devised three molecular cores that have be prepared and studied in the context of this work for the use as photocatalysts in electron transfer processes. These

compounds are the Perylene-bis(dicarboximide) (PDI), that are well-known *n*-type semiconductors, the Perixanthene-monoimide (PXXIM) considered a building block for the preparation of a new class of O-doped PAHs with excellent carrier-transport and injection properties studied by the group of professor Bonifazi, and the Naphthalimide with outstanding ICT electronic structure and desirable photophysical properties and a relative simple synthetic process.

The results highlight problems related to the solubility of the prepared compounds in the use of the hexane/perfluorohexane/water emulsion. On the other hand, micelles proved to be able to solubilize all the components needed for a photo-induced catalytic process without altering the photophysical properties of the Naphthalimide dye. Working with professor Bergamini in Bologna we characterised the UV, fluorescence and life-time of this dye in different micellar environment. In collaboration with Dr. Reddy's laboratories, Naphthalimide proved to be an efficient photocatalyst of the nickel-catalyzed decarboxylative arylation in bulk solution. However, the reaction is not occurring in micellar solution probably due to technical problems in the degassing of the water solution. Overall, micelles demonstrated to be a convenient media to organize all the components of the photocatalytic process in a small reacting volume at the interface with water.

Table of Contents

Abstract	2
Abbreviations	3
1 Introduction	5
1.1 Electron Transfer Reactions and Photocatalysis	6
1.2 Liquid-Liquid interfaces	10
1.2.1 Complex Emulsions	10
1.2.2 Surfactants and micellar aggregates	12
1.3 Organic Dyes	14
1.3.1 Perylene-bis(dicarboximide) (PDI)	15
1.3.2 Perixanthene Xanthene	16
1.3.3 Naphthalimide	17
1.4 Photocatalytic reactions at interfaces	19
2 Aim	23
3 Results and Discussion	25
3.1 Studies in hexane/perfluorohexane emulsion.	26
3.1.1 Synthesis of the PDI derivatives	29
3.1.2 Synthesis of the PXXMI derivatives	33
3.1.3 Solubility tests in complex emulsion	38
3.1.4 Modification of PXXMI structure to improve its solubility	41
3.2 Naphthalimides	45
3.2.1 Photophysical properties of Naphthalimides	49
3.2.2 Naphthalimides as Photocatalysts	53
3.2.3 Naphthalimides in Micellar Aggregates	56
4 Conclusion	65
5 Experimental part	67
5.1 Materials and general methods	67

5.1.1	Nuclear Magnetic Resonance	67
5.1.2	Luminiscence lifetime measurements	67
5.2	Experimental procedures	68
5.2.2	General procedures for the preparation of complex emulsion and micellar aggregates	69
5.2.3	General procedures for the synthesis of perylene derivatives	70
5.2.6	General procedures for the synthesis of substituted peryxanthene xanthenes	76
5.2.7	General procedures for the synthesis of Naphthalimides.	80
6	References	88

Abbreviations

AcOEt	Ethyl Acetate
APSET	Assembly promoted single electron transfer
CMC	Critical micellar concentration
CS	Charge separation
dba	Tris-dibenzylideneacetone
DCM	Dichloromethane
DIPEA	Diisopropylethylamine
DMF	Dimethylformamide
DMSO	Dimethylsulfoxide
dtbbpy	4,4'-Di-tert-butyl-2,2'-dipyridyl
ESI-MS	Electro-spray ionization mass spectroscopy
ET	Electron transfer
FET	Field-effect transistors
HRMS	High resolution mass spectroscopy
ICT	Internal charge transfer
NDI	Naphthalene diimide
OLED	Organic light-emitting diode
PAH	Polycyclic aromatic hydrocarbon
PDI	Perylene-bis(dicarboximide)
PXXIM	Perixanthene-monoimide
T _c	Low upper consolute temperature
TEA	Triethylamine

TFA	Trifluoroacetic acid
THF	Tetrahydrofuran
TLC	Thin layer chromatography

Introduction

Sunlight is one of the most powerful sources of energy on the Earth and in the past years many efforts have been directed toward its transformation in chemical energy and this is even more relevant in the context of a sustainable green economy.¹

In general, following light absorption several processes may take place, that in a properly designed photoactive artificial systems, may lead to the conversion of light energy into chemical energy *via* photoinduced electron process (Figure 1). The efficiency of these process is usually limited by factors like charge-charge recombination and stability of the photoactive systems calling for a careful design and optimization of the system.

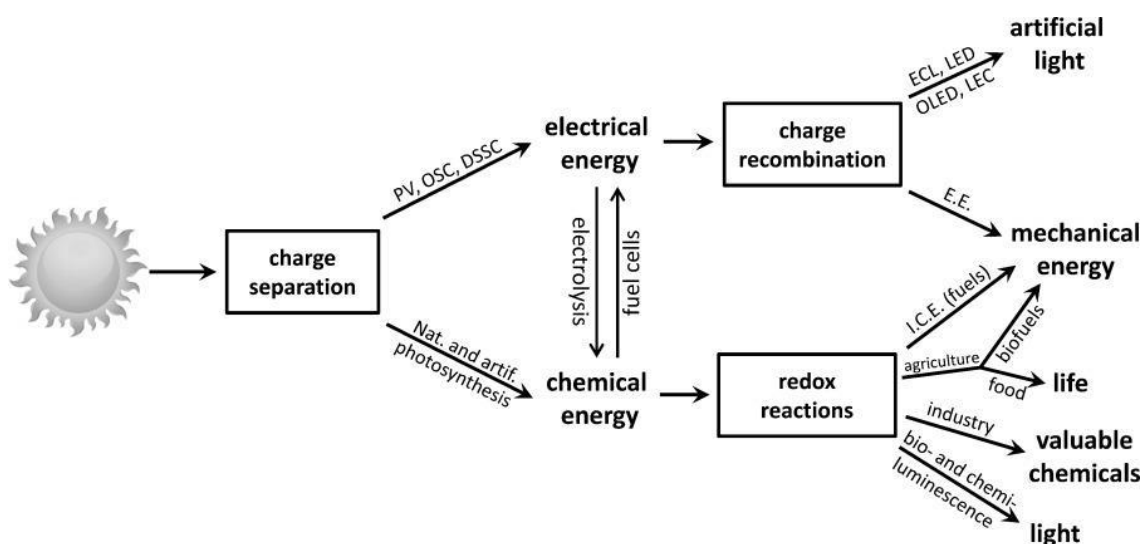


Figure 1. Schematic representation of light energy conversion. From reference 1.

The photoinduced electron transfer chemistry may be exploited for the generation of radical species that can trigger a variety of chemical reactions and the selection of a proper photoactive catalyst may activate molecules that do not absorb light promoting their transformation into valuable chemical products. Several examples demonstrate that photoredox catalysis can be successfully applied in sustainable free-radical-mediated processes for organic synthesis.² The proper selection of the photoredox catalyst and of the experiment conditions is a key factor in these reactions.

However, some issues limit the applicability and practical implementation of photocatalytic process in organic synthesis. In particular, the common use of high cost

metal catalysts (i.e. ruthenium/ iridium complexes) and the difficulty of the separation of the complex reaction mixture to recover the product and recycle the catalyst obstacle the scale up of these processes. Finally, the charge-charge recombination is a common problem that limit the overall efficiency of the process.³

Most of these limitations could be addressed in a system in which the different components are confined in different phases and the reaction takes place at the interphase. This Thesis work is focussed on the study of photoinduced processes at static liquid-liquid interphases (immiscible solvents/surfactant aggregates) as models or more complexes dynamic interphases implemented in microfluidic channels within the framework of the Phototrain processes.

1.1 Electron Transfer Reactions and Photocatalysis

When a molecule absorb light one electron is promoted from the ground state to an electronically excited state (Figure 2, left). Normally this is a singlet excited state (S_n) which can eventually evolve to a triplet state (T_n) via intersystem crossing. The electronically excited state has an extra amount of energy which can be dissipated through different processes such as non-radiative thermal deactivation (internal conversion), radiative emission (fluorescence or phosphorescence) or a chemical reaction (degradation) of the dye. Other possible deactivation pathways in the presence of a quencher (an acceptor) are energy or electron transfer from the excited dye to the quencher.⁴ In the case of organic quenchers, which usually adsorb at high energy making the energy transfer forbidden, electron transfer is the most common process and may result in oxidation or reduction of the quencher depending on the photochemical couple.⁵ In Figure 2 (right) is shown the reduction of the quencher (B) from the excited dye (A^*), which occurs spontaneously with a favourable ΔG and generates the radical anion of B (B^-).

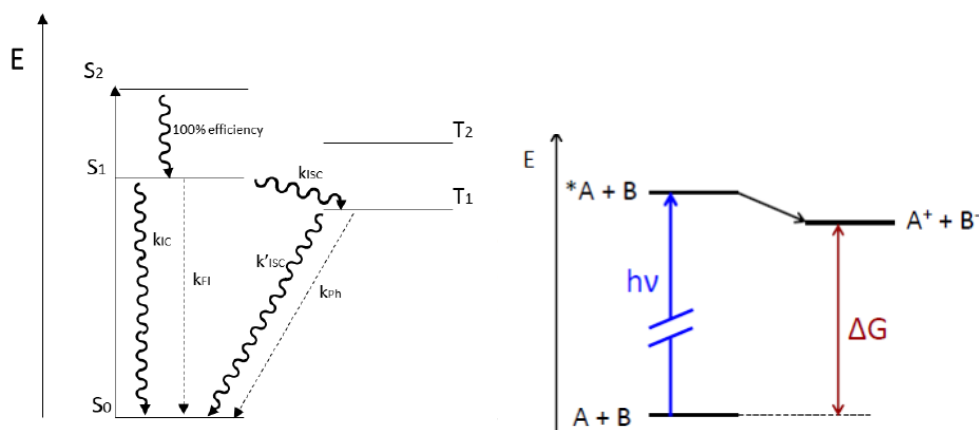


Figure 2. Left: Jablonski diagram for an organic molecule (S_n is a singlet state, T_n is a triplet state, k_{ISC} is the intersystem crossing rate constant, k_{IC} is the internal conversion rate constant, k_{FI} is the fluorescence rate constant and k_{Ph} is the phosphorescence rate constant). Right: Diagram of electron transfer reaction.

In general, a photoinduced oxidation of molecule B is possible, when reductive potential of dye A in its excited state (E^*_{red}) is more positive than oxidation potential of molecule B (E_{ox}). Similarly, a photoinduced reduction of B might occur when the oxidative potential of dye A in its excited state (E^*_{ox}) is more negative than reductive potential of B (E_{red}).⁶

In a typical photocatalytic cycle (Figure 3) the photocatalyst might oxidize or reduce the reactant X with the formation of product X' and modified (oxidized or reduced) catalyst C'.⁷ These two reactive species X' and C' diffuse away from each other, however if any of them cannot escape the solvent cage fast enough, back electron transfer reaction may take place and stop the desired chemical transformation. Once formed, X' might undergo secondary reaction (e.g. with other substrates) with the formation of a stable products Px. To close the catalytic cycle and restore catalyst, C' must react with an intermediate of the reaction or another molecule Y (called sacrificial agent).

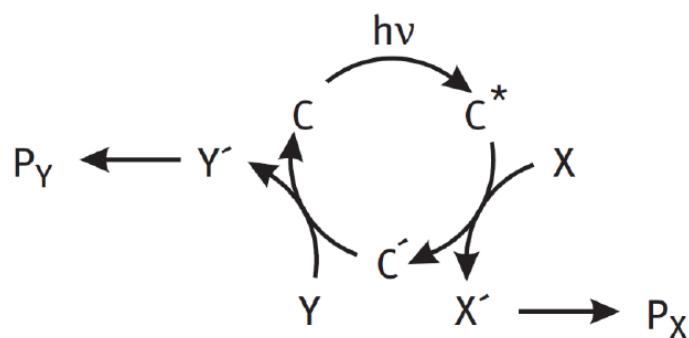


Figure 3. Schematic representation of a photocatalytic cycle.

As shown by MacMillan et al.⁸ these photoinduced catalytic processes have been performed mostly with the help of inorganic catalysts like Ruthenium and Iridium complexes. The photophysical properties of ruthenium bipyridine have been thoroughly studied, showing that $\text{Ru}(\text{bpy})_3^{2+}$ has a long-lived excited state lifetime (1100 ns) and excited state redox potentials of $E_{1/2}(\text{III}/\text{II}^*) = -0.81 \text{ V}$ and $E_{1/2}(\text{II}^*/\text{I}) = +0.77 \text{ V}$ vs SCE that allow it to engage in a variety of oxidative and reductive processes.⁹ In the case of $[\text{Ir}(\text{dFCF}_3\text{-ppy})_2(\text{dtbpy})](\text{PF}_6)$, initially reported for OLED and water-splitting applications, it has likewise become one of the most widely used photocatalysts in recent years.¹⁰ While it bears many similarities to $\text{Ru}(\text{bpy})_3^{2+}$, it offers a longer lived excited state lifetime (2300 ns) and greatly expanded redox window ($E_{1/2}(\text{Ir}(\text{III}^*/\text{II})) = 1.21 \text{ V}$ and $E_{1/2}(\text{Ir}(\text{III}^*/\text{IV})) = -0.89 \text{ V}$).¹¹ Figure 4 shows an example of a photocatalytic cycle applied to the catalysis of the copper-catalyzed trifluoromethylation of alkyl bromides reported by MacMillan group.¹² In this case, upon photoexcitation, the Ir(III) complex generates by single electron transfer (SET) a silicon-centered radical which in turn generates an alkyl radical by bromine extraction from an alkyl bromide. At the same time, SET between the Ir^{II} reductant and electrophilic trifluoromethylation reagent regenerates the photocatalyst and produces the trifluoromethyl radical. Rapid capture of this latter radical by a Cu^I complex produces a Cu(II)-CF₃ adduct which reacts with the alkyl radical formed in the photocatalytic cycle giving an alkyl-Cu(III)-CF₃ species, which upon reductive elimination affords the desired product and regenerates the Cu^I catalyst. Therefore, the combination of a photocatalytic cycle with a copper catalytic cycle allowed to overcome

These inorganic catalysts, despite their high efficacy, are also well known for their toxicity to the environment and for the waste they create.¹⁴ An organic photocatalyst, being biodegradable, is a more suitable catalyst in a green chemistry context. Moreover, in an industrial perspective, non-metal photocatalysts are more cost-effective and sustainable when compared with metal-based photocatalysts.¹⁵ As a consequence, organic chromophores have gained increasing attention in the photoredox catalysis.

The structural diversity of organic chromophores provides a wide range of diverse photophysical and electrochemical properties influencing their reactivity in the photoinduced electron transfer reactions. As a consequence, organic chromophores allow to perform a broad spectrum of chemical transformation similarly to their metal counterparts.¹⁶ Moreover, careful design of the molecular structure of organic dyes allows to gain control on the redox potentials of excited states enabling the development of chemoselective reactions activated by specific excitation wavelengths.¹⁷

This study will use as model reaction a dual catalytic cycle photocatalyst/nickel, similar to that proposed by MacMillan⁸, but with an organic photocatalyst as an alternative to Ir(III)-complexes and confining the reaction at static interphases.

1.2 Liquid-Liquid interfaces

The focus of this project is the study of photoinduced energy and electron transfer processes at liquid-liquid interfaces and for this investigation we choose to use complex emulsion and the micellar/water interphase as models for static liquid/liquid interfaces.

1.2.1 Complex Emulsions

Complex emulsions include multiple components emulsion with several interfaces in droplets and Janus droplets and have an important role in pharmaceuticals and medical diagnostic, in the creation of microparticles and capsules of food, in cosmetics, dynamic optics and chemical separations.¹⁸ Following the method described by Swager et al¹⁹ it's possible to create three-phase complex emulsions with highly controllable and reconfigurable morphologies. They did this exploiting the facts that fluorocarbons are

lipophobic as well as hydrophobic and that many fluorocarbon and hydrocarbon liquids are immiscible at room temperature but have a low upper consolute temperature (T_c) and mix with gentle heating. Fluorocarbon solvents were also chosen due to being inert materials with properties that can be used in ultrasound contrast agents and magnetic resonance imaging, in water repellent surfaces, as artificial blood and acoustically triggered release of payloads. The process to create these complex emulsions is a temperature-induced phase separation starting with the preparation of an emulsion of 1:1 volume ratio of hexane:perfluorohexane above T_c (22.65 °C, low upper consolute temperature) in an aqueous solution of the nonionic fluorosurfactant Zonyl (Zonyl FS-300: $F(CF_2)_xCH_2CH_2O(CH_2CH_2O)_yH$). When cooling the emulsion below T_c , structured complex droplets are formed with an internal spherical interface between hexane and perfluorohexane and with an increased interfacial area with respect to Janus droplets. These complex emulsions can be produced by simple shaking of hexane-perfluorohexane liquids in the surfactant solution (Figure 6a). As can be seen in Figure 6b, these droplets are polydisperse and their morphology and composition were uniform. The droplet morphology is directly controlled by interfacial tension which in turn is influenced by the concentration of Zonyl. As shown in Figure 6c, on decreasing the concentration of Zonyl the multiphase droplets will adopt three thermodynamically

permissible internal configurations: (1) liquid H encapsulated in liquid F, (2) liquid H and F form a Janus droplet, and (3) liquid F encapsulated in liquid H.

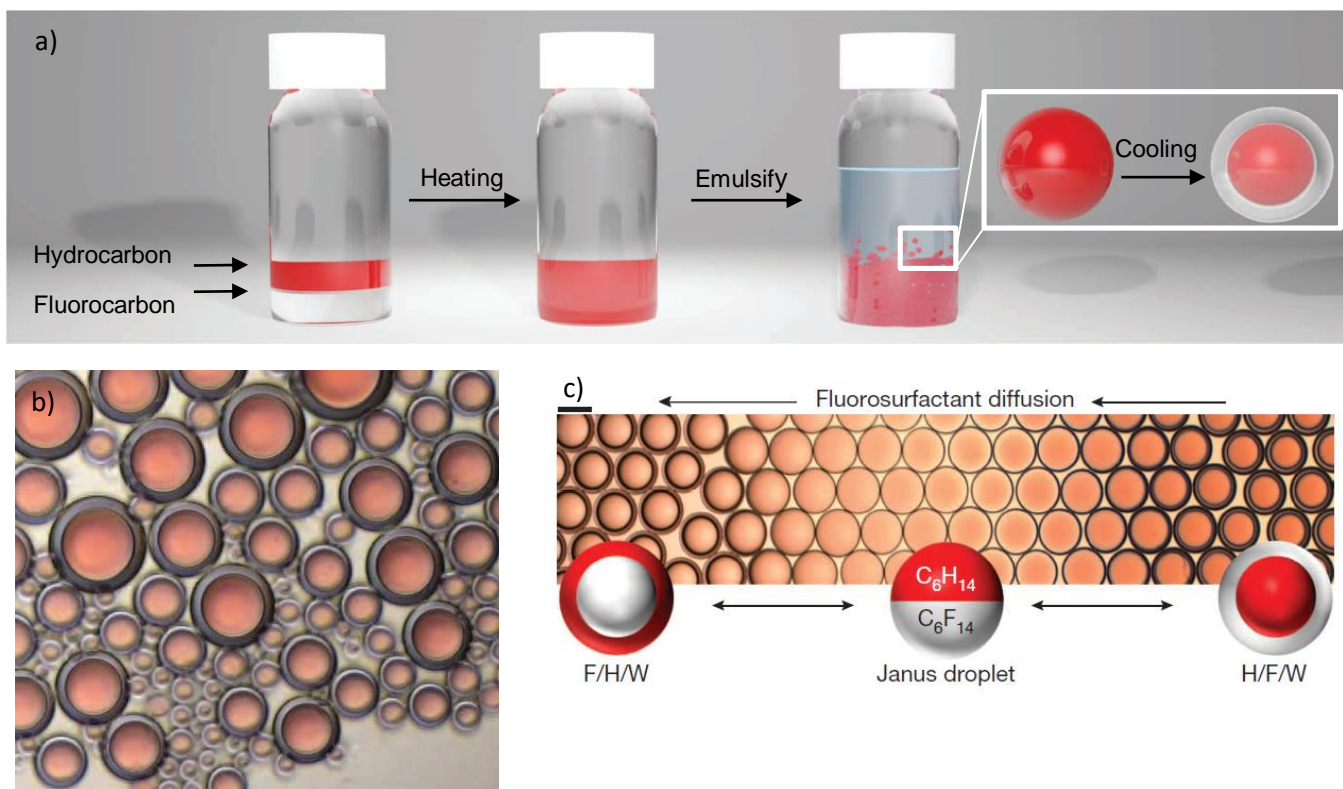


Figure 6. a) Procedure for preparation of complex emulsions; b) Example of a colored complex emulsion by microscope; c) Hexane–perfluorohexane droplets reconfigure in response to variation in the concentration of Zonyl from right (higher Zonyl concentration) to left (lower Zonyl concentration).

1.2.2 Surfactants and micellar aggregates

Surfactants are compounds able to decrease the interfacial tensions of liquid/solid, liquid/liquid and liquid/gas interfaces, due to their amphipathic nature usually related to a structure comprising a hydrophilic head group and a hydrophobic chain. They are used in various fields such as additives in food industry, cosmetics, tertiary recovery, washing agent, etc. In the field of nanotechnology surfactants were crucial inducing and capping agents able to assist the synthesis of different sized and functionalized nanomaterials.^{20,21} To give diversity to the functionality of surfactants novel surfactants have been synthesized recently such as gemini surfactants owning high surface activity, abundant self-assembly morphologies,^{22,23} and low critical micelle concentration, silicon surfactants,²⁴ degradable surfactants,²⁵ bola surfactants,²⁶ ionic liquid surfactants,^{27,28}

biological surfactants,²⁹ and fluorescent surfactants.^{30,31} In the case of aromatic fluorescent surfactants, their absorption and fluorescent spectra are sensitive to environment^{32,33} and this is an advantage when compared to other surfactants and allows for a study of the aggregation behaviour of the compound in various applications. To create the fluorescent surfactants, the ideal method is incorporating a chromophore group into a surfactant. This, however, creates the problem of using dyes with large molecular volume and poor water solubility as the chromophore group of the surfactant. Generally, the presence of aromatic rings in the core structure of the surfactant has significant influence on the aggregation behaviour of the surfactant resulting in a decrease of solubility in water, due to the presence of π - π interactions.^{34,35} Also, the absorption and emission spectra of these fluorescent surfactants are normally in the UV region, and easily interfered by other small aromatic molecules.

As an example a carbazole group has been introduced to the end the hydrophobic chain of imidazolium surfactant to give a fluorescent surfactant with improved micelle formation capabilities.³⁰ A group of fluorescent surfactants containing 2,4,6-trimethylphenyl groups were prepared recently. The resulted surfactants have strong π - π interactions between the nearby molecules and high packing density on the surface of water.³¹

One of the most interesting properties of surfactant is their ability to form aggregates in water. Above to a given concentration (critical micellar concentration, CMC) the surfactants self-assemble forming micelles.³⁶ Micelles are spherical aggregates with the hydrophobic chain of the surfactant buried in the interior and the hydrophilic head on the surface, in the contact with water (Figure 7). The superficial layer of the micelle has peculiar properties as it concentrates ions (at least in the case of charged surfactants) and create an interfacial region between water and the less polar interior. On the other hand, hydrophobic molecules tend to partition in the inner phase of the micelles. These abilities to compartmentalize and to concentrate different chemical species has been exploited in many field and in particular in the catalysis of chemical reactions.³⁷ In this thesis, we will explore micellar aggregates as reactors for photocatalytic reactions also preparing surfactants functionalized with organic dyes.

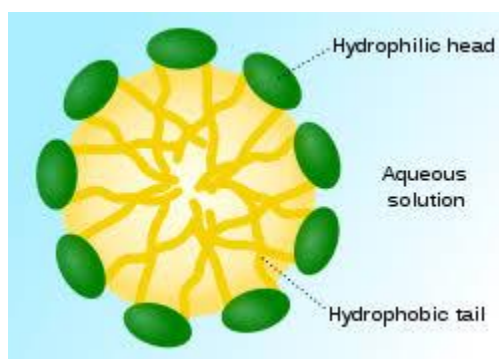


Figure 7. Schematic drawing of a micelle.

1.3 Organic Dyes

From the plethora of organic semiconductors available, PAHs (polycyclic aromatic hydrocarbons) have become more relevant. When compared to infinite grapheme, PAHs have non-zero tunable bandgaps and are therefore more useful as chromophores in antennae³⁸ or emissive molecular architectures³⁹ and as a general use in all optoelectronic applications that require this type of semiconductor.

With this general group of molecules as a tool,^{40,41} we need to tune the molecular HOMO-LUMO gap³⁸ to suit our ideal parameters. This can be done by 1) changing the molecular planarity by insertion of bulky substituents or bridging chains; 2) changing the size and edge of the carbon based aromatic framework; 3) changing the peripheral functionalization through the insertion of electron-donating or electron withdrawing substituents; 4) varying the aromatic properties of the constituent monomeric units; 5) promoting supramolecular interactions between individual molecules governing their organization into a condensed phase; 6) enclosing structural defects; and 7) replacing selected carbon atoms by isostructural and isoelectronic analogues like oxygen and silicon (i.e., doping). This heteroatom-doping approach in identifying the ideal chromophore is probably the most relevant,^{42,43} since without substantial perturbation of the structural stability of the molecule we can significantly change its optoelectronic properties⁴⁴.

Using these parameters and researching the properties of different PAHs we devised three molecular cores that will be prepared and analysed in the context of this work.

These compounds are the Perylene-bis(dicarboximide) (PDI), the Perixanthene-monoimide (PXXIM), and the Naphthalimide.

1.3.1 Perylene-bis(dicarboximide) (PDI)



Figure 8. Perylene structure and reactive areas of the compound. Some of the uses of perylene derivatives due to their self-organization properties.⁴⁵

Perylene-bis(dicarboximide)s (PDIs)⁴⁵⁻⁴⁸ are well-known n-type semiconductors with properties that allow the fabrication of field-effect transistors (FETs),⁴⁹ solar cells,⁵⁰ artificial photosynthesis, two-photon absorption dyes, molecular assembly, and photoinduced charge separation (CS). PDIs with fluorinated chains have also been used in FETs, to change the stability of the device in the air and more importantly make them stronger electron acceptors.⁵¹ As an example of a PDI as an organic semiconductor, Rabe et al.^{52,53} showed that a PDI containing branched aliphatic side chains could work as a good electron acceptor with a hexakis(dodecyl)hexabenzocoronene (HBC-C12) as an electron donor. This work also showed that the aromatic cores of the two components engaged in the electron transfer tend to form ADADAD periodic columnar stacks, with the side chains used to aggregate or disperse this staking.⁵⁴ In terms of our project this staking proves to be a problem due to the agglomeration of donor and acceptor molecules interfering with their dissolution at the liquid-liquid interface.

1.3.2 Perixanthene Xanthene

In the case of the O-doped analogue of anthanthrene, perixanthenoxanthene (PXX) is considered a building block for the creation of a new class of O-doped PAHs.⁵⁵⁻⁵⁷ When substituted with reactive groups (like imide) the PXX have excellent carrier-transport and injection properties, with easy processability, high thermal stability, and chemical inertness.⁵⁸ These properties make PXXs an excellent active organic semiconductor in transistors or rollable OLEDs.⁵⁹⁻⁶¹ For a PXX to be capable to perform as an active organic semiconductor good charge-transport properties, and good thermal and chemical stability of the π -conjugated system, that avoids parasitic oxidation of the catalyst, are needed.

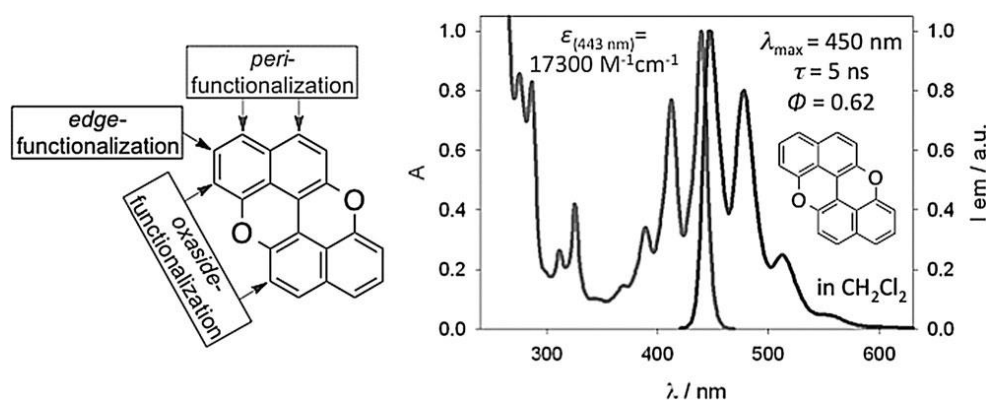


Figure 9. Structure of PXX and normalized absorption and emission spectra in CH₂Cl₂ at room temperature

Bonifazi et al,⁶² developed a synthetic strategy toward π -extended versions of PXX with the effect of increasing the HOMO energy levels of the compounds as a consequence of the improved electron donor properties.⁵⁵ They considered that PXX could be an excellent chromophore to promote exergonic photo-induced single electron transfer (SET), by studying the UV-Vis absorbing bandgap, with minor Stokes shift and strong charge injection.⁶³ By adding electron withdrawing groups (EWGs) in the peri-positions, the redox properties of PXXs excited states can be controlled,⁶⁴ by tuning the frontier orbital energy levels of the molecule. This conjecture led them to choose as mimic of perylene diimide (PDI)⁶⁵ the PXXMI (perixanthene-monoimide) and the PXXDI (perixanthene-diimide), that have one or two electron-depleting alkylimide groups

linked to the structural core of the compound, in order to promote electron transfer properties.^{65,66}

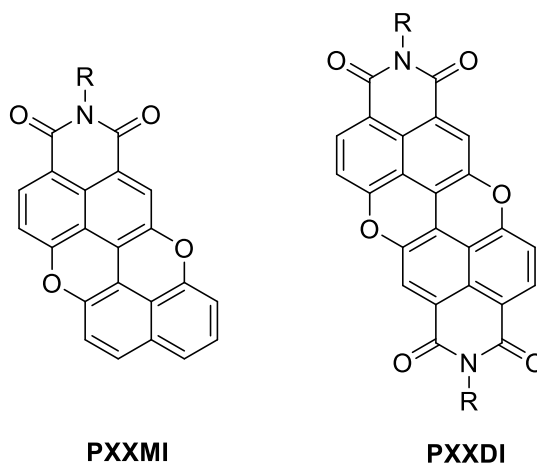


Figure 10. Structure of PXXMI and PXXDI prepared in the Bonifazi group (from reference 62).

The field of PXX doping with oxygen or silicon has been largely unexplored, so this work will also be important for the study of possible applications of these compounds as effective OSC (organic semiconductor) with tuneable optoelectronic properties and as a photocatalyst.

1.3.3 Naphthalimide

The Naphthalimides (NDI) substituted in position 4 with an amino group are functional dyes that have received great interest throughout the years due to their outstanding ICT electronic structure and desirable photophysical properties, like high fluorescence quantum yields, large Stokes shift, appropriate absorption, and emission wavelength. Due to their properties these molecules have been used as antiviral agents,^{67,68} as components in the design of molecular logic gates,⁶⁹ as fluorescent probes,^{70,71} to view laser activity,^{72,73} and as fluorescent sensors.^{74,75} In the case of fluorescent sensors these are very valuable in environmental important recognition processes. A system of 'on-off' fluorescent sensors based on simple naphthalimides has been reported in the literature for the detection of anionic surfactants and imaging of molecules based on

the electrostatic and hydrophobic interactions between sensors and surfactants.⁷⁶ Examples of Naphthalimides that can be used for the detection of anionic surfactants with both absorbance and fluorescence changes were reported by Li et al.⁷⁷ (Figure 11).

The cationic hydrophilic headgroups of the naphthalimides of Figure 11 ensure a strong electrostatic interaction with anionic surfactants reinforced by hydrophobic interactions between the alkyl chains. These interactions led to modification of the emission properties of the dye allowing successful sensing of the anionic surfactant. Unlike most traditional surfactants the use of NDI brings strong π - π interactions between the surfactant molecules and should have a significant effect on the surface activities of the surfactant and eventually of their photocatalytic properties.

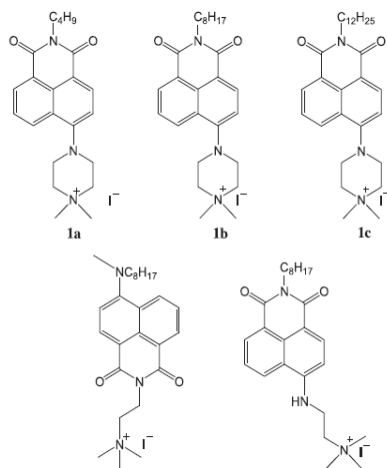


Figure 11. Naphthalimides prepared by Li et al. (from reference 77).

NDIs have two relevant positions in 4 and 5, and the imide group itself, that are suitable of being modified by reactive groups. In addition, unlike most PHAs, the NDIs have a smaller molecular volume, allowing for an increased solubility in aqueous solutions. Substitution in the 4 position with a donor amino group led to a strong ICT (internal charge transfer) effect that ensures very high fluorescence quantum yields, from 0.7 to 0.8, and strong sensitivity to environmental conditions.^{78,79} Thanks to these properties the NDI can be successfully used in the construction of fluorescent surfactants.

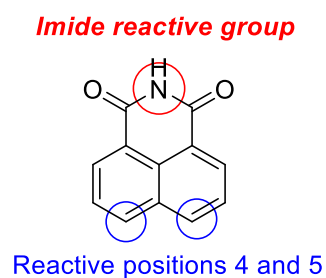


Figure 12. Reactive positions of the core Naphthalimide structure.

1.4 Photocatalytic reactions at interfaces

In the literature there are several studies regarding photocatalysis in nanophotoreactors, either inorganic structures or organized molecular assemblies (e.g., titania spheres, lipid vesicles, foams, oil-in-water emulsions), which show the today relevance of these topics in the field of material chemistry and energetics.⁸⁰ Other possible materials for photocatalysis are soft gels that can work as structured reaction vessels and reusable catalysts.⁸¹ However, the study of photochemical processes in gel media, using embedded reactants that do not participate in the viscoelastic network, is rather underexplored. One study by Bhat and Maitra⁸² in 2007 shows that a photodimerization of acenaphthylene occurs with higher syn/anti selectivity in bile acid-based hydrogels than in micellar solutions. Later Shinkai and coworkers⁸³ reported a selective photocyclodimerization of anthracene derivatives within an organogel matrix.

Many studies have been done to use photochemical catalysis in water splitting, however this has proved a challenge for the scientific community. Some information can be taken from these studies regarding electron transfer processes in water environments. The first is that a typical catalyst for these processes is composed of two subunits: a light absorbing photoredox active dye or sensitizer and the water oxidizing catalyst, this can be translated to an efficient single molecule photocatalyst with two reactive cores.⁸⁴ The second is that in biological photosynthesis, chromophores and catalytic units are bound to membranes, so when compared to homogeneous solution, these two dimensional assemblies increase the local concentration of the redox partners and shorten the average distance for electron transfer between them.⁸⁵

Another important aspect is the comparison between intra and intermolecular electron transfer. The reaction of electron transfer between photosensitizer and reduction catalyst is mainly done by covalent connection or assembly through bridging ligands. However, by embedding the components in a structured media it is possible to achieve efficient intramolecular electron transfer avoiding the use of bridging ligands. This self-assembling approach is much simpler and permits to easily vary compositions and ratios of the photosensitizer and catalyst. A study by König et al⁸⁶ showed that, in the case of hydrogen generation in pure water, the use of functionalized vesicle membranes by co-embedding of amphiphilic photosensitizers with amphiphilic cobalt-based hydrogen evolving catalyst results in high local concentration of the embedded photosensitizer and catalyst at the surface of the vesicle. Moreover, the use of vesicles allows to overcome the solubility problems that some photosensitizers and catalysts might have and can avoid the use of organic solvents. By incorporating the two redox-active subunits into lipid layers, König and co-workers obtained a two-dimensional arrangement that resulted in high local concentration of the components of the reaction. This assembly creates a close spatial proximity of the complexes without relying on direct covalent linkage between the components (unlike most intermolecular electron transfers reaction). The membrane fluidity of the vesicle membrane allows also a dynamic reorganization of the system. All these factors greatly improved the catalytic activity and accelerate the hydrogen generation process in pure water.

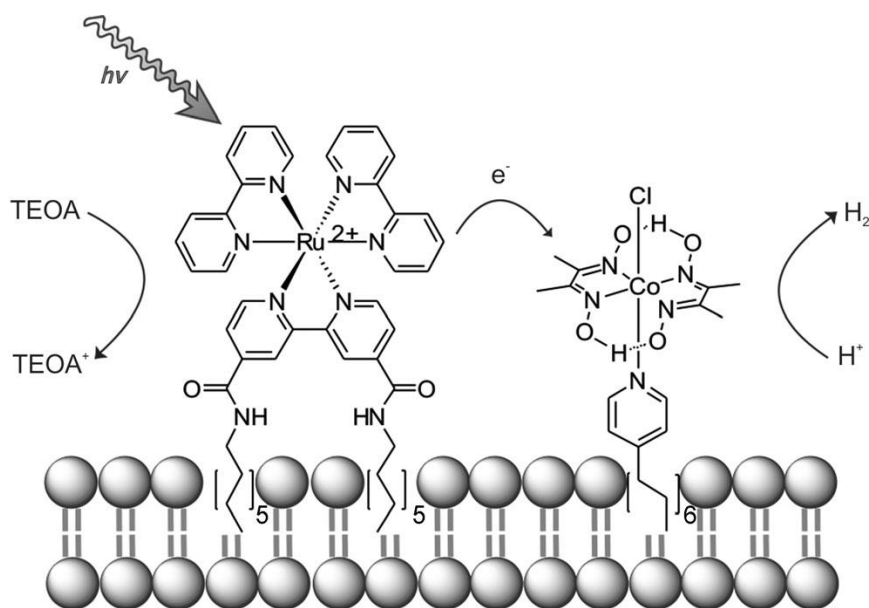


Figure 13. Self-assembled functionalized membranes for photocatalytic hydrogen generation as described by König et al., from reference 86.

Regarding the photocatalysts we plan to use, Xu et al⁸⁷ have designed a rapid and simple route to integrate probes for sensing Fe³⁺ ions in aqueous systems embedding a Naphthalimides derivative (NapTp) into water soluble surfactant micelles. The surfactant cetyltrimethyl ammonium bromide (CTAB) has a positively charged head group and a hydrophobic tail, and, when added in water forms positively charged micelle. In this work, Xu and co-workers trapped NapTp inside the hydrophobic core of

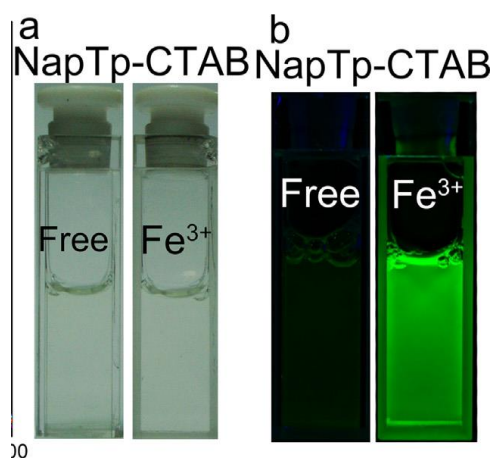


Figure 14. Fluorescence images of NapTp-CTAB and NapTp-CTAB + Fe³⁺ under U. V by Xu et al. (From reference 87)

CTAB micelles ensuring its solubility by assembly of NapTp-CTAB micelles. They observed that the NapTp-CTAB assemblies display a degree of optical changes with the change of concentration of Fe^{3+} ions, with a distinct color change of the solution (Figure 10).

A different work that applies an assembly promoted single electron transfer (APSET) strategy in which the reacting species are compartmentalized in a microheterogeneous aqueous solution (micelles) is the recent work of König et al.⁸⁸ With this they intend to increase the stability of an iridium photocatalyst and allow the engagement of non-activated alkyl chlorides in radical dehalogenation addition and cyclization reactions. The photoreductive APSET system they create allows visible light-induced activation of alkyl chlorides with reduction potentials, which in classical organic solvents reach -2.8 V versus SCE. The thus formed alkyl radicals react with alkenes forming new carbon-carbon bond. The micellar solutions are able to stabilize the Iridium complex by non-covalent interactions and to compartmentalize the reacting species. Although this work focused in radical dehalogenations, addition and cyclization reactions using metal based catalysts, this Thesis project intends to use similar compartmentalization strategy and non-covalent interactions to achieve similar results using organic catalysts.

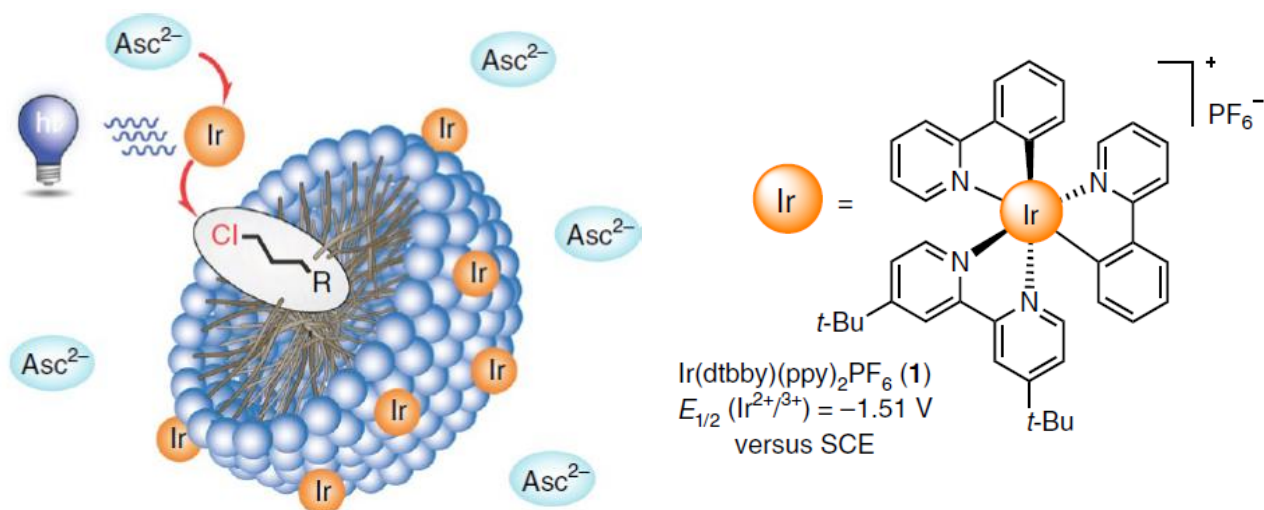


Figure 15. Schematic representation of the assembly-promoted single electron transfer (APSET); Asc^{2-} = ascorbate.⁸⁹

Aim

Aim of the project is the study of photochemical processes at the static interphase between two immiscible liquids as a model of the more complex dynamic liquid-liquid interphases which will be implemented in microfluidic devices within the frame of the PHOTOTRAIN project. As a first system we will investigate a ternary emulsion water/fluorohexane/hexane, which allows to easily obtain stable hydrocarbon/fluorocarbon interfaces, using amphipathic dyes functionalized with fluorocarbon chains. The idea is that the fluorocarbon chain will insert in the fluorohexane phase anchoring the dye at the interface between the two organic solvents.

As a first test compound we will use a dye, known as perylene, that has well known photophysical properties. The dye will be modified by appending a C₁₂-fluorocarbon amine. As a second test molecule we will use a different dye with the perixantene (PXX) core developed in the Bonifazi's group which will also be functionalized with a C₁₂-fluorocarbon amine. The dyes will then be incorporated at the liquid-liquid interface and their photophysical properties and photocatalytic behaviour will be investigated. As reference compounds the analogous dyes functionalized with a C₁₂-hydrocarbon amine will be prepared. These dyes will presumably be confined in the hexane phase.

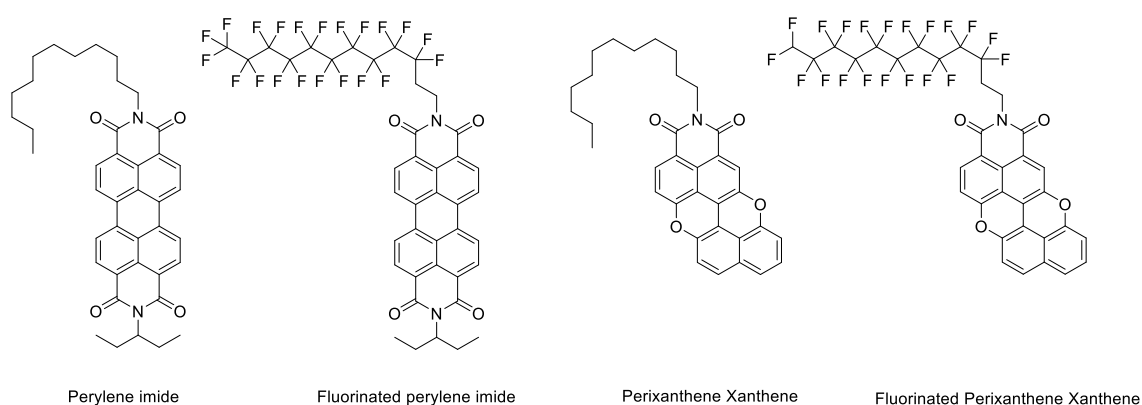


Figure 16. Prepared dyes for the inclusion in a water/fluorohexane/hexane ternary emulsion.

Other liquid-liquid interfaces will be used, such as the water/micellar interface, where we will attempt to apply derivatives of Naphthalimide as amphipathic dyes. The naphthalimide core will be functionalized with uncharged and positively or negatively charged chains so that it will be integrated at the interface between water and micelles.

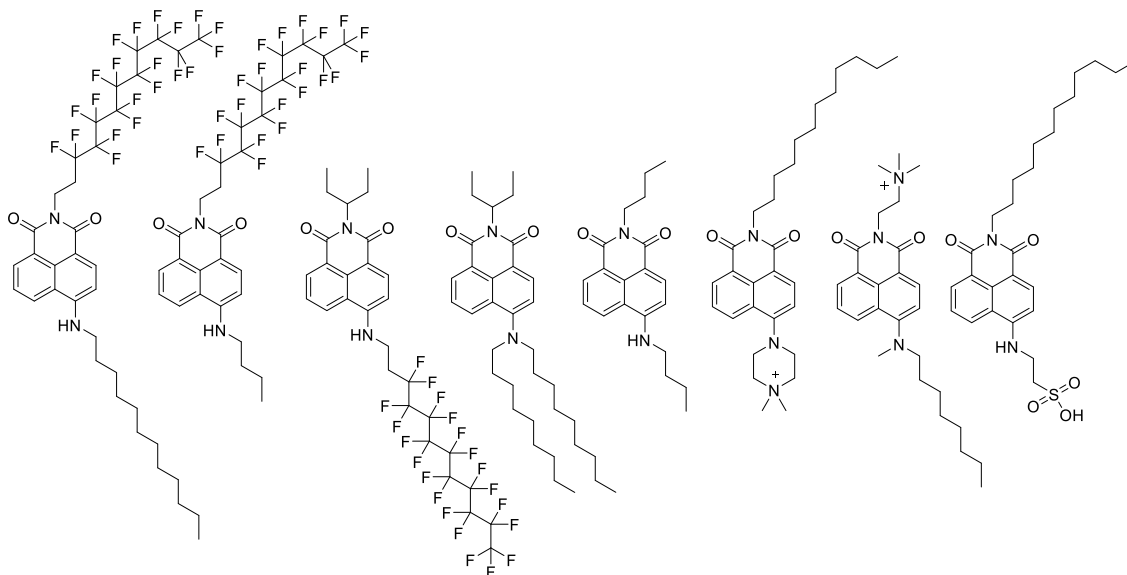


Figure 17. Prepared Naphthalimides for the inclusion in a water/fluorohexane/hexane ternary emulsion and micellar solutions.

If any of the dyes prepared successfully dissolves at the interface between the two liquids, we will continue to the next step of the project that is the study of the electron transfer capabilities of these molecules when integrated at the interface. For this purpose, we will also use a model reaction exploiting our dyes as photocatalysts and we will investigate how the photophysical properties of the catalysts affect the yields of those reactions in comparison with the same reaction performed in bulk solvent. This will be done with the help of the colleagues in the PHOTOTRAIN project and in particular the team in Dr. Reddy's laboratories in Cambridge and the group of professor Bergamini at the University of Bologna.

Results and Discussion

This work will focus on the study of photoinduced energy and electron transfer processes and photocatalytic reactions at static liquid-liquid interfaces between two immiscible solvents. However, the simple use of two immiscible liquids like, for example, water/DCM or hexane/perfluorohexane does not ensure a large contact area between the solvents and this limits the number of possible phenomena occurring making difficult to study the process. For example, the interfacial area of two immiscible liquids contained in a 25 ml round-bottom flask is only few cm^2 and this will strongly reduce the rate of a photocatalytic reaction occurring at the interphase making difficult to isolate and characterize the products which are formed in a very small amount, unless a very long reaction time is allotted. One easy way to overcome this problem is the use of an emulsion in which the contact area between the two immiscible liquids is much greater. Indeed, in a surfactant stabilized oil in water emulsion containing 10 ml of oil and with droplets size of $1\ \mu\text{M}$ the surface contact area between oil and water can be estimated as large as $30\ \text{m}^2$, and will increase strongly as the size of the droplets will decrease.⁸⁹

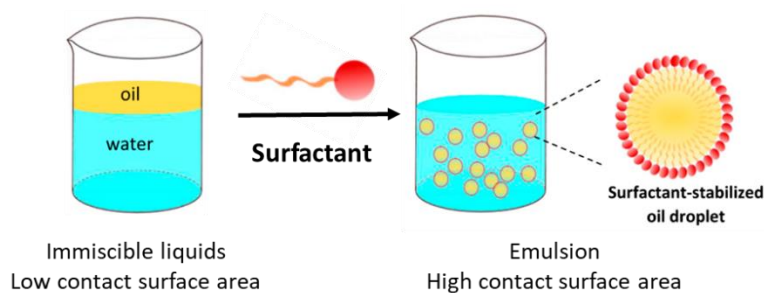


Figure 18. picture comparing the different contact surface area between two immiscible liquids obtained by simple mixing (left) and by formation of an oil in water emulsion stabilized by a surfactant (right).

3.1 Studies in hexane/perfluorohexane emulsion.

For the above illustrated reasons, we directed our attention to emulsion systems and as a first choice we selected a complex hexane/perfluorohexane/water emulsion stabilized by a surfactant that ensure a great contact area between two immiscible organic solvents (hexane and perfluorohexane). Such kind of emulsions have been recently reported by the group of Swager¹⁹ and its formation exploits the facts that fluorocarbons are lipophobic as well as hydrophobic and that many fluorocarbon and hydrocarbon liquids are immiscible at room temperature but have a low upper consolute temperature (T_c) and mix with gentle heating.⁹⁰ Hexane and perfluorohexane have a T_c of 22.65 °C.⁹¹ Therefore, it is possible to exploit a temperature-induced phase separation to control the formation and the properties of a hexane/perfluorohexane emulsion. The complex emulsion is simply prepared by firstly emulsifying a 1:1 volume ratio of hexane and perfluorohexane above T_c in an aqueous solution of Zonyl FS-300 (Zonyl), which is a nonionic fluorosurfactant with the linear chemical formula $F(CF_2)_xCH_2CH_2O(CH_2CH_2O)_yH$, and then by cooling below T_c (Figure 19a). This process lead to the formation of structured complex droplets (Figure 19b) with an inner core of hexane covered by a layer of perfluorohexane in contact with the water phase and stabilized by the surfactant [hexane-in-perfluorohexane-in-water (H/F/W) double emulsion]. These complex emulsions are readily produced in bulk by shaking warm hexane–perfluorohexane liquid in a surfactant solution (Figure 19c). Although the droplets are polydisperse, the morphology and composition of the droplets is highly uniform. Moreover, and very importantly for our work, chemical partitioning during phase separation gave directed compartmentalization of solutes. This has been demonstrated by adding the hydrocarbon-soluble Nile Red dye (green) and the water soluble Rhodamine B dye (red) during the preparation of the emulsion and after cooling below T_c and droplets formation the two dyes are confined in the hexane core and interstitial water, respectively (Figure 19d).

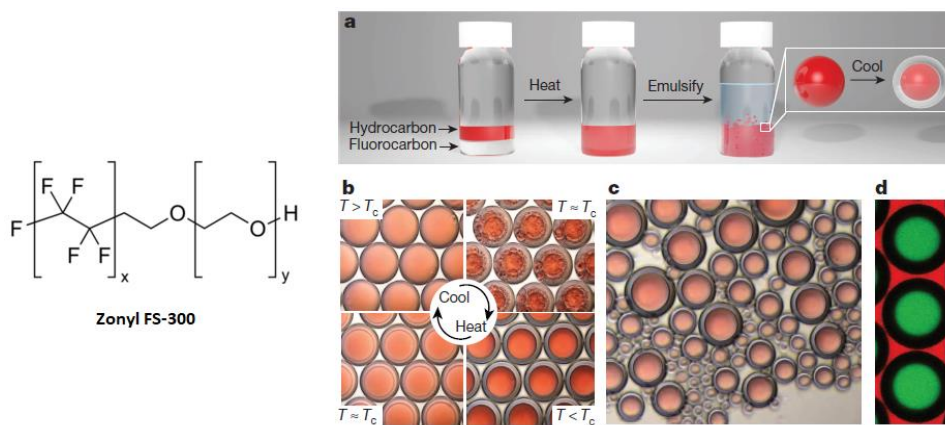


Figure 19. Structure of Zonyl FS-300 and formation of the complex hexane-in-perfluorohexane-in-water emulsion. a) Protocol for emulsion formation. b) Above T_c , hexane and perfluorohexane are miscible and emulsified in aqueous 0.1% Zonyl (top left). Below T_c , hexane and perfluorohexane phases separate to create a hexane-in-perfluorohexane-in water (H/F/W) double emulsion (bottom right). Hexane is dyed red. Scale bar, 200 μm . c) Emulsions of uniform composition made by bulk emulsification (such as shaking). Scale bar, 100 μm . d) Lateral confocal cross-section of H/F/W double-emulsion droplets. Hydrocarbon-soluble Nile Red dye (green) selectively extracts into hexane. Rhodamine B dyes the aqueous phase (red). Scale bar, 100 μm . Monodisperse droplets in b and d were made using a microcapillary device. The picture was reproduced from reference 19.

Elaborating on these facts we speculated that one possibility to confine a photoactive molecule at a liquid-liquid interface was to design an “amphipathic” molecule with a fluorophilic portion appended to a photoactive lipophilic core. This idea is schematically illustrated in Figure 20. The fluorophilic portion, such as a fluorinated hydrocarbon, will dissolve preferentially in the perfluorohexane phase while the lipophilic dye will interact more favourably with the hexane phase. In this way the molecule will partition preferentially at the interphase between the two immiscible solvents. On the contrary, a fully hydrocarbon molecule will dissolve only in the bulk hexane phase. If the hydrocarbon core is a fluorescent dye it would be therefore possible to investigate its behaviour (Emission wavelength, quantum yield, life time, etc.) at the interphase, for example, in the presence of a quencher dissolved in the bulk hexane or confined at the interphase and compare it with the behaviour of the same dye dissolved in bulk hexane. In such a way we will be able to test if our strategy for the confinement of a photoactive molecule at the interface of the immiscible liquids is working or not.

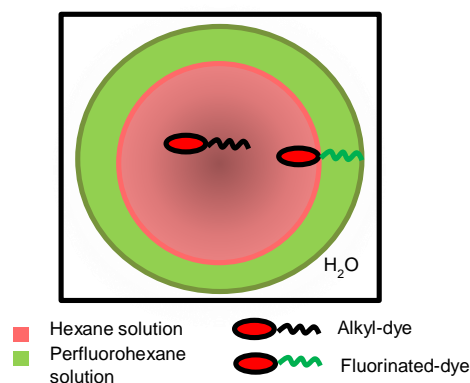


Figure 20. Schematic representation of an “amphiphilic” dye confined at the hexane/perfluorohexane interphase with the fluorophilic chain dipped in the fluorinated solvent and the fluorescent core in the hydrocarbon phase. A fully hydrocarbon dye is represented dissolved in the hexane phase.

To test this working hypothesis we selected two different fluorescent dyes. The first one is a perylene diimide (PDI) dye and it was chosen because it is a very popular, deeply investigated fluorescent molecule which has been used in several different systems, as a n-type semiconductor to use in FETs (Field-effect transistors) and solar cells,⁹² and because its asymmetric functionalization is relatively easy. The second one is a *peri*-xanthenoxanthene imide (PXXMI) which has been recently reported by the group of Bonifazi.^{62,93} This dye belongs to a family of molecules derived by the *peri*-xanthenoxanthene core, the O-doped analogue of anthanthrene, and depending of the substitution patterns their photophysical properties and redox potentials can be finely tuned. In particular, PXXMI can be considered as an analogue of PDI bearing one electron withdrawing imide group at the *peri*-position. Interestingly, and potentially very important for our work, PXXMI is an effective photocatalyst of the dehalogenation of organic compounds and, for example, when irradiated at 520 nm in a degassed solution in the presence of DIPEA it is able to convert quantitatively PhCOCH₂Br in PhCOCH₃ after 24 h in CH₃CN.

To adapt these dyes to our scope we have to modify them by appending a perfluorinated alkyl chain so that to ensure the “amphipathic” character needed for their confinement at the hexane/perfluorohexane interphase. The easiest synthetic approach is the use of the imide moiety as anchoring point by reaction with the proper functionalized amine in the formation of the imide group. Our targets **PDI-F** and **PXXMI-F** are illustrated in Figure 21 together with the alkyl analogue which will be prepared for comparison studies.

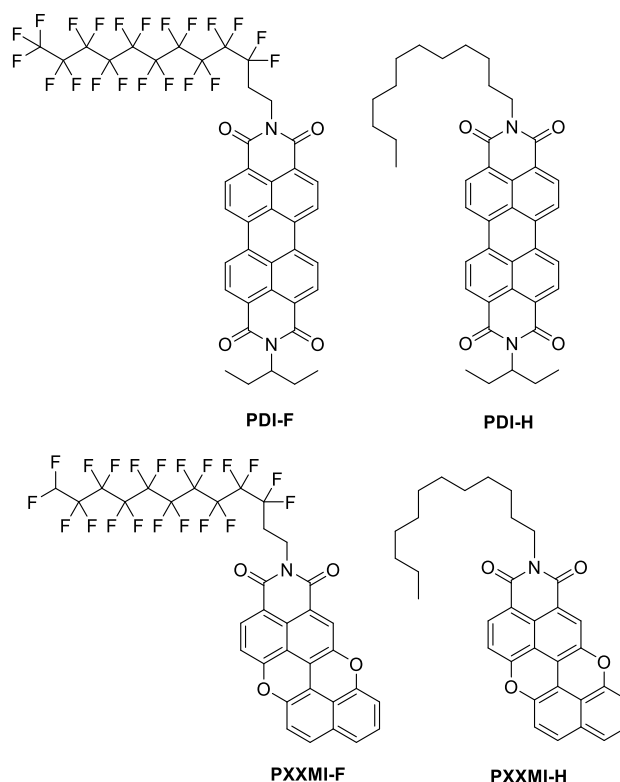
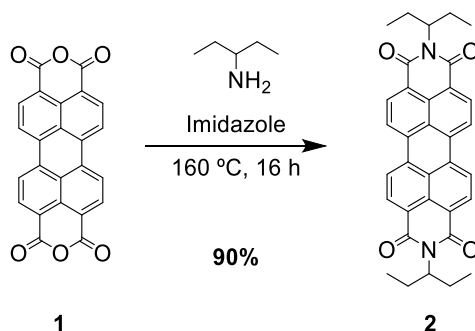


Figure 21. Fluorinated and alkylated dyes investigated in this Thesis.

3.1.1 Synthesis of the PDI derivatives

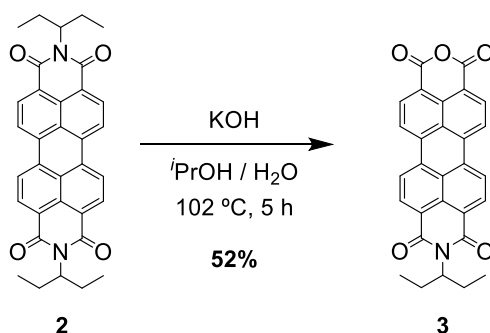
The **PDI-F** and **PDI-H** compounds are non-symmetrically substituted PDI derivatives and therefore the imide groups have to be introduced in different synthetic steps. This type of functionalization is reported in the literature⁹⁴⁻⁹⁶ and starts with the formation of a symmetric diimide using the commercially available 1-ethylpropylamine. The amine is reacted with the perylene dianhydride in imidazole at 160 °C for 16 hours affording after

purification by filtration in basic water (20% KOH), suspension in methanol and filtration, the desired diimide in a 90% yield (Scheme 1).



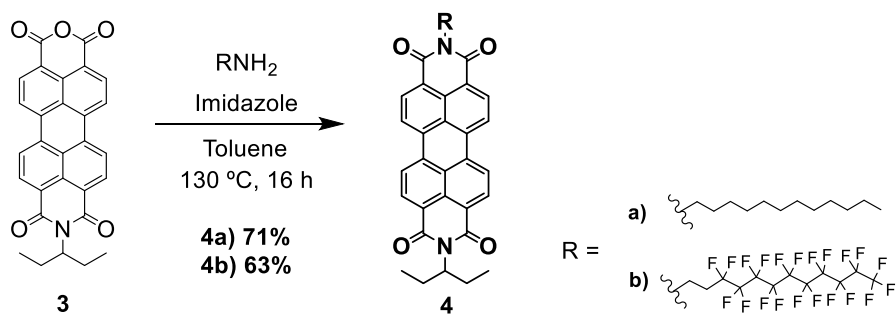
Scheme 1. Synthesis of the N,N'-Bis(3-pentyl)perylene diimide, first step of the synthesis of the PDI derivatives.

The next step is the removal of one of the imides to form a non-symmetric perylene derivative substituted with an anhydride on one side and an imide group on the other side. This is made by hydrolysing one of the two diimide groups with KOH (10%) in isopropanol/water at 105 °C leading to the di-carboxylic acid that in the same reaction conditions is spontaneously transformed in the corresponding anhydride. The reaction is little selective and after purification by washing with basic water (5% KOH) and chloroform, compound **3** is obtained in 52 % yield.



Scheme 2. Synthesis of the imide anhydride perylene precursor (**3**), second step of the synthesis of the PDI derivatives.

The final step for this synthetic pathway is the formation of the imide with dodecylamine and with 1*H*,1*H*,2*H*,2*H*-perfluorododecyl amine to give **PDI-H** e **PDI-F**, respectively. While dodecylamine is commercially available the fluorinate analogue was synthesized



Scheme 4. Synthesis of PDI-F (**4b**) and PDI-H (**4a**).

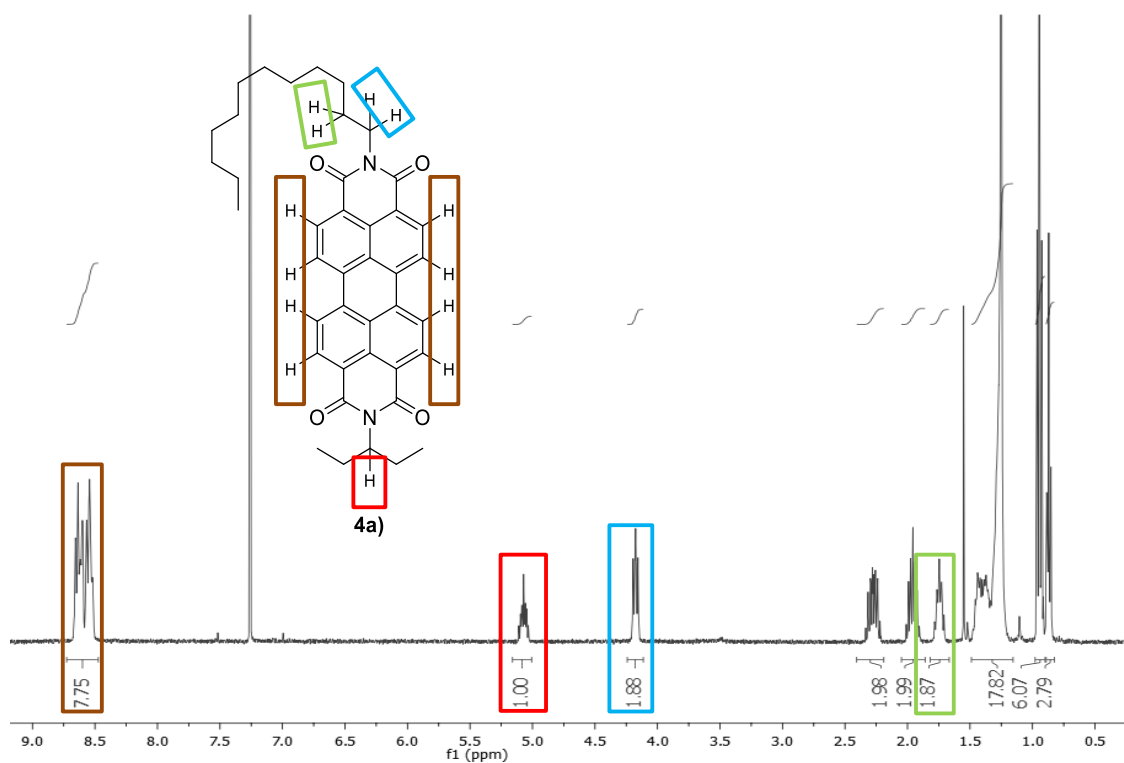


Figure 22. NMR spectra of PDI-H (**4a**) (CDCl_3 , 400 MHz).

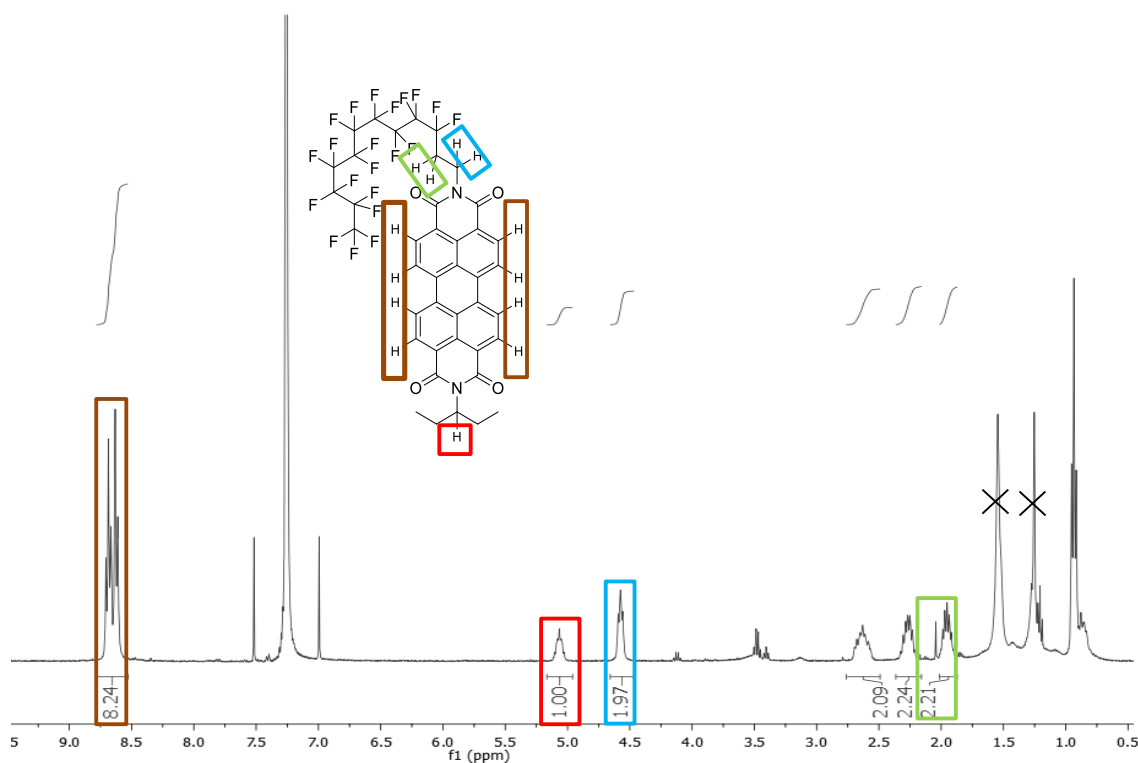
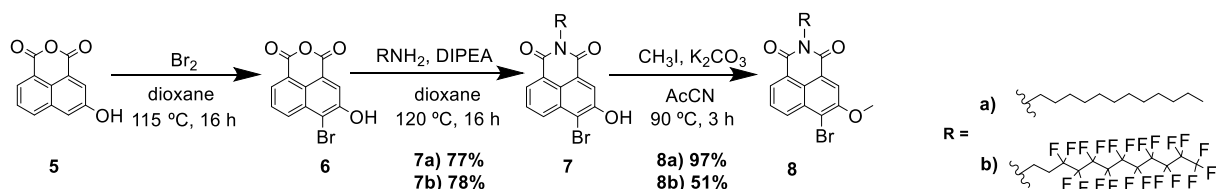


Figure 23. NMR spectra of PDI-F (**4b**) (CDCl_3 , 400 MHz).

3.1.2 Synthesis of the PXXMI derivatives

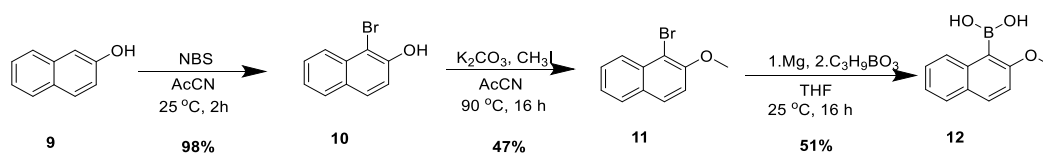
Next, we decided to synthesize the perixanthene xanthene derivative that, as stated before, has photocatalytic properties that we can attempt to study at the liquid-liquid interface. The synthesis of this compound was studied extensively by the Bonifazi group^{55,62}, and starts from the commercially available 3-hydroxy-naphthal anhydride which is firstly brominated in the 4 position of the naphthalene ring by using bromine in dioxane. The brominated product was not purified and the crude of the reaction was directly used in the next step of the synthesis. This step is the formation of the imide derivative by reaction of the anhydride moiety with a primary amine functionalized with the desired chain. The reaction is performed in dioxane at 120 °C and using diisopropylamine as a base. The primary amines used were the same used in the synthesis of the PDI derivatives, and after purification, via removing the dioxane and a silica column in chloroform, we obtained an overall yield on the two steps of 77% for **7a** and 78% for **7b** (respectively the compound functionalized with hydrocarbon chain and

fluorinated chain). Finally, the hydroxy group was methylated by reaction with methyl iodide in acetonitrile and using as base potassium carbonate. The crude was first washed with brine/dichloromethane and then purified on silica column with hexane and ethyl acetate as eluent (ratio 8:2). Compound **8a** and **8b** were obtained in 97% and 51% yield, respectively. These compounds are stable intermediates that are the starting point of the next reaction that is, as we will see, the most demanding in terms of yields.



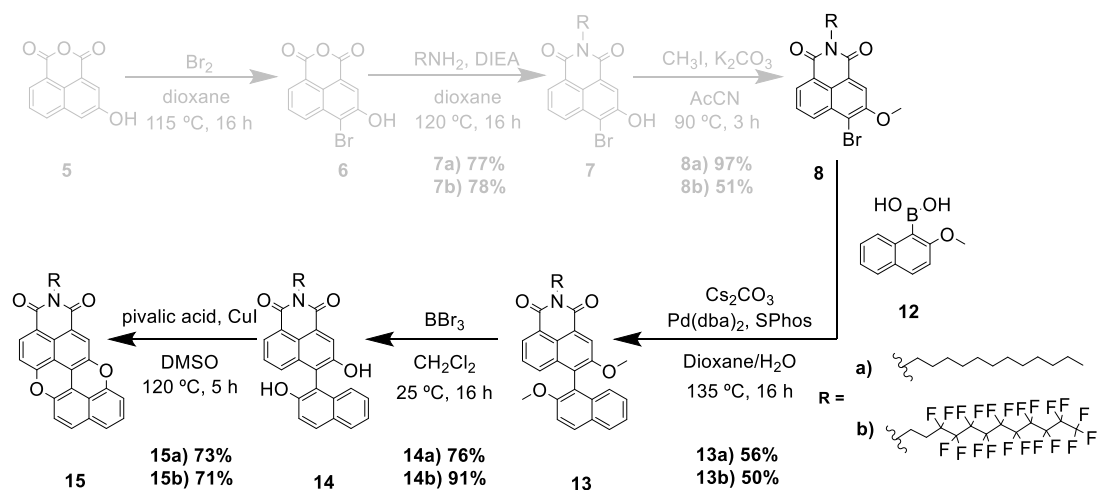
Scheme 5. Formation of precursor bromo-methoxy-naphthalene imide, first part of the synthesis of PXXI derivatives.

To complete the synthetic pathway, we needed to prepare the second precursor which is the 2-methoxy-naphthaleneboronic acid (**12**). This compound will be used in a Suzuki coupling to create the core structure of the perixanthene xanthene product. The synthesis starts from the commercially available 2-hydroxynaphthalene (**9**) which is brominated in the α -position with *N*-bromosuccinimide in acetonitrile. After purification by washing with ethyl ether and water and a silica column in hexane with 5% ethyl acetate the product was obtained in the excellent yield of 98%. Compound **10** was then methylated using methyl iodide in a procedure similar to the one used to prepare compound **8**, the main difference being that the reaction takes more time (16h compared to 3h). This resulted in **11** being prepared with a yield of 47%. The final component for the Suzuki reaction was then prepared by firstly making a Grignard derivative (magnesium in anhydrous THF) which was then reacted with trimethyl borate added drop-wise due to the high exothermal reaction. Compound **12** was finally obtained with a 51% yield. This low yield was expected due to the instability of the product, since it can be easily oxidized forming the de-brominated methoxy-naphthalene side-product as seen in the crude of the reaction as an impurity.



Scheme 6. Formation of precursor 2-methoxy-naphthaleneboronic acid, second part of the synthesis of PXXI

The two compounds prepared (**8** and **12**) were linked together via a Suzuki coupling in dioxane using as catalyst bis(dibenzylideneacetone)palladium(0) ($\text{Pd}(\text{dba})_2$), 2-dicyclohexylphosphino-2',6'-dimethoxybiphenyl (SPhos) as ligand and cesium carbonate as base. The reaction was done in anhydrous conditions and the work-up of the crude was done by filtration on celite followed by purification of the residue on a silica column using hexane with 5% ethyl acetate as eluent. Compounds **13a,b** were obtained with a yield of 56% and 50% (**13a** and **13b**, respectively). This reaction is easily affected by the conditions used and the yield may change depending on the reagents or on the correct degassing of the reaction environment. In any case we did not optimize the reaction conditions. The next step was the de-methylation of the methoxy groups using boron tribromide in dichloromethane leading to the free hydroxy group. A simple extraction with water and ethyl acetate and a silica column with hexane:ethyl acetate (7:3) afforded pure products with 76% yield for **14a** and a surprisingly high yield for the fluorinated derivative **14b** of 91%. Finally, the perixanthene xanthene core was obtained by ring-closing *via* cyclisation with pivalic acid and copper iodide in DMSO at 120 °C. The reaction was stopped after 5 hours by adding acidic water (1M HCl), followed by an extraction with chloroform and a column purification of the crude using dichloromethane as eluent. To remove all impurities, the products were recrystallized from diethyl ether. **PXXMI-H (15a)**, with the perixanthene xanthene functionalized with a dodecylamine, was obtained with a 73% yield, while **PXXMI-F (15b)**, with the perixanthene xanthene functionalized with a 1*H*,1*H*,2*H*,2*H*-perfluorododecyl amine, was obtained with a 71% yield.



Scheme 7. Synthesis of PXXMI-H (**15a**) and PXXMI-F (**15b**), third part of the synthesis of perixanthene xanthene imide derivatives.

With this synthesis we have prepared a perixanthene xanthene functionalized with a fluorinated chain **PXXMI-F** that should go at the interface between the fluorinated solution and the hydrocarbon solution. We also prepared a perixanthene xanthene with a hydrocarbon chain **PXXMI-H** that should work as a control molecule. The structure of the two derivatives is reported in full in Figure 24.

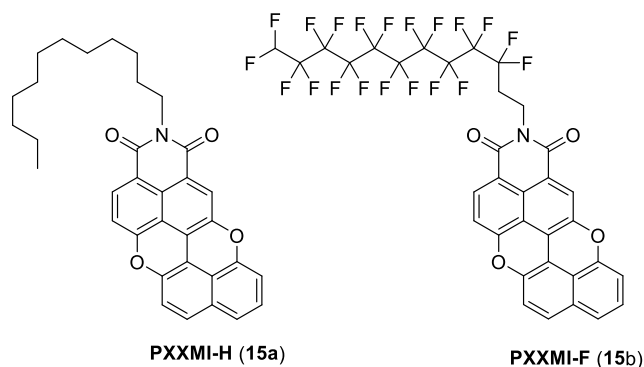


Figure 24. Perixanthene xanthene imides prepared using procedures from Scheme 5 to 7, **PXXMI-H (15a)** is the control compound, functionalized with an alkyl chain, **PXXMI-F (15b)** is the dye functionalized with a fluorinated chain.

PXXMI-H was characterized by ^1H -, ^{13}C -NMR and ESI-MS while in the case of **PXXMI-F** the ^{13}C -NMR was not recorded for the low solubility of the compound and the characterization was limited to ^1H -, and ESI-MS. Figure 25 reports, as an example, the ^1H -NMR and COSY spectra of **PXXMI-H**.

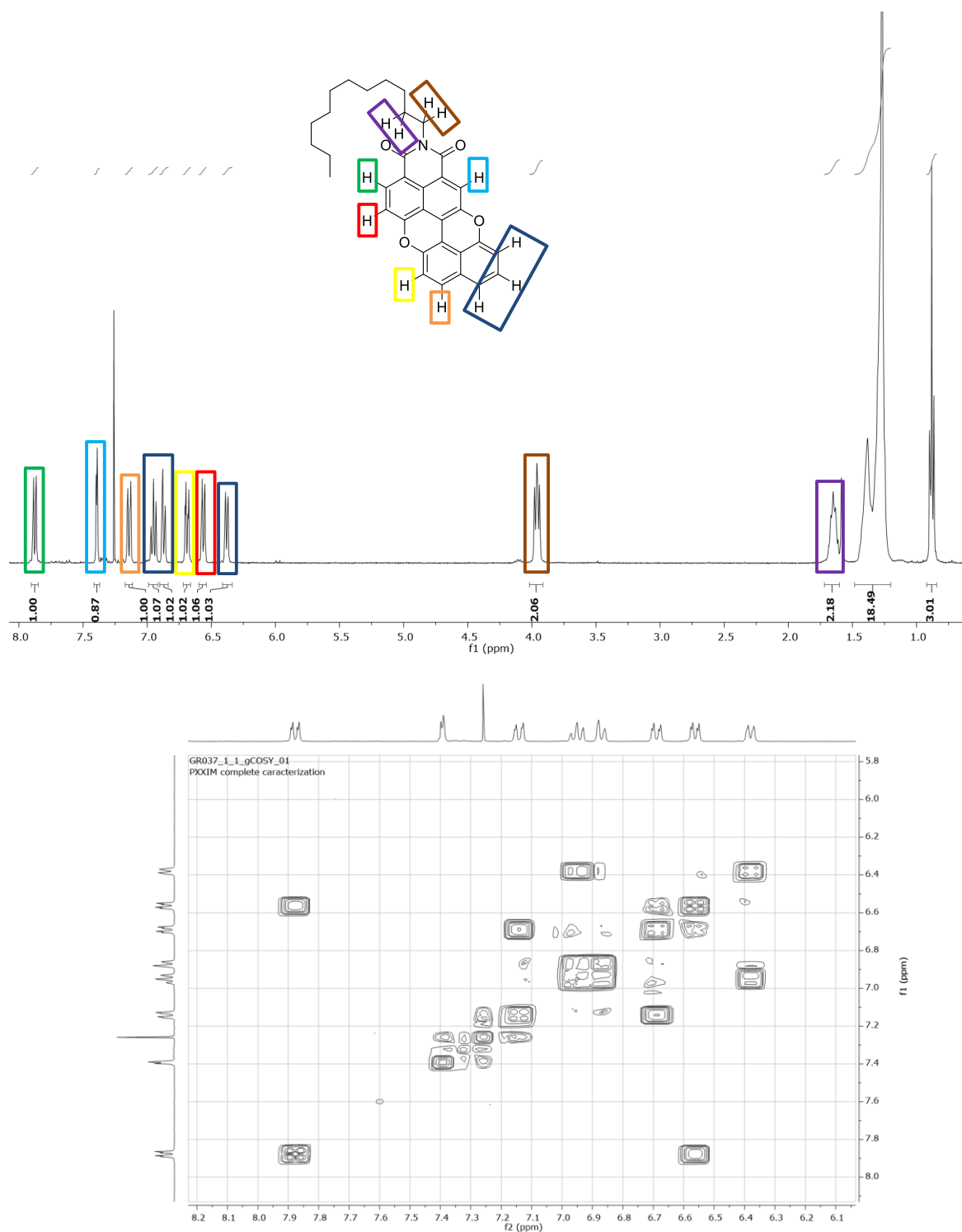


Figure 25. ¹H-NMR spectra of **PXXMI-H (15a)** in CDCl₃ (top) with peak attribution made on the basis of the 2D-COSY experiment (bottom).

In the proton spectrum of **PXXMI-H** the typical pattern of the aromatic signals characteristic of the perixanthene xanthene imide is observed between 8.0 and 6.2 ppm.

The other identifiable signals are the NCH_2 and NCH_2CH_2 of the methylene groups closer to the imide nitrogen at 3.96 and 1.63 ppm, respectively. The other signals with lower ppm are characteristic of a long hydrocarbon chain. The resonances of the aromatic protons were assigned with the aid of 2D-COSY experiment and are indicated in Figure 25.

Using these compounds, we decided to test their solubility in the complex emulsion starting from the non-fluorinated compounds: the perylene with a hydrocarbon chain **PDI-H** and the perixanthene xanthene with a hydrocarbon chain **PXXMI-H**.

3.1.3 Solubility tests in complex emulsion

The complex emulsion is prepared as described in paragraph 3.1 In detail the fluorocarbon and hydrocarbon solvents, in equal amounts, are added to a flask and the two phases solution is heated at 40 °C until it becomes one single phase. Then a 0.1% volume in water solution of Zonyl FS-300 is added and the suspension is mixed and stirred, either by manually shaking of the vial or by magnetically stirring. Formation of the emulsion is signalled by the appearance of an opalescent milky suspension. Finally, the suspension is cooled in ice leading to the formation of a hexane-in-perfluorohexane-in-water (H/F/W) double emulsion in which the droplets have an internal interphase hexane/perfluorohexane.

The solubility tests were initially performed with the non-fluorinated compounds that should be soluble in the hexane phase. In the case of **PDI-H** the emulsion was initially prepared using 2 mL of hexane, 2mL of fluorohexane and 4 mL of water with Zonyl. **PDI-H** (10 mg) was added to the hexane phase before mixing with the other emulsion components but it resulted to be very little soluble. Indeed, as can be seen from Figure 26, the hexane phase turn orange due to the solubilisation of some **PDI-H** but most of the compound forms crystals in suspension or attached to the walls of the vial. Preparation of the emulsion did not increase the solubility and crystals of **PDI-H** are clearly visible also in the emulsified phase (Figure 26, picture on the right). To increase the solubility a test was also performed using 5 ml of hexane, 5 ml of fluorohexane and 2 ml of toluene in 6 ml of water and zonyl. The amount of **PDI-H** used was the same (10

mg) which decreased the overall concentration of the compound to about one third. The toluene was added in the attempt to decrease the intermolecular π - π interactions in **PDI-H** which are responsible for the stacking and aggregation of the compound and, eventually, to its very low solubility in hexane (and in general in many solvents). However, the addition of toluene did not have any substantial effect and the solubility of the compounds remains very low with very little **PDH-I** dissolved and with a lot of precipitate in suspension or attached to the vial walls.

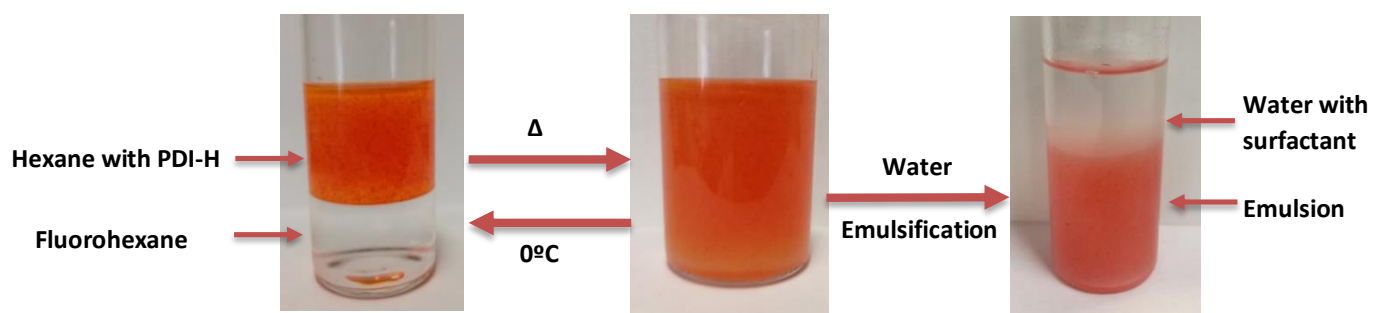


Figure 26. Emulsion test using non-fluorinated **PDI**.

Next the solubility of the fluorinated perylene **PDI-F** was tested using the same conditions as used for the first test of **PDI-H** (2 ml of hexane, 2 ml of fluoro-hexane, 4 ml of water with Zonyl) but with only 1 mg of **PDI-F**. The results show that the compound does not stay in any of the phases, but instead goes to the interface between the solvents or to the walls of the flask as undissolved crystals. Indeed, as can be seen in Figure 27, none of the two solvents became coloured. Formation of the emulsion did not improve the situation and the suspension remains uncoloured with clearly visible crystals of undissolved **PDI-F**. Unfortunately, and as expected due to fluorinated derivatives having generally a lower solubility than their hydrocarbon counterparts, the compound is again not soluble in the complex emulsion of hexane and fluoro-hexane.

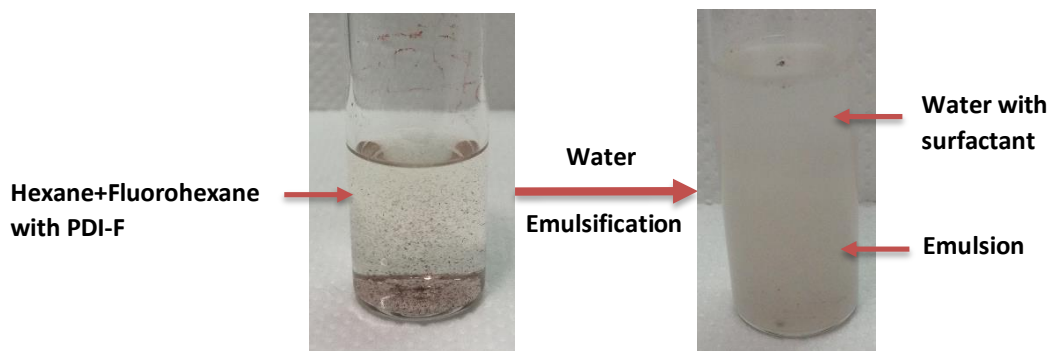


Figure 27. Emulsion test using fluorinated **PDI**.

Similar results were obtained in the tests with the derivatives of the perixanthene xanthene. In the case of **PXXMI-H** the experiment was made in the same condition of the **PDI-H** (2 ml of each organic solvent, 4 ml of water and Zonyl and 10 mg of compound) and again we found that the compound stays mostly undissolved in the hydrocarbon phase of the solution in the flask (Figure 28).

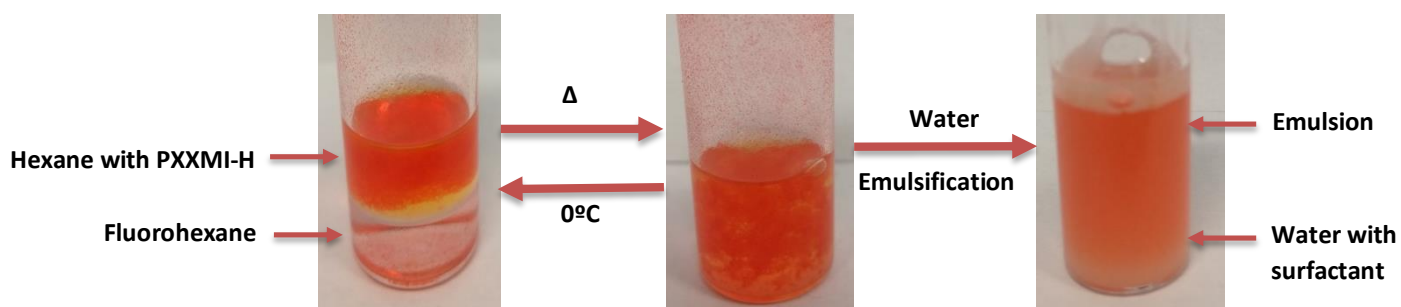


Figure 28. Emulsion test using non-fluorinated **PXXMI**.

When we tested the solubility of the perixanthene xanthene functionalized with the fluorinated chain **PXXMI-F** and using the same procedure and concentration used for **PXXMI-H** we observed a similar result to the fluorinated perylene **PDI-F** with the compound staying mostly at the interface and on the walls of the flask, and completely undissolved.

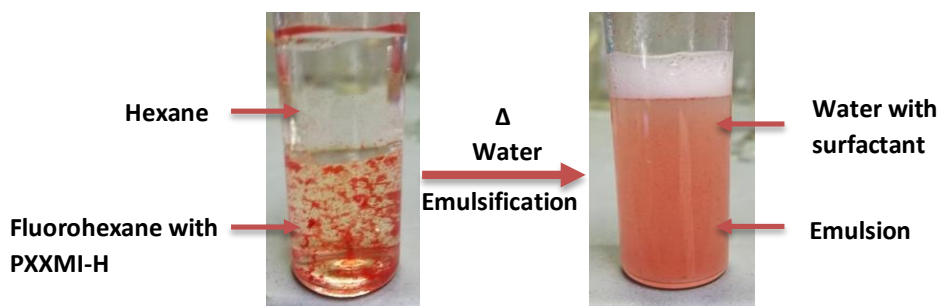


Figure 29. Emulsion test using fluorinated **PXXMI**.

3.1.4 Modification of PXXMI structure to improve its solubility

Due to the insolubility of the perixanthene xanthene derivatives we decided to modify the structure of this compound to improve its solubility. The lack of solubility of PXXMI, has been attributed to the aggregation of the PXX core due to the planarity of the structure which favours π - π stacking. In order to avoid this phenomenon two possible modifications of the PXX core can be envisaged (Figure 30): a) the use of a branched amine instead of a linear one as imide substituent, and b) the insertion in the aromatic portion of substituents that break the planarity of the molecule such as *o,o*-dimethylphenyl group which, due to the steric encumbrance of the methyl substituents, cannot adopt a coplanar conformation with the PXX core. As a first attempt we started to prepare a branched alkyl amine planning to prepare the fluorinated analogue if the solubility tests give positive results. We also decided to increase the overall length of the alkyl chains hoping to improve the solubility in hexane.

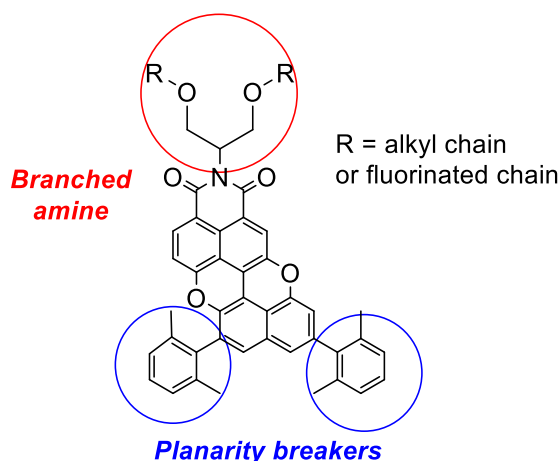
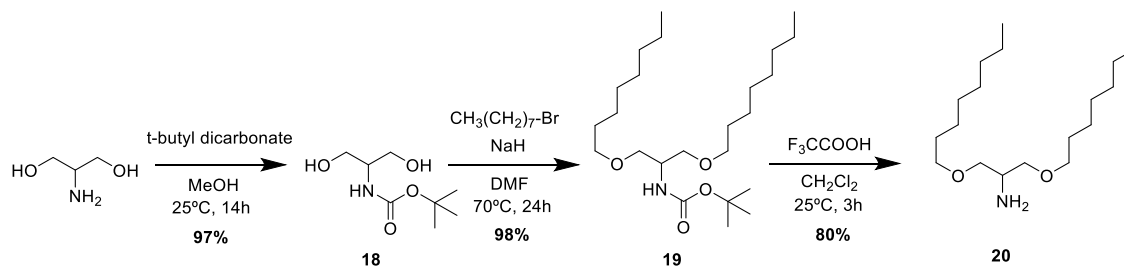


Figure 30. Possible modifications of the PXX core to improve its solubility.

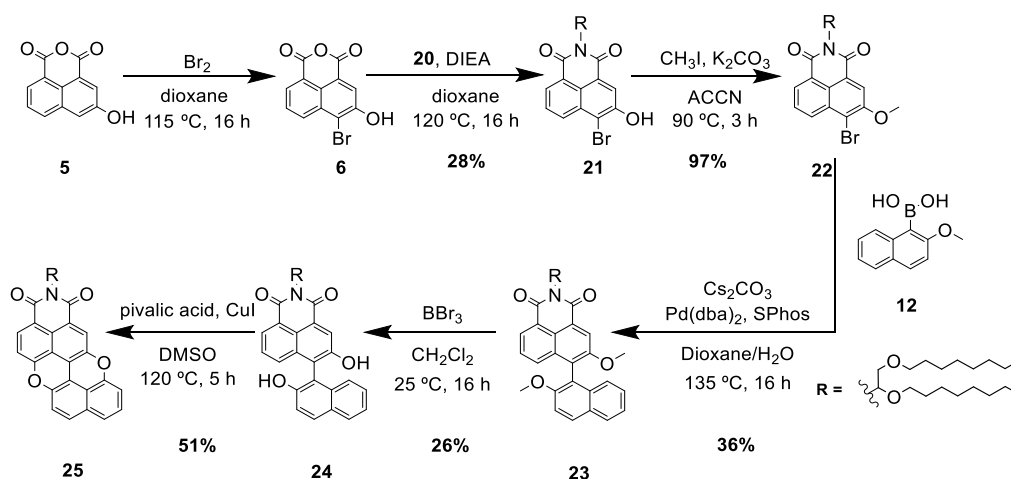
The synthetic pathway to prepare this modified **PXXMI-2H** is similar to the synthesis of the **PXXMI** used before (Scheme 7), but because branched amines of the desired length are not commercially available, we needed to prepare it from scratch (Scheme 8). The synthesis of the amine begins with the commercially available 2-amino-1,3-propanediol, which is BOC-protected on the amine moiety using *tert*-butyl-dicarbonate in methanol with a 97% yield. The two hydroxyl groups were then alkylated with bromooctane in DMF using NaH as base. The yield of this reaction is dependent on the halogenated species used, but since bromooctane is very reactive we obtained an excellent 98% yield.

Compound **19** was finally deprotected with TFA in DCM to give the desired branched primary amine **20**, with a 80% yield.



Scheme 8. Synthesis of alkyl branched amine needed for the preparation of **PXXMI-2H**.

The amine **20** was used in the preparation of **PXXMI-2H** using the same synthetic scheme used before (Scheme 9). However, using the branched amine **20** instead of the linear dodecylamine resulted in a lowering of the yield of almost all the synthetic steps. Intermediates **21**, **23** and **24** and product **25** were obtained with a yield of 28%, 36%, 26% and 51%, respectively, that compares with the yields of 77%, 56%, 76% and 73% obtained for the corresponding compounds with the linear amine. The reason for this general lowering of the reaction yields was not investigated and the reactions were not optimized because the final scope was to obtain some compound for the solubility tests.



Scheme 9. Synthesis of modified **PXXMI-2H** with a branched alkyl chain.

The solubility in the emulsion of the PXXMI modified with the branched alkyl chain was tested using the same procedure describe before, with 1mg of **PXXMI-H2**, 2 ml of hexane and 2 ml of fluorohexane. As expected the compound remains in the hexane phase that became slightly coloured however the solubility was still too low for any for any photophysical tests to be performed.

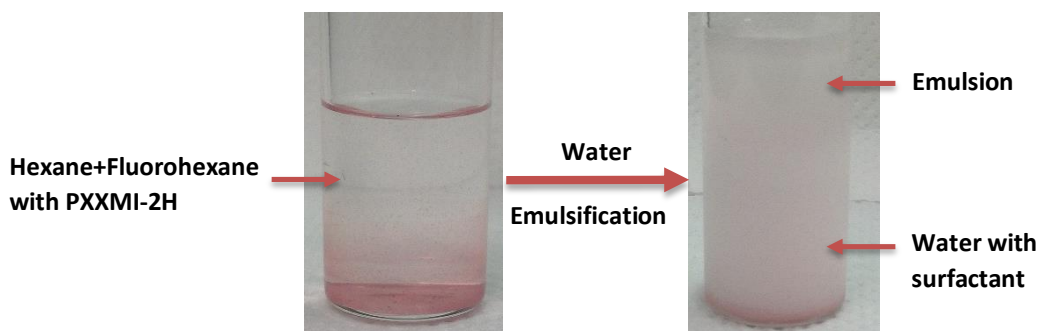
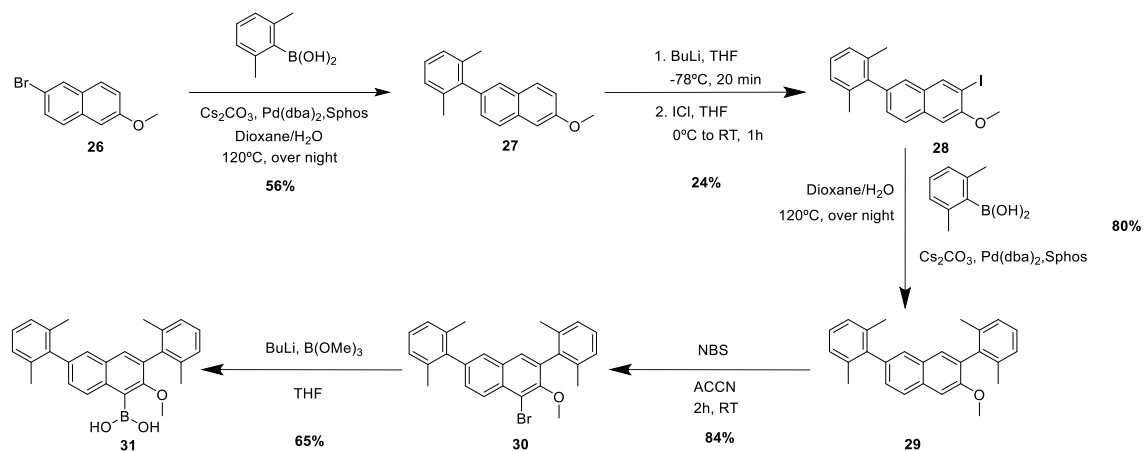


Figure 31. Emulsion test using branched chain PXXMI-2H.

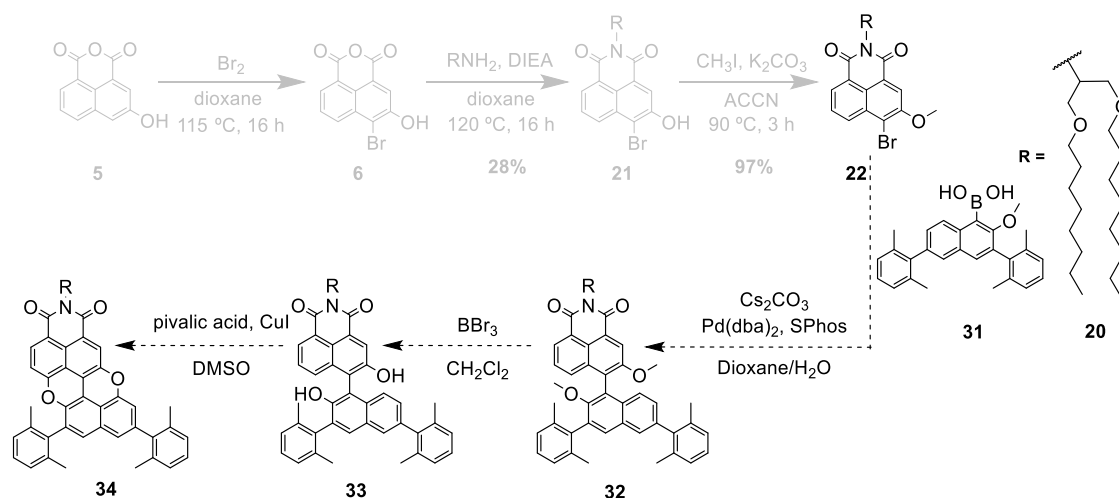
These results show that the modification at the level of the imide substituent is not enough to ensure solubility to the PXXMI derivative. We therefore decided to modify also the PXX core by adding two *o,o*-dimethylphenyl substituents to the aromatic portion. These groups, due to the presence of the ortho-methyl substituents, cannot adopt a coplanar conformation with the PXX core making the π - π stacking process less favourable.

We planned to use the same intermediate compound with the branched amine (**22**) for the top of the PXX structure, while, for the bottom part of the PXX core, we followed the synthetic pathway shown in Scheme 10. The synthesis starts from the Suzuki coupling between 2-bromo-6-methoxynaphthalene (**26**) and 2,6-dimethylphenylboronic acid to give intermediate **27**. This compound was treated with BuLi followed by a chloriodide solution in THF to give the iodide substituted derivative **28**. A second Suzuki coupling between **28** and 2,6-dimethylphenylboronic gives the naphthalene **29** bearing the two *o,o*-dimethylphenyl groups. This compound was brominated with *N*-bromosuccinimide

and transformed in the boric acid derivative **31** ready for the Suzuki coupling with compound **22** (Scheme 11).



Scheme 10. Synthesis of boronic acid reagent **31** functionalized with two *o,o*-dimethylphenyl groups.



Scheme 11. Synthetic scheme for the preparation of the modified PXXMI with a branched alkyl chain and two *o,o*-dimethylphenyl groups.

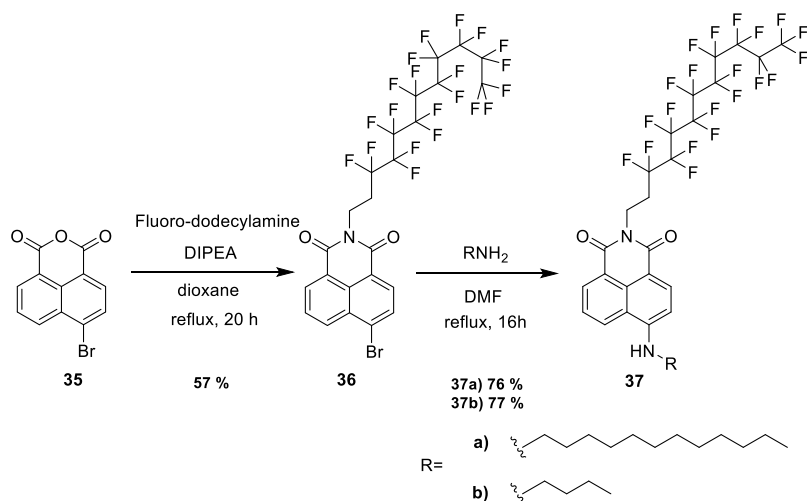
Unfortunately, the Suzuki coupling between **22** and **31** failed and **32** was obtained in very low yields (from 1 to 5%). Despite different attempts we were not able to improve the yield of this reaction and this is probably the consequence of the low reactivity of **22** (see above). At this point, due to the difficulty experienced with the synthesis which is really time consuming and also due to the fact that we were not sure that the final

product would have been really soluble in the complex emulsion, we decide to change target and we chose 4-amino-naphthalimides as fluorescent core of our molecules.

3.2 Naphthalimides

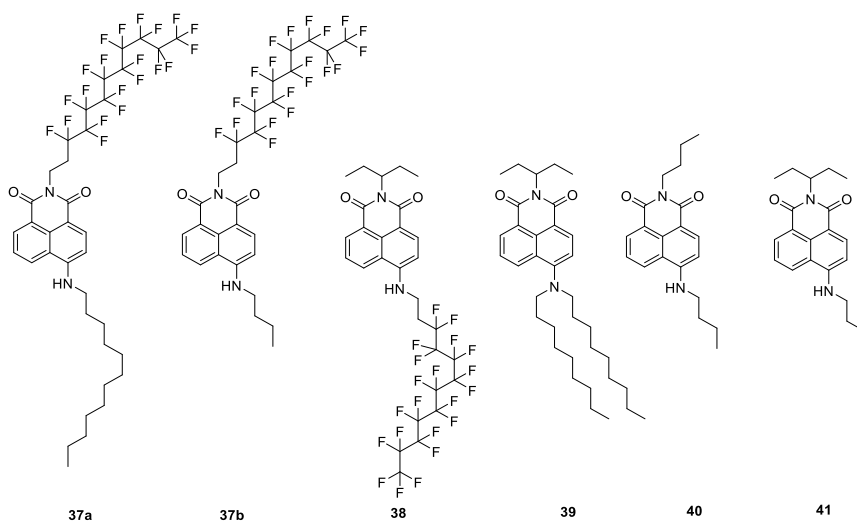
As explained in the introduction the Naphthalimides that we are using have two reactive sites that can be functionalized to adjust them to any experiment intended. The first site is the imide group that can be modified using different primary amines and the second is the group in the 4-position, which can be a secondary or a primary amine bearing different substituents. The presence of the amine moiety in the 4-position is essential to ensure high fluorescent emission to the dye. The synthesis of these compounds is also much more time and cost effective than the synthesis of the Perixanthene xanthene derivatives allowing us to easily screen several different compounds to optimize their solubility and reactivity.

The synthesis of functionalized 4-aminonaphthalimides starts from the commercially available 4-bromo-1,8-naphthalic anhydride which is transformed in the corresponding imide by reaction with a primary amine. The reaction is performed in refluxing dioxane in the presence of DIPEA. The yield of the reaction depends on the primary amine used and in the case of the 1H,1H,2H,2H-perfluorododecyl amine shown in Scheme 12 was 57%. The substituents in 4-position is then introduced by a nucleophilic aromatic substitution of the 4-bromo substituent with a primary or a secondary amine. This reaction is performed at high temperature in polar solvents like ethanol, butanol, diethylene glycol, or in the case below dimethylformamide. In the example shown in Scheme 12 the bromo derivative **36** was reacted with *n*-dodecylamine or with *n*-butylamine yielding the desired products **37a,b** with a 76% and 77% yield, respectively.



Scheme 12. Standard synthesis of 4-aminonaphthalimides.

Using this synthesis, we prepared a small library of naphthalimides with fluorinated or hydrocarbon chains and linear or branched chains. This will allow for a comprehensive study on the solubility of naphthalimides and on their photophysical properties.



Scheme 13. List of Naphthalimides prepared using procedure from Scheme 12, to be used with the hexane-fluorohexane complex emulsion.

Naphthalimides **37a** and **37b** share the same perfluorinated chain but differ for the length of the alkyl chains, and have been prepared to test their solubility in the hexane-fluorohexane complex emulsion also evaluating the effect of the different

fluorinated/non-fluorinated balance. Compound **38** was prepared to investigate the effect on the solubility when the alkyl chain and the fluorinated chain have their position inverted. It also demonstrates that the synthetic procedure is flexible enough to allow different design of the final compounds. Naphthalimide **39** was prepared as a test for the synthesis of a branched fluorinated derivative. However, the yield of this compound proved to be very low and the synthesis of the branched fluorinated naphthalimide proved to be unfeasible. Compounds **40** and **41** were prepared to serve as the simplest naphthalimide derivative to be used in model reactions as photocatalysts (**40** is a linear naphthalimide and **41** has a branched chain).

The analysis of the ^1H -, ^{13}C -NMR and ESI-MS of naphthalimides derivatives showed the characteristic signals of the naphthalimide core and of the appended chains. As an example Figure 32 reports the ^1H -NMR spectra of compound **37a**.

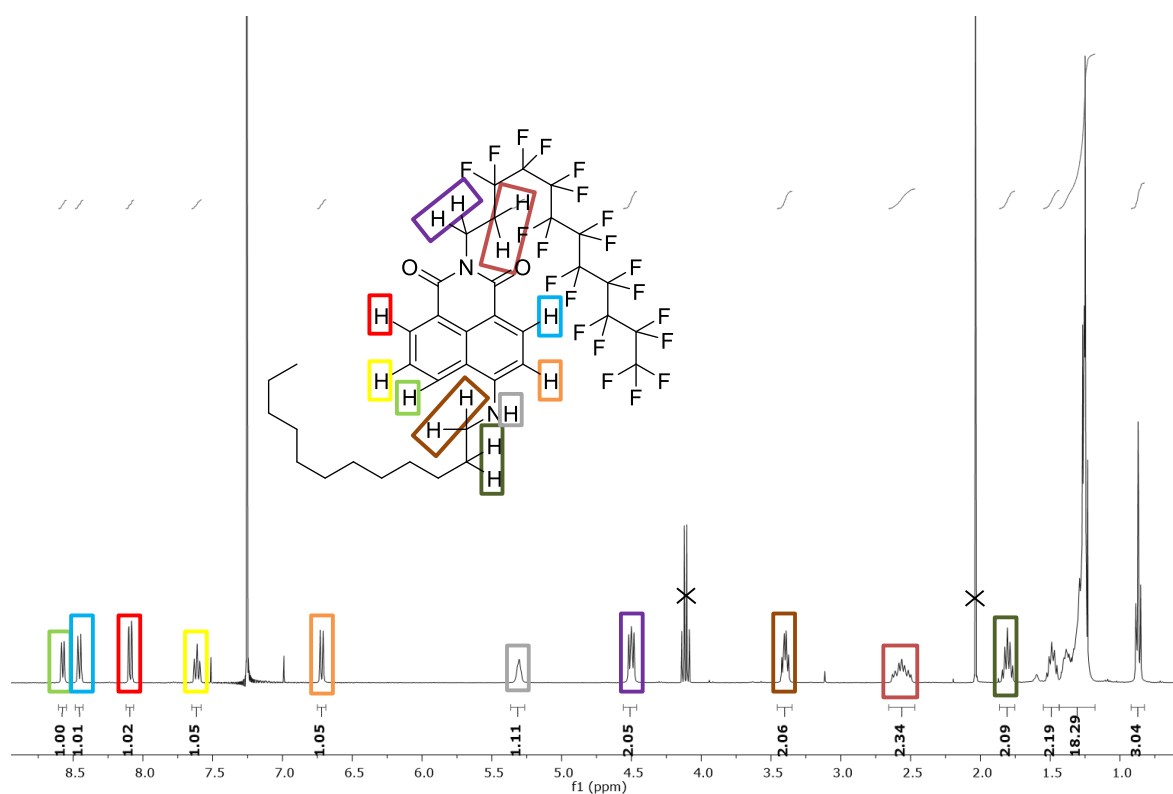


Figure 32. ^1H -NMR spectra in CDCl_3 and peak attribution of Naphthalimide **37a**.

By analysing this proton NMR spectra we can easily identify the aromatic proton signals of the compound between 6.5 and 8.7 ppm. On the basis of their multiplicity and ppm values this signals can be reasonably assigned to the different aromatic protons as indicated in Figure 32. At about 5.3 ppm a broad singlet can be identified as the proton of the amine group. The other proton signals identifiable are the protons of the two CH₂ that are connected to the NH group, and the protons of the two CH₂ that are next to the imide group. These have a higher multiplicity due to being part of a fluorinated chain and therefore showing the coupling with the fluorine atoms. Finally, at low ppm values the characteristic signals of the linear hydrocarbon chain appended in position 4 are found.

The solubility tests of compound **37a** and compound **37b** in hexane and perfluorohexane are shown in Figure 33 and 34. Regrettably, the two naphthalimides are very little soluble in the hexane solution and they are practically not soluble in the fluorohexane solution with very little difference between the two compounds. Unfortunately, when tested in the emulsion, the solubility of **37a** and **37b** proved to be too low for any photophysical tests to be performed, as shown in Figure 35. We therefore decided to move to surfactant aggregates as a different model of a static liquid-liquid interface.

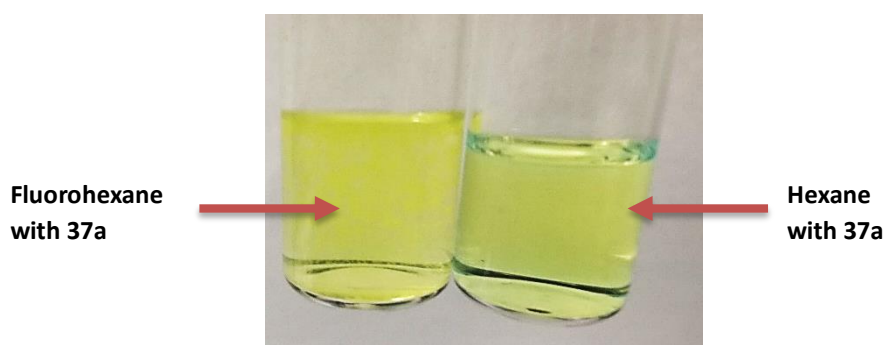


Figure 33. Solubility test of naphthalimide **37a** in fluoro-hexane and hexane.

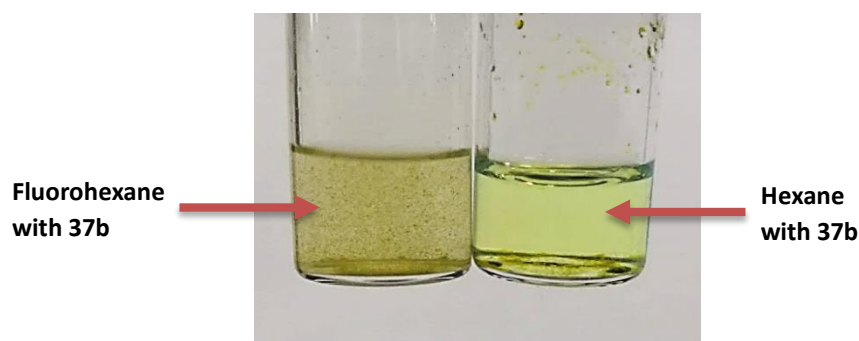


Figure 34. Solubility test of naphthalimide **37b** in fluorohexane and hexane.

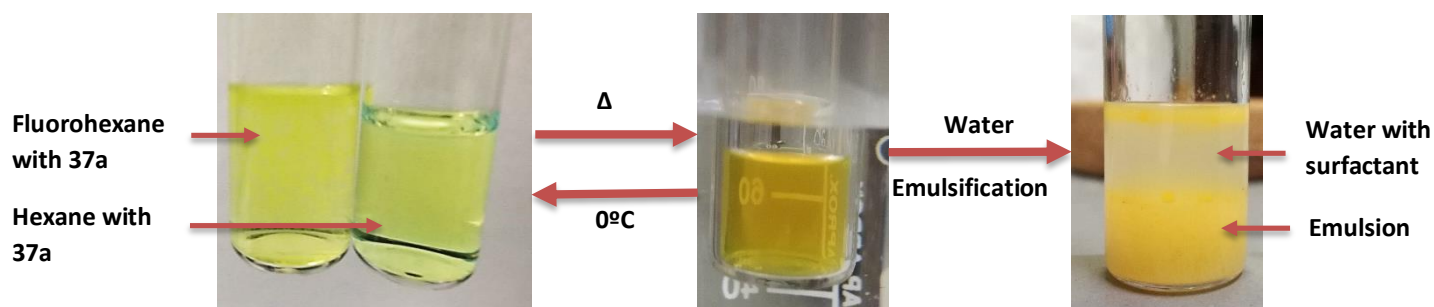


Figure 35. Emulsion test using naphthalimide **37a**.

3.2.1 Photophysical properties of Naphthalimides

Before to investigate the possibility to use naphthalimides as photocatalysts we performed some photophysical characterization aimed to determine if the excited state of the fluorophore is quenched by some sacrificial electron donor. This quenching experiments are useful to verify if the dye can perform an efficient electron transfer between its excited state and an electron donor and thus potentially perform a photocatalytic reaction. Moreover, in the perspective to move in water solution we also wanted to verify the effect of the solvent polarity on this process.

Figure 36 reports the normalized UV-Vis and Emission spectra of the compound **37a** in DCM. The naphthalimide has strong absorption bands at 258, 282 nm and when excited at 431 nm shows an intense emission band centered at 500 nm.

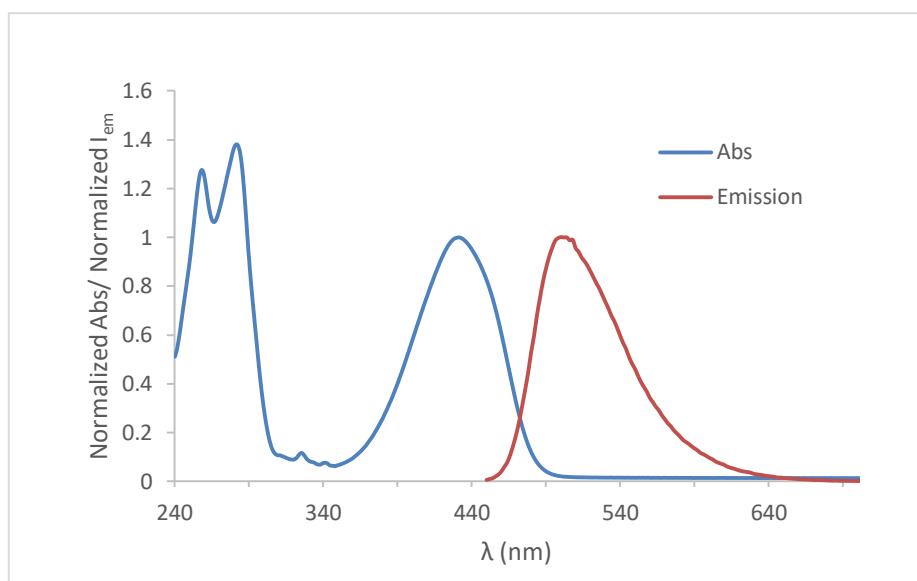


Figure 36. Normalized absorption and emission ($\lambda_{\text{ex}} = 431 \text{ nm}$) spectra of **37a** in DCM.

Among the most common sacrificial agents used for quenching experiments, triethylamine (TEA) was chosen as an efficient electron-donor. Figure 37 shows the UV-Vis and fluorescence spectra of compound **37a** recorded at increasing concentration of TEA. The effect of TEA on the UV-Vis spectra of **37a** is negligible and only a small decrease of absorbance is observed due to dilution, ruling out a ground state interaction between the dye and the amine. On the other hand, a clear decrease of the fluorescence intensity of **37a** is observed upon addition of TEA (Figure 37, bottom). This dynamic quenching effect is indicative of an electron transfer from the electron rich amine to the excited state of the dye leading to its deactivation. As expected, similar results were obtained with compound **37b** indicating that the length of the alkyl chain does not influence the photophysical properties of the naphthalimides.

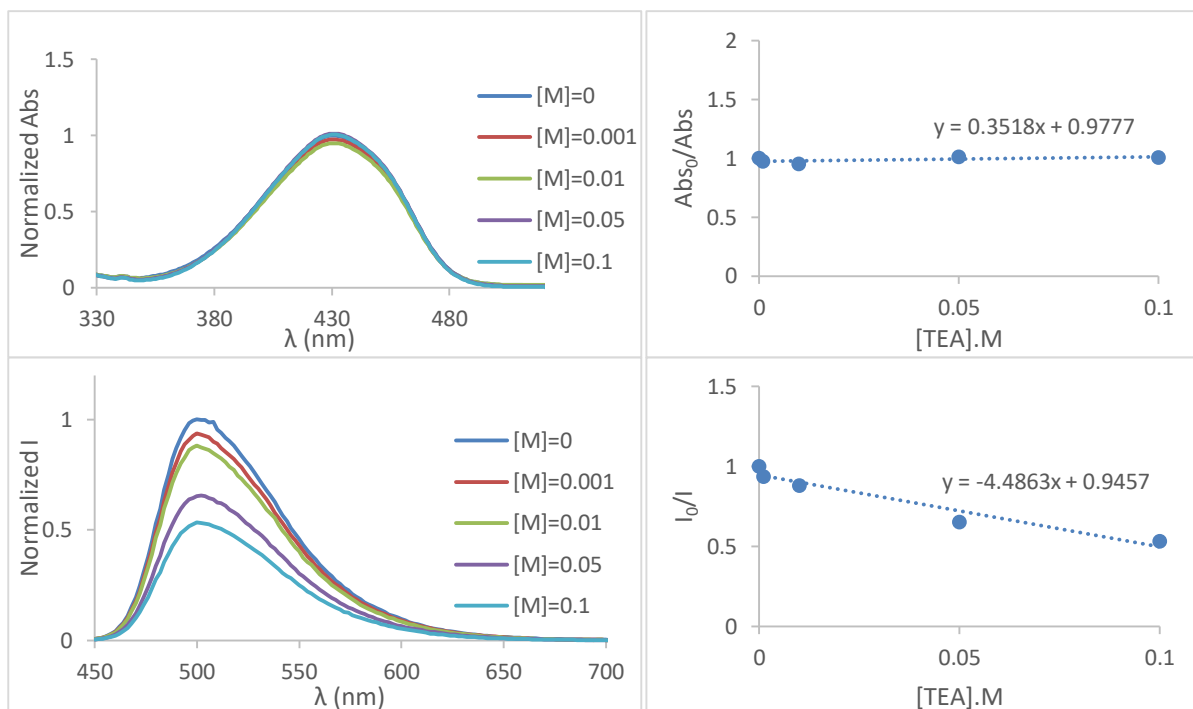


Figure 37. UV-Vis spectra (top-left) and emission spectra ($\lambda_{\text{ex}} = 431$, bottom-left) in DCM of **37a**, absorption at 430 nm (top-right) and emission at 500 nm (bottom-right) recorded at increasing concentration of TEA.

The next step was to study the effect of the solvent polarity on the photophysical properties of the naphthalimides. Figure 38 show the UV-Vis and fluorescence spectra of compound **37a** in DCM, acetonitrile (MeCN), isopropanol, and methanol (MeOH). In the UV-Vis spectra the effect of the polarity of the solvent is small with a little bathochromic effect observed in the alcoholic solvents. On the other hand, the effect on the fluorescence spectra is more relevant with a shift of the emission maxima toward longer wavelengths on increasing polarity of the solvent. This effect was expected and it is related to the ICT nature of the excited state of naphthalimides. The ICT state is more polar than the ground state and it is stabilized by polar solvents leading to a decrease in energy difference between the two state and to a less energetic transition.

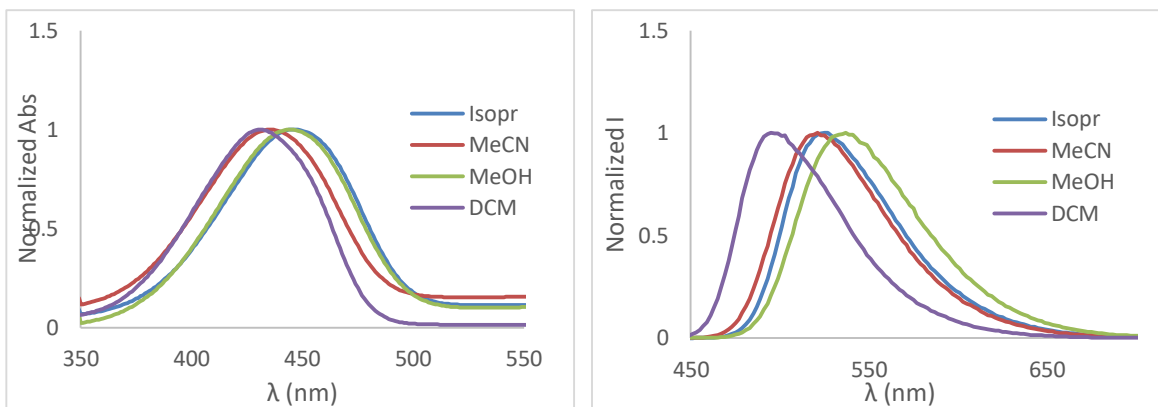


Figure 38. UV-Vis spectra (left) and emission spectra (right) of **37a** in different solvents.

The quenching experiments with TEA were repeated with **37a** in acetonitrile and isopropanol and also in this case a decrease of the fluorescence emission of the dye on increasing the concentration of TEA was observed without effects on the UV-Vis spectra. The data were fitted with the Stern-Volmer equation where I and $I_{[Q]}$ are the fluorescence intensity in the absence and in the presence of the quencher (TEA), respectively, $[Q]$ is the concentration of the quencher and K_{SV} is the Stern-Volmer constant which is the bimolecular quenching constant. The results of the fitting are shown in Figure 39.

$$\frac{I_0}{I_{[Q]}} = 1 + K_{SV} \cdot [Q]$$

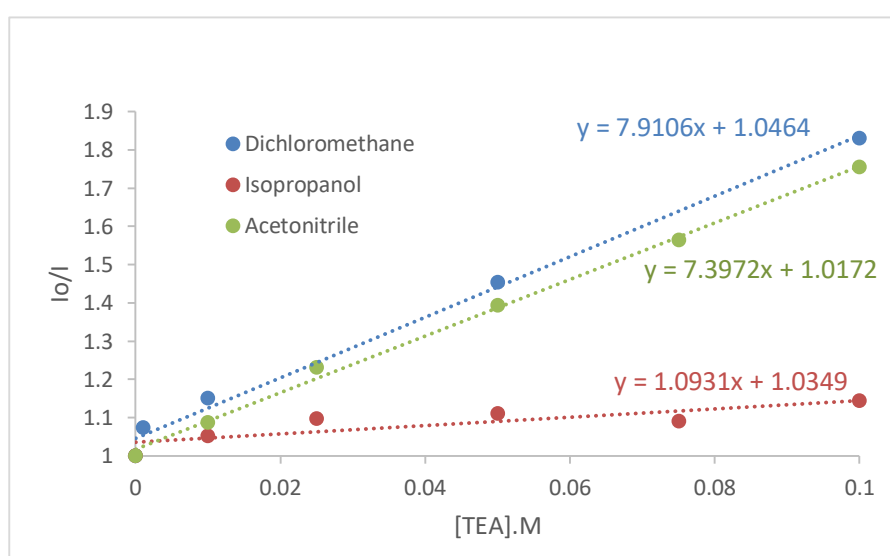


Figure 39. Stern-Volmer fittings of the quenching experiments of **37a** with TEA as the quencher in different solvents.

The results of Figure 34 show that the K_{sv} is similar in DCM and acetonitrile but it is lower in isopropanol. Therefore, the ET process from TEA to the dye becomes less efficient in alcoholic solvents respect to DCM and MeCN and this may represent a problem for the study of the photocatalytic properties of naphthalimides in micellar solution which are prepared in water.

3.2.2 Naphthalimides as Photocatalysts

Before to start the experiments in micellar solution we investigated the ability of the naphthalimides to act as photocatalyst in standard bulk condition using an organic solvent to have a homogeneous solution. These experiments were performed at the Dr. Reddy's laboratories. As a model reaction we choose the photoredox nickel-catalyzed decarboxylative arylation described by MacMillan et al.⁹⁸ This reaction uses two inorganic catalysts $NiCl_2$ and an Ir(III) complex. This latter acts as the photocatalyst. We replaced the Ir(III) complex with the Naphthalimide **40**, which is a simple and easily synthesized naphthalimide derivative that can serve as a model for other naphthalimides. The reaction is performed in DMF starting from 0.6 mmol of the *N*-Bocproline and 0.2 mmol of 4-bromoacetophenone, 0.004 mmol of **40**, 0.02 mmol of $NiCl_2$ glyme, 0.03 mmol of ditert-butylbipyridine (dtbbpy) as ligand for Ni(II), and Cs_2CO_3 as a base (0.6 mmol). The reaction mixture is degassed to avoid oxygen and irradiated with a blue LED light for 24 h at 25°C.

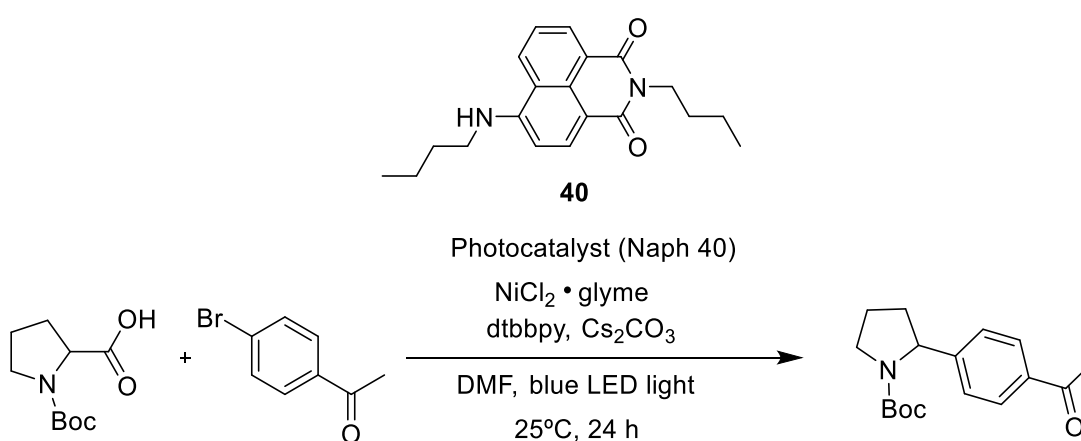


Figure 40. Model reaction tested using Naphthalimides as photocatalysts.

After irradiation the solvent is evaporated and the reaction crude is analysed with ^1H -NMR adding a known amount (0.2 mmol) of trimethoxybenzene as internal standard. Figure 41 shows the NMR spectra of the crude where is possible to identify at 7.9 ppm and 7.25 the two doublets of the aromatic protons of the product and at 4.8 and 4.95 ppm two broad singlets which correspond to the resonance of the $\text{C}_\alpha\text{-H}$ proton in two rotamers of the product. Integration of these signals against the $-\text{OCH}_3$ and aromatic signals of the internal standard allowed to calculate the amount of product present and the yield of the reaction. In this case the reaction resulted in a 35% yield of our desired product.

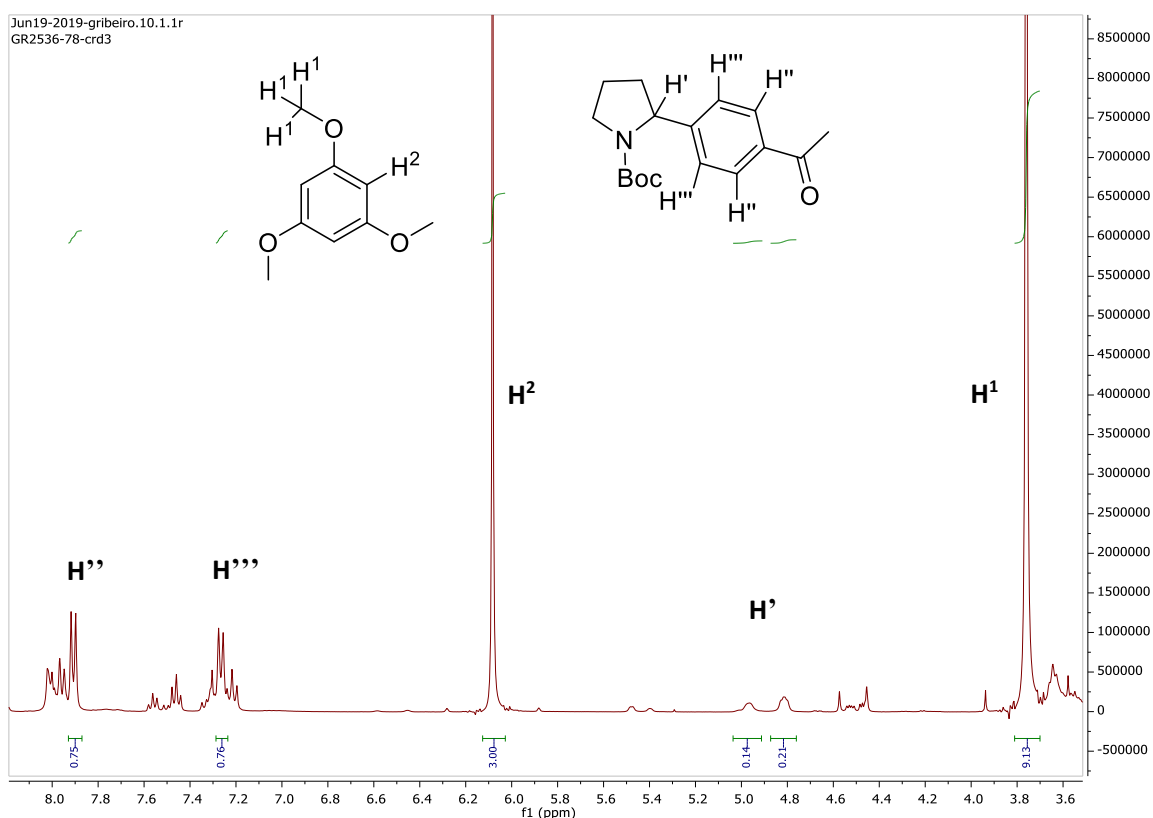


Figure 41. NMR spectra of the crude of the reaction using trimethoxybenzene as an internal standard.

After this initial promising result, we tried to optimize the reaction by changing the ligand of the NiCl_2 complex. We tested the ligands 4,4'-di-tert-butyl-2,2'-dipyridyl, 2,2'-dipyridyl, 1,10-phenanthroline, (s)-4-tert-butyl-2-(2-pyridyl)oxazoline, 2,2-bis((4s)-(-)-4-isopropyl oxazoline)propane and 4,7-Dimethoxy-1,10-phenanthroline. The yields of the reactions performed using the different ligands are presented in the Table below.

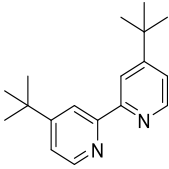
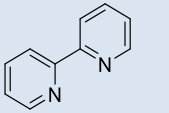
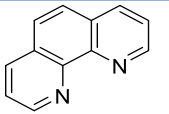
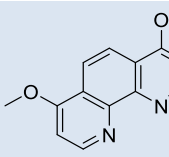
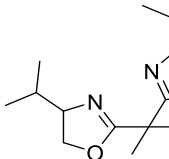
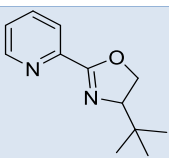
Ligand	Structure	Yield
4,4'-di-tert-butyl-2,2'-dipyridyl		35%
2,2'-dipyridyl		25%
1,10-phenanthroline		20%
4,7-Dimethoxy-1,10-phenanthroline		10%
2,2-bis((4S)-(-)-4-isopropyl oxazoline)propane		0%
(S)-4-tert-butyl-2-(2-pyridyl) oxazoline		0%

Table 1. Results of the reaction optimization by changing the ligand of the NiCl₂ complex

Clearly the best ligand for this reaction is dtbbpy and with all the other ligands the yields are lower or, in some cases, the reaction does not occur. With these results we decided to continue using di-tert-butyl-dipyridyl as ligand and tested if different length of the chains and the presence of fluorinated chains on the naphthalimide core could affect the reaction yield. By using compound **37a** and **41** as photocatalyst in the reaction of Figure 40, we obtained a 15% yield of the product in both cases. The yield is lower with respect to the reaction performed with **40** but still demonstrate that also these compounds can be used as photocatalysts.

We also tested a different substrate instead of the Boc-L-Pro to verify the scope of the reaction with other carboxylic reagents. The compound tested is shown in Figure 42 and it was already prepared in Dr. Reddy's labs. Unfortunately, the reaction only resulted in a very low yield of 5%.

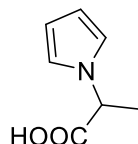


Figure 42. Alternative reagent used for reaction of Figure 40.

These experiments proved that the Naphthalimides can successfully be used as photocatalysts in the photoredox nickel-catalyzed decarboxylative arylation reaction.

3.2.3 Naphthalimides in Micellar Aggregates

After all the tests using the complex emulsion of hexane and fluorohexane, it became clear that no positive results would be achievable using this model interface. Therefore, we decided to switch to a different liquid-liquid interface: the water-micellar interface.

To maximize the interaction between the naphthalimide derivatives and the micellar aggregates we decided to prepare amphiphatic compounds decorating the naphthalimide core with a long alkyl chain and either a positively or a negatively charged group. By using the same synthetic procedure described above for the synthesis of naphthalimide derivatives we were able to prepare three amphiphatic compounds (Figure 43).

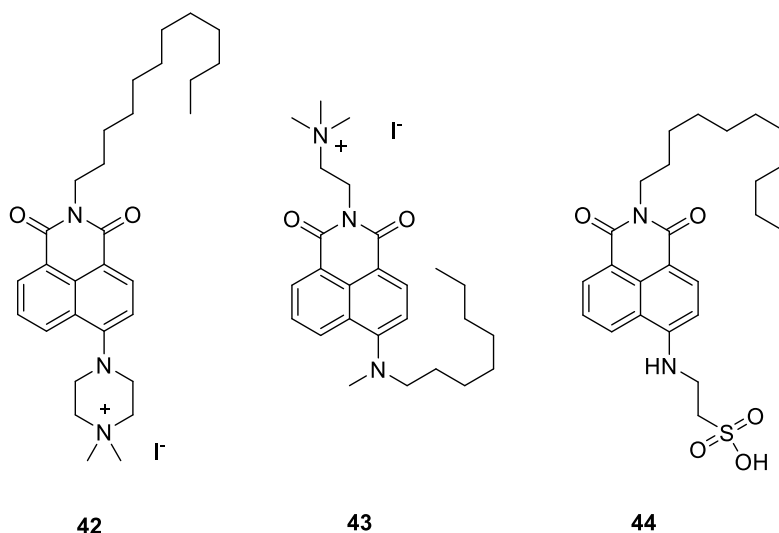


Figure 43. Structures of the amphiphilic Naphthalimides prepared using the synthetic procedure from Scheme 12.

As a first characterization of the system we investigated the solubility of the naphthalimides and of the other reagents used in the photocatalytic reaction in micellar aggregates. To do this we used four different surfactants that can be used to form micelles, in order to find the ideal one to use in the reactions. These surfactants have different characteristics: CTABr is positively charged, SDS is negatively charged while Brij-35 and TRITON X-100 are neutral. The micelles were formed by simply adding the surfactant to water, stirring and heating slightly to completely dissolve the surfactant, using amounts of surfactant always above the CMC (Critical Micellar Concentration), which is specific for each surfactant. The CMC is indeed a property of each surfactant, that determines at which concentration in water the surfactant starts forming stable micelles in solution. The CMC values are indicated for each surfactant in Figure 44.

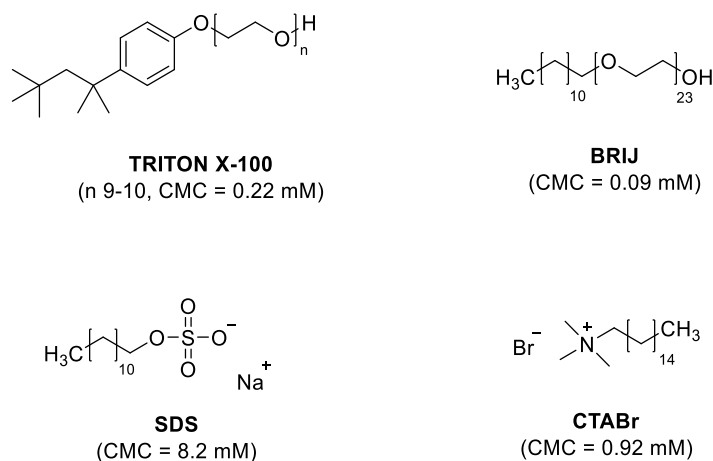


Figure 44. Structure of the surfactants used for micelles preparation.

The solubility tests were made using the positively charged naphthalimide **42** and concentration of surfactant 10 times or 50 times their CMC. The micellar solutions were prepared in water and then the reagents that are insoluble in water, the Nickel complex, the ligand ditert-butylbipyridine (dtbbpy) and the bromo-Acetophenone, were added. The suspensions were then mixed and gently heated to favour the solubilisation of the components. By simply observing the vials shown in Figure 45 we can clearly see that these compounds are soluble in SDS micelles at 10 times the CMC and in CTABr micelles at 50 times the CMC. However, for Triton and Brij the solubility is too low even using 50 times the CMC. Further tests using this method showed that the solubility becomes acceptable at 300 times the CMC for Brij and 500 times for Triton.

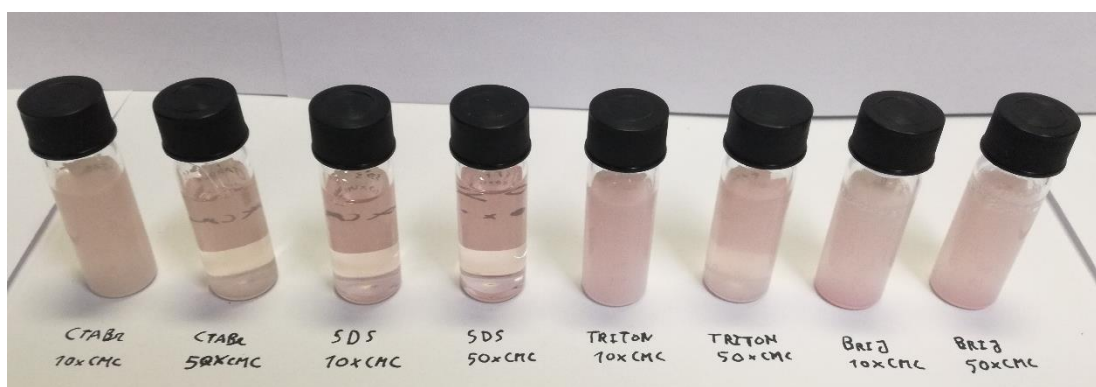


Figure 45. Solubility test using the surfactants from figure 44, naphthalimide **42**, the Nickel complex and bromo-acetophenone.

After these solubility tests we investigated the photophysical properties of compound **42** in the different surfactant aggregates. Figure 46 shows the normalized UV-Vis spectra of compound **42** in water and in surfactant aggregates. The effect of the aggregate on the UV-Vis spectra of the naphthalimide is almost negligible, with a small shift of the position of the maximum toward shorter wavelengths observed in the case of SDS, suggesting that inclusion in the aggregate do not influence the properties of the compound.

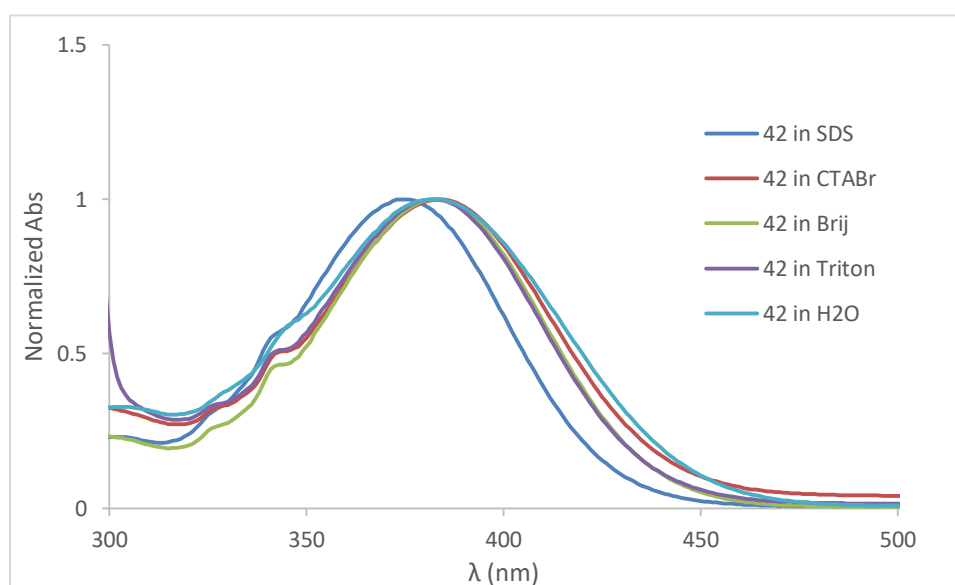


Figure 46. UV-Vis spectra comparison of **42** ($2.6 \times 10^{-4} \text{M}$) in a Micellar/water solution of CTABr (50xCMC), SDS (10xCMC), Brij (300xCMC) and TRITON (500xCMC).

For each of the micellar solutions we then added bromo-acetophenone, and Nickel complex with ditert-butylbpyridine (dtbbpy). The UV Vis spectra of this solutions are reported in Figure 47. In all cases we did not observed effects on the naphthalimide absorption band at around 384 nm ruling out interactions between the dye and the other components of the mixture at the ground state.

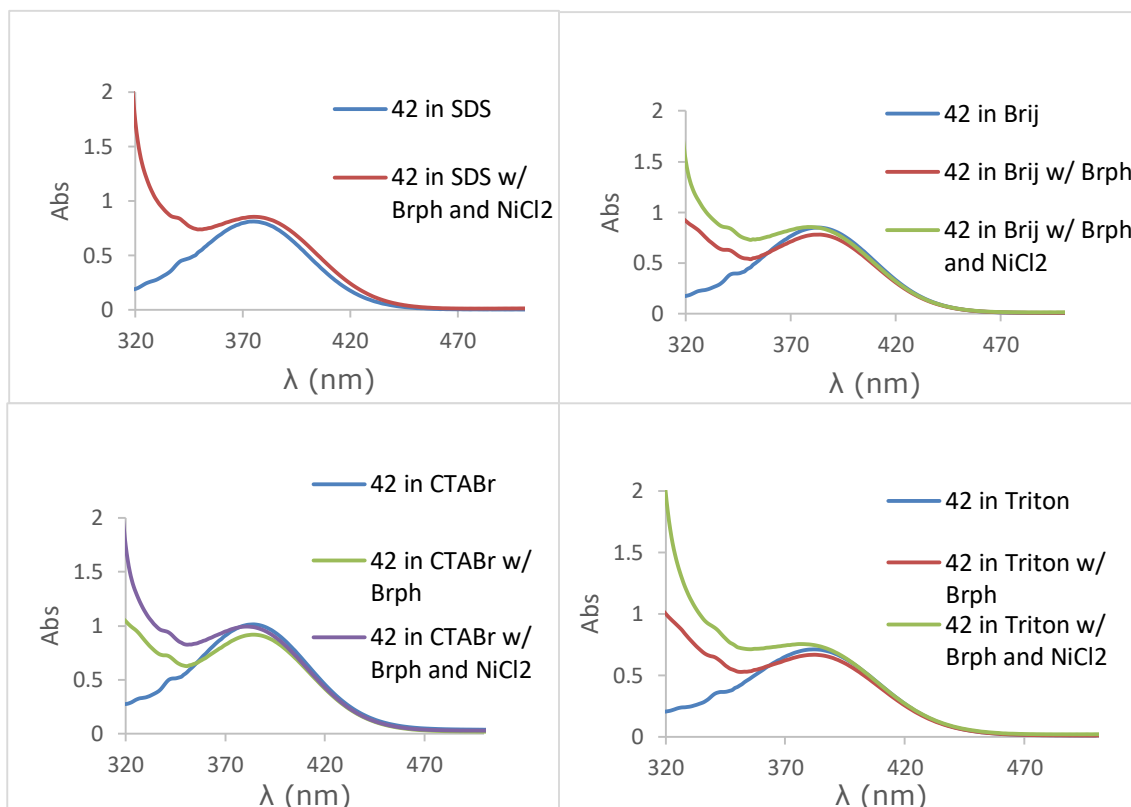


Figure 47. UV-Vis spectra of **42** ($2.6 \times 10^{-4} \text{M}$) with Bromoacetophenone (1×10^{-2}) and Nickel complex (1×10^{-3}) in a micellar/water solution of CTABr (50xCMC) (bottom-left), SDS (10xCMC) (top-left), Brij (300xCMC) (top-right), and TRITON (500xCMC) (bottom-right).

Next, we measured the fluorescence spectra of the naphthalimide for each of the micellar solutions in the absence and in the presence of bromo-acetophenone and Ni complex (Figure 48). In each cases, we observed a quenching of the fluorescence emission when the Nickel complex is added, while there is no quenching with the addition of bromo-acetophenone suggesting that the Ni complex can be engaged in ET processes with the excited dye.

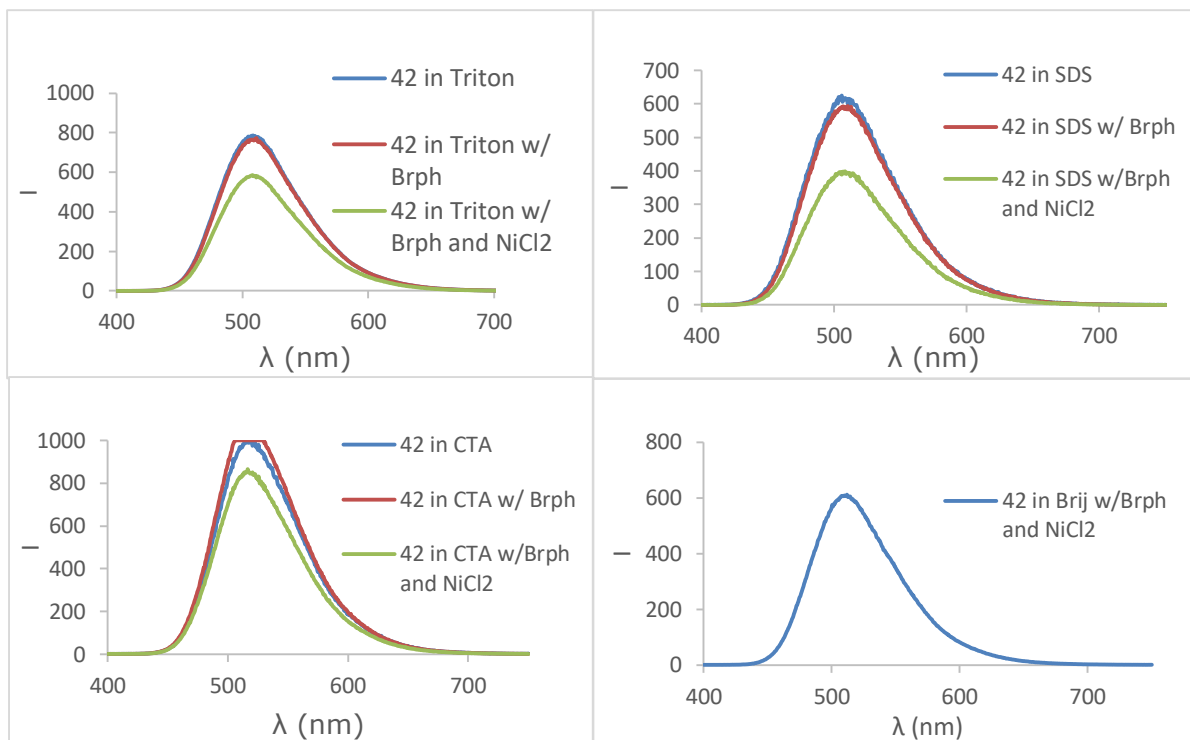


Figure 48. Fluorescence spectra of **42** ($2.6 \times 10^{-4} \text{M}$) with Bromoacetophenone (1×10^{-2}) and Nickel complex (1×10^{-3}) in a micellar/water solution of CTABr (50xCMC) (bottom-left), Brij (300xCMC) (bottom-right) SDS (10xCMC) (top-right), and TRITON (500xCMC) (top-left).

Finally, we measured the life-time of the emission of naphthalimide **42** in each of the water/micellar solutions in the absence and in the presence of bromo-acetophenone and Ni complex (Figure 49).

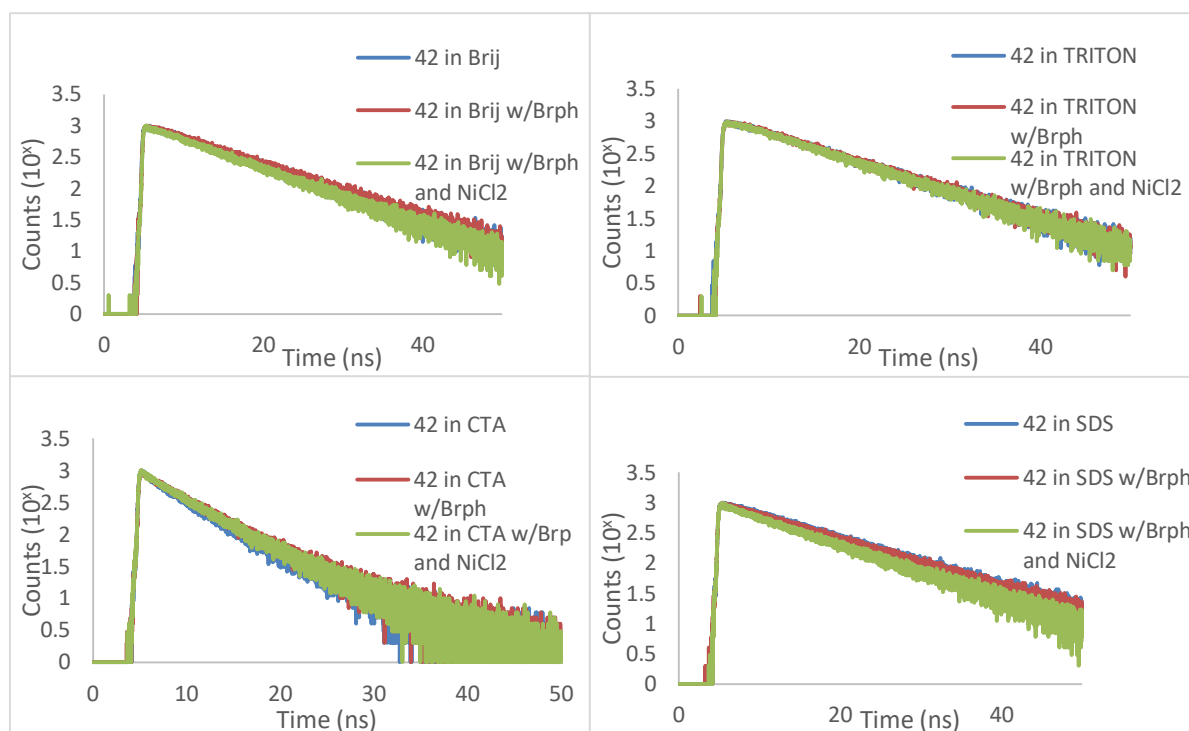


Figure 49. Fluorescence decay of **42** ($2.6 \times 10^{-4} \text{M}$) in a micellar/water solution of CTABr (50xCMC) (bottom-left), SDS (10xCMC) (bottom-right), Brij (300xCMC) (top-left) and TRITON (500xCMC) (top-right).

The graphs of Figure 49 are plotted in a semi-logarithmic scale and fitting the data with the equation:

$$\ln I(t) = -t/\tau + \ln A_1$$

where $I(t)$ is the fluorescence intensity at time t , A_1 is a pre-exponential factor and τ is the life-time of the excited state, allows to determine the life-time of the fluorescent dye in the different conditions. This is shown in Figure 30 in the case of Brij while all the data obtained are reported in Table 2.

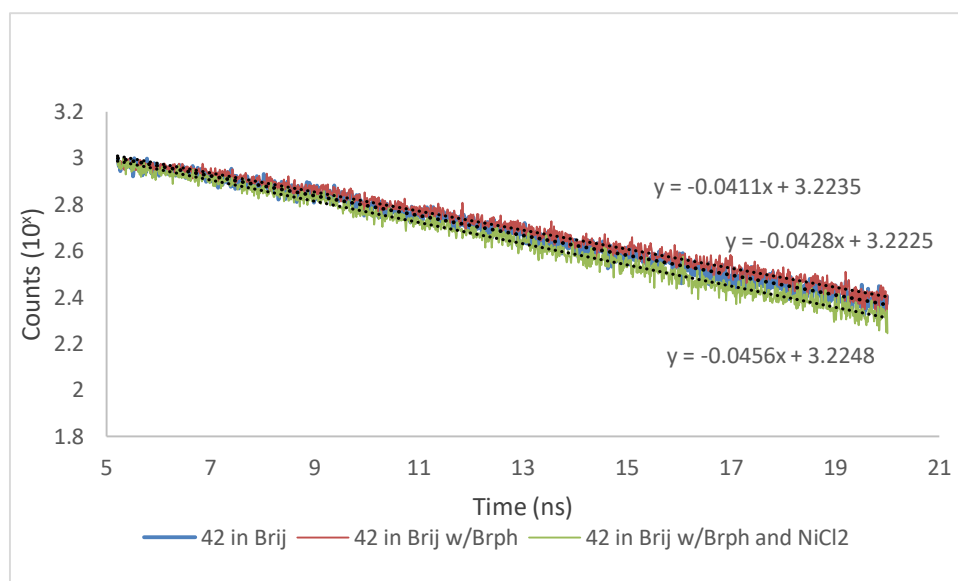


Figure 50. Fitting of the fluorescence decay of **42** ($2.6 \times 10^{-4} \text{M}$) with Bromo-acetophenone (1×10^{-2}) and Nickel complex (1×10^{-3}) in a micellar/water solution of Brij (300xCMC).

	Surfactant with 42	Surfactant with 42+Bromo-acetophenone	Surfactant with 42+Bromo-acetophenone+Nickel complex
Brij	23.4	24.3	21.9
TRITON	24.7	25.1	23.9
CTABr	10.7	12.1	11.6
SDS	27.3	26.3	22.0

Table 2. Life-time (ns) for **42** in the micellar aggregates in the absence or presence of 4-bromo acetophenone and Nickel complex.

The data of Table 2 show that the life-times of naphthalimide **42** are similar in the different micellar aggregates with the exception of CTABr in which the life-time is shorter. Addition of bromo-acetophenone has little effect on the life-time of the dye in accord with the observation that this compound does not act as a quencher of the fluorescence emission of the dye. On the other hand, also the Nickel complex has little effect on the life-times while it is able to quench substantially the fluorescence emission of the dye (Figure 48). This suggest a static quenching effect of the Nickel complex which can be ascribed to the confinement at close distance of the dye and of the metal complex at the micellar surface. Further experiments are, however, required to confirm this hypothesis.

Finally, we tested the ability of naphthalimide **42** to act as a photocatalyst in the model nickel-catalyzed decarboxylative arylation reaction (Figure 40). The reaction was performed by dissolving in SDS 0.03 mmol of the of *N*-Bocproline and 0.09 mmol 4-bromoacetophenone, 0.016 mmol of **42**, 0.003 mmol of NiCl₂ glyme, 0.003 mmol of ditert-butylbipyridine (dtbbpy) as ligand for Ni(II), and Cs₂CO₃ as a base (0.09 mmol). The reaction mixture was degassed by bubbling argon under sonication to avoid oxygen and irradiated with a blue LED light for 24 h at 25°C. The products were extracted from the water solution with CH₂Cl₂ and, after drying and evaporation, analysed by ¹H-NMR. Regrettably we did not observe the formation of the reaction product. Even changing the concentration of Nickel ligand complex by increasing the amount from 0.003 mmol to 0.011 mmol, doubling the concentration of **42** (with 0.026 mmol), or increasing the concentration of SDS from the 0.02M used to 0.08M, we were not able to observe the product of the reaction. This may be the result of the difficulty to exclude oxygen from the reaction mixture because the bubbling of argon is not really efficient due to the formation of soap bubbles. More experiments are required to optimize the system

Conclusion

The research carried out in this Thesis focused on the study of photochemical processes at the static interphase between two immiscible liquids as a model of the more complex dynamic liquid-liquid interphases which are the final goal of the Phototrain project.

We tested different liquid-liquid systems, using previously studied photoactive compounds (perylene, perixanthene xanthene and naphthalimide) to be applied as photocatalysts. After completing the synthesis of perylenes with fluorinated and alkyl chains and the synthesis of perixanthenes xanthenes with fluorinated and alkyl chains with success, these compounds were tested in a complex emulsion made by fluoro-hexane/hexane/water stabilized by a fluorinated surfactant. However, the synthesized dyes proved to be very little soluble in the emulsion hampering any photophysical characterization of the system and their use as photocatalysts.

Attempts to improve the solubility of the perixanthenes xanthenes derivatives were directed toward the preparation of compounds with substituents able to avoid intermolecular π - π stacking of the large flat aromatic core by decreasing the planarity of the molecule. However, the synthesis proved to be too demanding and the perixanthenes xanthenes derivatives were abandoned in favour to the more versatile and synthetically accessible 4-aminonaphthalimides dye.

Synthetic modification of the 4-aminonaphthalimides core allowed to create a library of naphthalimides with different properties. Using naphthalimides functionalized with a fluorocarbon and alkyl chain we characterized the absorption and emission properties of these molecules, and concluded, via studies on the quenching of their fluorescence, that they could be used as electron acceptors in an electron transfer reaction. Following this we made solubility tests of these compounds in the complex emulsion. Unfortunately, also in this case the solubility of the compounds in the emulsion was too low to allow further characterization.

In the Dr. Reddy's labs the naphthalimides were studied as photocatalyst using the photoredox nickel-catalyzed decarboxylative arylation as model reaction. The results were encouraging and in the best condition a 35 % yield of product was obtained proving

that the naphthalimide can act as an organic photocatalyst able to replace the traditionally used inorganic photocatalysts.

Following this positive result, we attempted the study of the reaction at a different liquid-liquid interface, the micellar/water interface. Amphipathic derivatives of 4-amino naphthalimide were prepared and the solubility of the different components of the reaction was tested in micellar aggregates made by different surfactants (cation, anionic and neutral) showing a good overall solubility. The photophysical properties (absorption, emission and life-time) of the reagents and of the catalysts were studied and the results suggest a static quenching effect of the Nickel complex on the 4-amino naphthalimide derivative which can be ascribed to the confinement at close distance of the dye and of the metal complex at the micellar surface. Further experiments are, however, required to confirm this hypothesis.

Finally, the model photocatalytic reaction was tested in the micellar conditions. Unfortunately, no product was found, which may be the result of the difficulty to exclude oxygen from the reaction mixture because the bubbling of argon is not really efficient due to the formation of soap bubbles. More experiments are required to optimize the system which is however promising due to the observed interaction between the Nickel complex and the excited state of the dye.

Experimental part

5.1 Materials and general methods

The reagents and solvents have been purchased from Sigma-Aldrich or Alfa Aesar and used without further purification. Column chromatography was performed on silica gel 60 (Merck, 230–400 mesh ASTM), eluting with solvents mixtures as specified below. The reactions were monitored by TLC (silica gel/ UV 254, 0.20 mm, glass or aluminum support). UV-Vis spectra were recorded on an Agilent Cary 60 spectrometer in a quartz cuvette (1 cm optic path length). Fluorescence emission spectra were recorded on a Varian Cary Eclipse spectrofluorometer in a quartz cuvette (1 cm optic path length). Mass spectra have been acquired using a Bruker Esquire 4000 ESI-MS instrument or a Bruker micrOTOF-Q for HRMS by Dr. Fabio Hollan of the Department of Chemical and Pharmaceutical Sciences of the University of Trieste. Only molecular ions and major peaks are reported.

5.1.1 Nuclear Magnetic Resonance

NMR spectra were recorded on a Varian 500 MHz (125 MHz for carbon) or a Varian 400 MHz (101 MHz for carbon). Chemical shifts are reported as parts per million (ppm) relative to the solvent residual signal as internal reference. Coupling constants (J) are quoted in Hertz (Hz). The s, d, t, q, m, and bs signal notations indicate respectively: singlet, doublet, triplet, quartet, multiplet and broad signal.

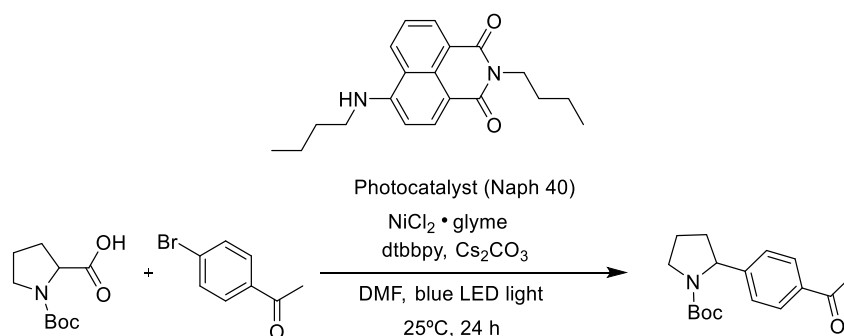
5.1.2 Luminiscence lifetime measurements

Excited state lifetimes in the range 0.5 ns-30 μ s were measured with an Edinburgh Instrument time correlated single-photon counting technique. The excitation impulse is obtained by a gas discharge lamp (model nF900, filled with nitrogen or deuterium, depending on excitation requirements) delivering pulses of 0.5 ns width at a frequency comprised between 1 and 100 kHz or by a pulsed diode laser (406 nm Picoquant). A photomultiplier tube (Hamamatsu R928P) cooled at -20°C and suitably amplified is used as stop detector.

Lifetimes in the range between 10 μ s and 5 s were measured with the same Perkin Elmer LS 50 spectrofluorimeter employed for the luminescence spectra acquisition. In this case the excitation pulse is generated by a Xe lamp (5-50 Hz) and the emission decay directly recorded. The experimental error on the lifetime measurements is \pm 10%.

5.2 Experimental procedures

5.2.1 Procedure for the photoredox catalysis



Reaction in DMF: In a separate flask a mixture of NiCl₂.glyme (0.02 mmol) and 4,4'-di-tert-butyl-2,2'-dipyridyl (8.05 mg, 0.03 mmol) was prepared in DMF (5 ml). At the same time, in a dried Schlenk kept under N₂, the desired photocatalyst (0.004 mmol), 4'-Bromoacetophenone (0.2 mmol) and Boc-L-proline (0.6 mmol) and anhydrous DMF (5 ml) were added. After some minutes the solution with NiCl₂ is mixed with the solution with the photocatalyst in the Schlenk tube, and Cesium carbonate (0.6 mmol) is added. The reaction mixture was deoxygenated by bubbling with N₂ for 15 minutes. The reaction was then left under stirring over night at room temperature under irradiation with blue LED lights. Work up was done by first diluting with dichloromethane (10 ml), washing first with water saturated with Na₂CO₃, then with water and finally with brine. The solvent was finally evaporated and the crude was analysed by NMR after addition of 0.02 mmol of trimethoxybenzene as internal standard.

Reaction in micellar environment: In a separate flask a solution of NiCl₂.glyme (0.009 mmol) and 4,4'-di-tert-butyl-2,2'-dipyridyl (0.028 mmol) was dissolved in 2-methoxyethanol (1 ml) and left stirring for 2 hours at 140°C. In a dried Schlenk 4'-Bromoacetophenone (0.05 mmol), 50 μ l of the Nickel/ligand solution where dissolved in 200 μ l of 2-methoxyethanol. In a separate flask a micellar solution was prepared with

water (5 ml) and the desired surfactant, via the general “procedure for Micellar solutions preparation” described below. The micellar solution was added to the solution in the Schlenk. Boc-L-proline (0.148 mmol), the photocatalyst **42** (0.004 mmol), and Cesium carbonate (0.15 mmol) were dissolved in the solution in the Schlenk. The reaction mixture was degassed by bubbling argon under sonication. The reaction mixture was then left stirring under irradiation with blue LED lights at room temperature for 16 hours. Dichloromethane (5 ml) was added and a small amount (0.5 ml) of Brine is used to perform an extraction. A new extraction is done with chloroform and Brine (3 times). The combined organic layers were dried with MgSO₄. The solvent was finally evaporated and the crude was analysed by NMR after addition of 0.02 mmol of trimethoxybenzene as internal standard.

5.2.2 General procedures for the preparation of complex emulsion and micellar aggregates

Procedure for the complex emulsion preparation

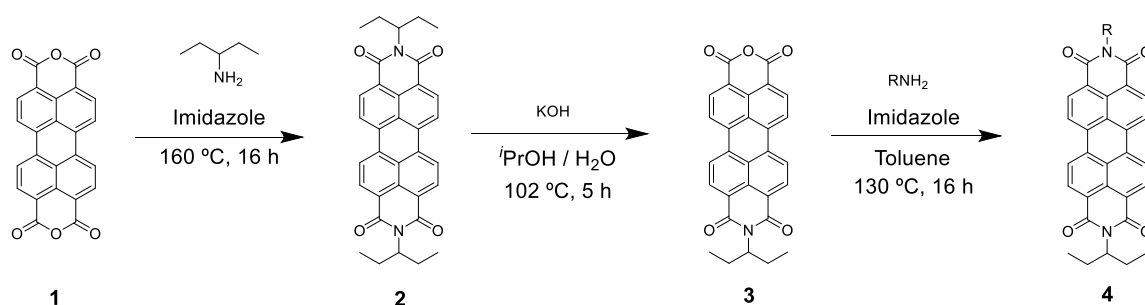
In a small flask the hydrocarbon and fluorocarbon liquids of choice were heated with a heated water bath until a single phase is formed. The temperature required varied depending on the solutions. Water with 0.1% Zonyl FS-300, a non-ionic fluorosurfactant, is added to the flask and the solutions were emulsified in bulk by shaking via magnetic stirrer or by sonication. Hexane–perfluorohexane emulsions, have to be cooled to induce phase separation and were, therefore, chilled on ice. Emulsions were observed to be stable during the time periods used (of the order of days). Longer-term stability experiments were not conducted.

Procedure for Micellar solutions preparation

In a small flask the desired surfactant was added. Water is the added to dissolve the surfactant. The concentration of surfactant used has to be above the predefined CMC for each surfactant. To create the micelles cycles of sonication intercalated with heating the flask with a standard heater, until eventually the solution goes from an opaque to a completely clear solution. This proves that the surfactant molecules reorganized to form micellar structures. Water-Micellar solutions were observed to be stable during the time

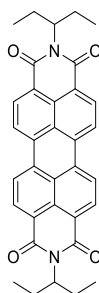
periods used (of the order of days). Longer-term stability experiments were not conducted.

5.2.3 General procedures for the synthesis of perylene derivatives



In a dried round bottom flask, the commercially available 1-ethylpropylamine (4 eq) and perylenetetracarboxylic dianhydride (1 eq) are added to imidazole (20 ml) in Ar atmosphere. The mixture is stirred for 16 hours at 160 °C. The reaction is diluted with water with KOH (20%) and suspended in methanol. The insoluble perylenetetracarboxylic di-imide **2** is then collected by filtration. Di-imide **2** is then hydrolysed with KOH (10%) (50 eq) in isopropanol/water (9/1) (156 ml) at 105 °C for 5 hours. The resulting solution is then poured into acidic water (1 M HCl), and the product collected by filtration, and washed with water three times. The product is extracted with chloroform to obtain the compound perylenetetracarboxylic mono-imine anhydride **3**. A selected primary amine (1 eq) is then added to compound **3** (1 eq) and imidazole (11 eq) in toluene (45 ml) and heated at 130 °C for 16 hours. The reaction mixture is then diluted with acidic water (1 M HCl) and extracted with dichloromethane. The organic phase was dried with MgSO₄, filtrated and the solvent was evaporated. The crude was purified by silica gel column (in dichloromethane) to obtain the red solid **4** as the final product.

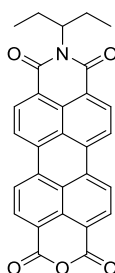
Compound 2



The compound has been synthesized using the general procedures for the synthesis of perylene derivatives.

Yield 90%. **¹H-NMR** (400 MHz, CDCl₃): 0.93 (t, J = 7.48 Hz, 12H), 1.95 (m, 4H), 2.27 (m, 4H), 5.07 (m, 2H), 8.64 (m, 8H). **¹³C-NMR** (101 MHz, CDCl₃) δ 134.48, 129.59, 126.42, 123.01, 57.70, 25.01, 11.34. **ESI-MS** Calculated: 530.62, Found: 531.22 [M+H]⁺.

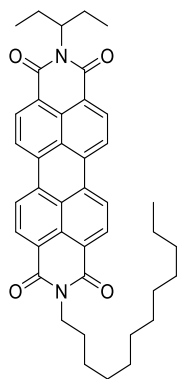
Compound 3



The compound has been synthesized using the general procedures for the synthesis of perylene derivatives.

Yield 52%. **¹H-NMR** (400 MHz, CDCl₃): 0.93 (t, 12H), 1.95 (ddd, 4H), 2.27 (ddd, 4H), 5.07 (m, 2H), 8.64 (m, 8H). **¹³C-NMR** (101 MHz, CDCl₃) δ 159.98, 133.55, 123.90, 55.06, 30.92, 25.28, 24.99, 11.33, 9.74, 1.00. **ESI-MS** Calculated: 461.12, Found: 461.47 [M]⁺.

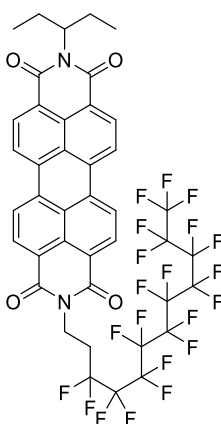
Compound 4a



The compound has been synthesized using the general procedures for the synthesis of perylene derivatives and using dodecylamine.

Yield 71%. **¹H-NMR** (400 MHz, CDCl₃): 0.86 (t, J= 6.56 Hz, 3H) 0.95 (t, J= 7.45 Hz, 6H), 1.26 (m, 18H), 1.74 (dt, J= 7.80, 7.65 Hz, 2H), 1.96 (dt, J= 14.88, 7.58 Hz, 2H), 2.27 (m, 2H), 4.17 (t, J= 7.60 Hz, 2H), 5.07 (tt, J= 9.50, 5.85 Hz, 1H), 8.58 (m, 8H). **¹³C-NMR** (101 MHz, CDCl₃) δ 163.28, 134.53, 134.29, 131.28, 129.52, 129.28, 126.37, 123.19, 123.00, 122.92, 57.75, 40.68, 31.91, 29.69, 29.64, 29.62, 29.60, 29.56, 29.36, 29.34, 28.10, 27.15, 25.02, 22.68, 14.10, 11.36. **ESI-MS** Calculated: 628.81, Found: 667.9 [M+K]⁺.

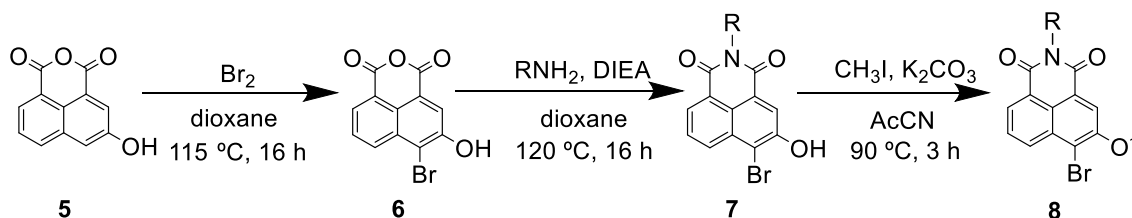
Compound 4b



The compound has been synthesized using the general procedures for the synthesis of perylene derivatives and using 1H,1H,2H,2H-perfluorododecyl amine which was prepared by a reported procedure.

Yield 63%. **¹H-NMR** (400 MHz, CDCl₃): 0.93 (t, J= 7.42 Hz, 6H), 1.95 (dt, J= 13.87, 6.81 Hz, 2H), 2.26 (dt, J= 13.99, 7.97 Hz, 2H), 2.63 (m, 2H), 4.57 (t, J= 7.59 Hz, 2H), 5.06 (m, 1H), 8.66 (m, 8H). **ESI-MS** Calculated: 1006.13, Found: 1024.3 [M+NH₄]⁺, 862.4, 409.2.

5.2.4 General procedures for the synthesis of peryxanthene xanthenes (1st step)



This synthesis was developed by the group of professor Bonifazi (reference 62).

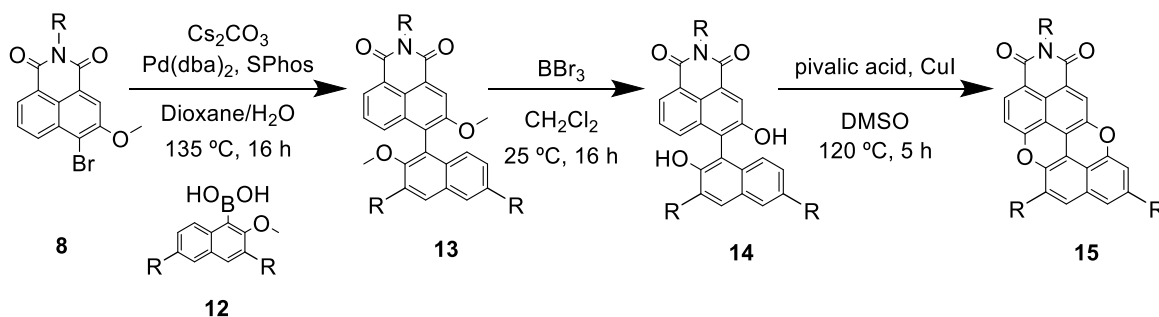
In a single-necked round bottom flask, 3-hydroxy-1,8-naphthalenic anhydride **5**, was dissolved in dioxane (50 mL) and bromine (2.6 eq.) was added. The resulting solution was heated under reflux for 2.5 hours, then cooled down to room temperature and the solvent evaporated under reduced pressure. The solid residue was suspended in water (75 mL) and filtered to give **6** as a yellow solid.

In a single-necked round bottom flask to a suspension of bromo-derivative **6** in dioxane (75 ml), diisopropylethylamine (2 eq.) was added. The solution turned to a red color. Afterwards, the proper primary amine (1.5 eq.) was added. The reaction mixture was heated under reflux for 20 hours. During this period the reaction mixture passed from a suspension to brown solution. Then solvent was evaporated under reduced pressure and the solid residue suspended in $\text{HCl}(\text{aq})$ (10 % w/w) and extracted with CHCl_3 . The combined organic layers were dried over MgSO_4 , filtered and evaporated under reduced pressure. The crude material was purified by silica gel chromatography (pentane/ AcOEt 2/1), affording **7** as a yellow solid.

In a single-necked round bottom flask, imide-derivative **7** was dissolved in boiling acetonitrile (155 ml). Potassium carbonate (1 eq.) was added, the solution turned to red, subsequently methyl iodide (1.2 eq.) was added and the reaction mixture heated under reflux for 4 hours. During this period the reaction mixture turned from red to yellow. Then, solvent was evaporated under reduced pressure, the solid residue was suspended in water and extracted with CHCl_3 . The combined layers were dried over MgSO_4 , filtered

and evaporated under reduced pressure. The crude material was purified by silica gel chromatography (pentane/AcOEt 10/1) to afford **8** as a yellow solid.

5.2.5 General procedures for the synthesis of peryxanthene xanthenes (2th step)



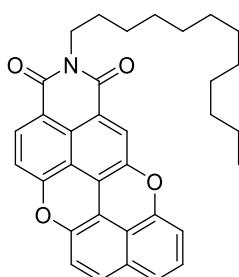
This synthesis was developed by the group of professor Bonifazi (reference 62).

In a single-necked round bottom flask methoxy-imide-derivative **8** and cesium carbonate (3 eq.) were suspended in dioxane (50 ml) and water (4 drops) and the resulting mixture degassed for 20 minutes. Subsequently, 2-methoxy-naphthaleneboronic acid derivative **12** (prepared by the general procedures for the synthesis of substituted peryxanthene xanthenes described below) (2 eq.), $\text{Pd}(\text{dba})_2$ (0.05 eq.) and SPhos (0.1 eq.) were added to the reaction mixture; the resulting suspension was degassed for other 20 minutes and heated under reflux for 16 hours under N_2 . The reaction suspension was then filtered over celite[®] and the residue concentrated in vacuo. The crude was purified by silica gel chromatography (hexane/ AcOEt, from 10/1 to 10/3) to give **13** as a yellow solid.

In a single-necked round bottom flask oven dried, binaphthyl-imide-derivative **13** was dissolved in dry CH_2Cl_2 (50 ml), cooled at 0°C and BBr_3 (10 eq., 1 M in dichloromethane) was added. The resulting solution was stirred overnight at room temperature. Afterwards reaction mixture was poured on crushed ice and extracted with AcOEt. The organic layers were dried over MgSO_4 , filtered and evaporated under reduced pressure. The crude was purified by silica gel chromatography (hexane / AcOEt 5/2) to give **14** as a yellow solid.

In a single-necked round bottom flask, bi-naphthalyl-imide-derivative **14**, pivalic acid (2 eq.) and CuI (3 eq.) were dissolved in DMSO (4 ml). The reaction mixture was heated at 120°C under air for 5 hours. The resulting solution was poured in water and extracted with CHCl₃. The combined organic layers were dried over MgSO₄, filtered and evaporated under reduced pressure. The crude material was purified by silica gel chromatography (CH₂Cl₂) affording **15** as a red solid.

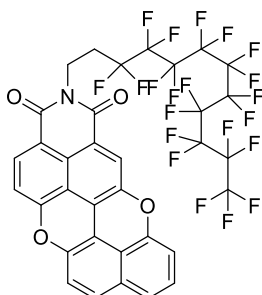
Compound 15a



The compound has been synthesized using the general procedures for the synthesis of peryxanthene xanthenes (step1) and (and step2) using dodecylamine.

¹H-NMR(400 MHz, CDCl₃): 0.87 (t, J= 6.55 Hz, 3H), 1.29 (m, 18H), 1.63 (m, 2H), 3.96 (t, J= 7.47 Hz, 2H), 6.38 (d, J= 7.65 Hz, 1H), 6.56 (d, J= 8.35 Hz, 1H), 6.69 (d, J= 9.26 Hz, 1H), 6.87 (d, J= 8.19 Hz, 1H), 6.95 (t, J= 7.97 Hz, 1H), 7.14 (d, J= 9.16 Hz, 1H), 7.39 (s, 1H), 7.88 (d, J= 8.59 Hz, 1H). **¹³C NMR** (101 MHz, CDCl₃) δ 162.60, 162.44, 156.29, 151.62, 144.66, 144.49, 132.90, 130.96, 128.94, 128.08, 125.62, 120.74, 120.41, 120.04, 119.94, 118.07, 117.58, 116.85, 115.26, 109.93, 109.90, 109.50, 40.54, 31.93, 29.68, 29.66, 29.64, 29.42, 29.37, 28.02, 27.24, 22.69, 14.12. **ESI-MS** Calculated: 519.24, Found: 540.4 [M+Na]⁺.

Compound 15b

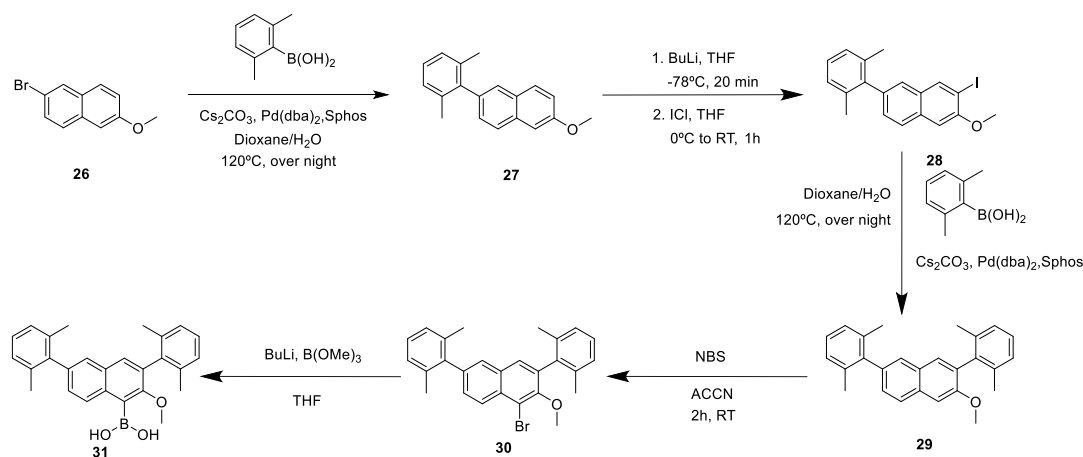


The compound has been synthesized using the general procedures for the synthesis of peryxanthene xanthenes (step1) and (step2) using 1H,1H,2H,2H-perfluorododecyl amine .

$^1\text{H-NMR}$ (400 MHz, CDCl_3): 2.57 (m, 2H), 4.51 (t, $J = 8.41$ Hz, 2H), 6.84 (d, $J = 6.86$ Hz, 1H), 7.03 (d, $J = 8.31$ Hz, 1H), 7.16 (d, $J = 9.16$ Hz, 1H), 7.30 (m, 2H), 7.57 (d, $J = 9.24$ Hz, 1H), 8.04 (s, 1H), 8.32 (d, $J = 8.32$ Hz, 1H). **ESI-MS** Calculated: 897.04, Found: 915.6 $[\text{M}+\text{NH}_4]^+$.

5.2.6 General procedures for the synthesis of substituted peryxanthene xanthenes

Dimethylbenzene modification



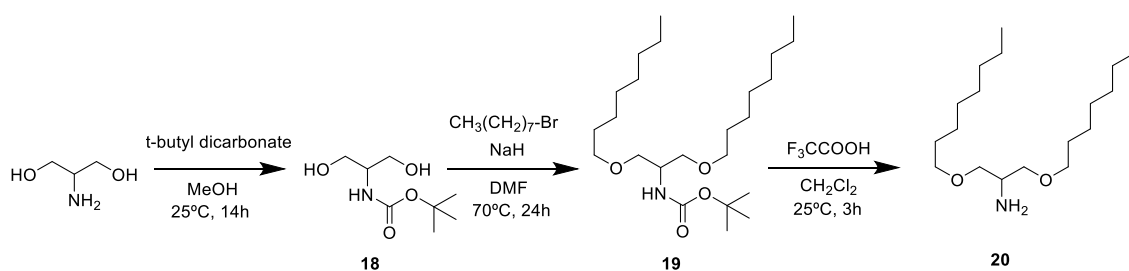
For the bottom part of the PXX core we started with the commercially available Bromomethoxy naphthalene **26** (1eq) dissolved in dioxane (15 ml). The solution was added to a Schlenk tube and degassed *via* freeze-pump-thaw cycles (5 cycles). Dimethylbenzene boronic acid (2 eq), Sphos (0.2 eq), and Bis(dibenzylideneacetone)palladium(0) ($\text{Pd}(\text{dba})_2$) (0.1 eq) were then added followed by Cesium carbonate (3 eq). The reaction mixture was stirred for 16 hours at 120 °C. After this Suzuki reaction is finished the suspension is filtered on Celite® and the solvent is evaporated in vacuum. The crude material was purified by silica gel chromatography (Hexane/ AcOEt 9/1) affording **27** as a yellow viscous liquid. To add the second di-methyl phenyl group we need to functionalize the compound with an Iodide in order to do a second Suzuki coupling. This iodination reaction is done by adding to a Schlenk tube compound **27**, and after 5 cycles of freeze-pump-thaw degassing, anhydrous THF (2 ml) is added under Ar. Using liquid

Nitrogen the solution is cooled to -78°C and butyl lithium (1.6 eq) is added drop wise. Iodochloride (1 eq) is diluted in 2ml of anhydrous THF and added to the solution. The reaction is left stirring for 1 hour at 25°C . After the reaction is finished the solution is quenched with water and washed with water saturated with NH_4Cl , and water saturated with $\text{Na}_2\text{S}_2\text{O}_3$. Each washing is done three times. The water phase was finally extracted with diethyl ether. The organic layers were dried over MgSO_4 , filtered and evaporated under reduced pressure. The crude was purified by silica gel chromatography (hexane/dichloromethane 9/1) to give **28**.

The following Suzuki coupling uses the same amounts and procedure as the first one, but using compound **28** as the starting material. Compound **28** was dissolved in dioxane (15 ml), added to a Schlenk flask and degassed *via* freeze-pump-thaw cycles (5 cycles). Dimethylbenzene boronic acid (2 eq), Sphos (0.2 eq), and Bis(dibenzylideneacetone)palladium(0) ($\text{Pd}(\text{dba})_2$) (0.1 eq), and cesium carbonate (3 eq) were then added. The reaction mixture was stirred for 16 hours at 120°C . After this Suzuki reaction is finished the suspension is filtered on Celite[®] and the solvent is evaporated in vacuum. The crude material was purified by silica gel chromatography (Hexane/AcOEt 9/1) affording **29** as a yellow solid.

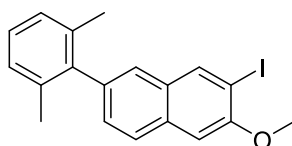
The last step is the bromination of compound **29** which is performed by dissolving **29** and bromo succinimide (1eq) in a round bottom flask with acetonitrile (5 ml). The reaction mixture is then heated at 70°C for 2 hours. Solvent is evaporated and residue dissolved in diethyl ether. Extracted with water 3 times and organic layers dried with MgSO_4 filtered and evaporated under reduced pressure, to obtain the brominated compound **30** as a white solid. To obtain the final boronic acid the compound **30** dissolved in anhydrous THF (3 ml) was added to a Schlenk tube and degassed by 5 cycles of freeze-pump-thaw. The solution is cooled to 0°C and magnesium (1.2 eq) is added to form the Grignard reagent. The reaction mixture is left stirring for 1 hour at 50°C under argon. Then the Schlenk tube was cooled to -78°C with liquid Nitrogen and trimethyl borate (3.4 eq) is slowly added. The reaction is left at 25°C under stirring for 16 hours. When finished the solution is washed with water and extracted with diethyl ether three times. After the solvent is evaporated we obtain the final product **31** as a white solid.

Branched amine modification



The synthesis of the amine begins by dissolving the commercially available 2-amino-1,3-propanediol in a solution of Methanol (50 ml) in a round bottom flask. Di-tert-butyl dicarbonate (1.1 eq) is added to the solution and the reaction mixture is left in room temperature for 16 hours. The solvent is evaporated in vacuum. The crude is used directly in a silica gel chromatography (Dichloromethane/Methanol 9/1). The product recovered **18** is a white solid. In an oven dried round bottom flask **18** is dissolved in anhydrous DMF (50 ml). Sodium hydride (5 eq) is dissolved in the mixture and the solution is cooled with an ice/water bath. The desired amine (4 eq) (1-bromooctane in this case) is slowly added to the reaction mixture. Reaction left for 16 hours at 70°C. The solution is cooled in a ice/water bath and a few droplets of water are added to quench the solution. An aqueous solution saturated with NH₄Cl is added and an extraction is done with ethyl acetate. Organic phase washed with brine 3 times and dried with MgSO₄. Product purified by silica gel chromatography (hexane / AcOEt 9/1) to give **19** as a white solid. The deprotection of **19** is done by dissolving the compound in dried Dichloromethane (40 ml) in a dried round bottom flask. Trifluoro acetic acid (20 ml) was added dropwise in an Argon environment. The reaction mixture is left under Argon for 3 hours at room temperature. The solvent is evaporated under vacuum and the crude is purified by silica gel chromatography (Dichloromethane/Methanol 9/1) affording the final product **20** as a white solid.

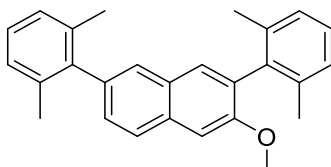
Compound 28



The compound has been synthesized using the general procedures for the synthesis of substituted peryxanthene xanthenes the dimethylbenzene modification.

¹H-NMR(400 MHz, CDCl₃): 2.02 (s, 6H), 4.03 (s, 3H), 7.16 (m, 3H), 7.29 (d, J= 8.37 Hz, 1H), 7.42 (s, 1H), 7.57 (s, 1H), 7.93 (d, J= 8.35 Hz, 1H), 8.45 (s, 1H). **¹³C-NMR** (101 MHz, CDCl₃) δ 139.21, 136.27, 128.68, 127.36, 127.20, 126.78, 126.26, 105.40, 56.42, 20.88. **ESI-MS** Calculated: 388.25, Found: 409.2 [M+Na]⁺, 425.1.

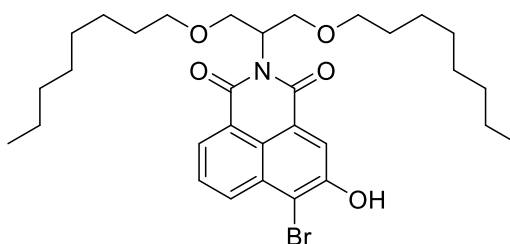
Compound 29



The compound has been synthesized using the general procedures for the synthesis of substituted peryxanthene xanthenes the dimethylbenzene modification.

¹H-NMR(400 MHz, CDCl₃): 2.02 (s, 6H), 3.89 (s, 3H), 7.14 (m, 6H), 7.27 (dd, J= 8.33, 1.69 Hz, 1H), 7.58 (m, 3H), 7.98 (d, J= 8.38 Hz, 1H). **¹³C-NMR** (101 MHz, CDCl₃) δ 136.80, 136.42, 136.41, 129.61, 127.89, 127.33, 127.27, 127.08, 127.05, 126.53, 105.31, 55.61, 21.05, 20.65. **ESI-MS** Calculated: 366.50, Found: 367.2 [M]⁺, 389.2 [M+Na]⁺, 316.2.

Compound 21

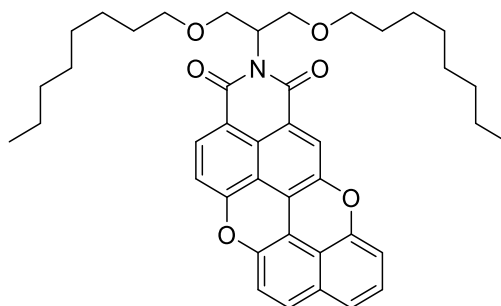


The compound has been synthesized using the general procedures for the synthesis of peryxanthene xanthenes (1st step) using the general procedures for the synthesis of substituted peryxanthene xanthenes the branched amine modification.

¹H-NMR (400 MHz, CDCl₃): 0.82 (t, 6H), 1.15 (m, 20H), 1.49 (m, 4H), 3.42 (m, 2H), 3.53 (m, 2H), 3.87 (t, J= 5.67 Hz, 2H), 4.11 (t, J= 8.32 Hz, 2H), 5.66 (tt, J= 7.99, 5.86 Hz, 1H), 6.71 (s, 1H), 7.75 (t, J= 8.52 Hz, 1H), 8.18 (s, 1H), 8.25 (d, J= 8.50 Hz, 1H), 8.45 (d, J= 7.23 Hz, 1H). **¹³C-NMR** (101 MHz, CDCl₃) δ 164.26, 163.69, 158.36, 151.95, 131.29, 128.41, 123.93, 112.99, 71.89, 71.21, 70.79, 68.69, 64.92, 54.70, 52.20, 42.80, 31.81, 31.77,

31.72, 29.52, 29.48, 29.36, 29.34, 29.26, 29.23, 29.21, 29.19, 27.53, 26.71, 26.10, 26.07, 22.63, 22.61, 14.07, 14.05. **ESI-MS** Calculated: 589.24, Found: 588.7 [M - H]⁻.

Compound 25

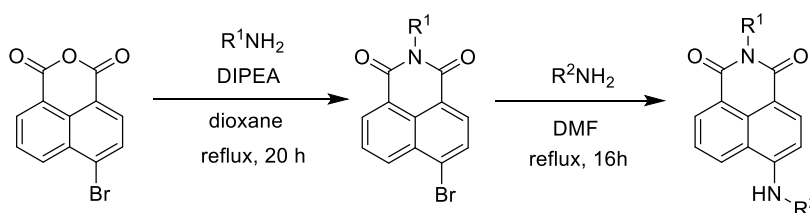


The compound has been synthesized using the general procedures for the synthesis of peryxanthene xanthenes (step1) and (and step2) and using the general procedures for the synthesis of substituted peryxanthene xanthenes the branched amine modification.

Due to low solubility the ¹H-NMR and ¹³C-NMR spectra were not possible for compound.

ESI-MS Calculated: 649.34, Found: 666.6 [M+NH₄]⁺.

5.2.7 General procedures for the synthesis of Naphthalimides.

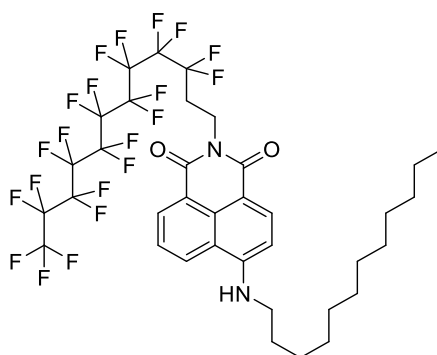


To make the synthesis of these compounds we add commercially available bromo-naphthalanhydride to a round bottom flask. diethylene glycol (10ml) is added, depending on the solubility and boiling point of the components of the reaction isopropanol, 1-butanol, ethanol, and dimethyl formamide can be used instead of diethylene glycol. The desired primary amine is then added (4 eq) and the reaction is left stirred for 5 hours under reflux (130 °C for diethylene glycol). The work up is done by addition of water to reaction mixture and extraction with dichloromethane (5 times). The organic layers are dried over MgSO₄, filtered and evaporated under reduced

pressure. The crude is purified by silica gel chromatography (hexane/chloroform 8/2) to give the desired imide.

The second step is done by dissolving the above product in diethylene glycol (3ml). Again depending on the solubility and boiling point of the components of the reaction isopropanol, 1-butanol, and dimethyl formamide can be used instead of diethylene glycol. The desired amine (4 eq) is added and the reaction is again left stirring for 5 hours under reflux (130 °C for Diethylene glycol). For the work up we use a similar procedure with addition of water and extraction with dichloromethane (5 times). The final product is obtained by purification on silica gel column with chloroform/methanol (9.7/0.3).

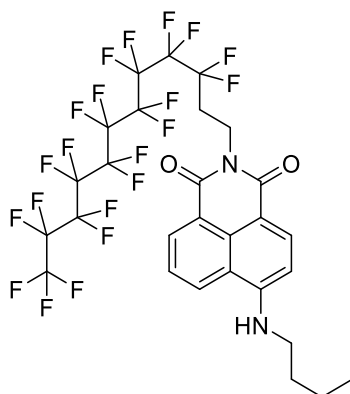
Compound 37a



The compound has been synthesized using the general procedures for the synthesis of naphthalimides. The solvent used was DMF.

¹H-NMR(400 MHz, CDCl₃): 0.87 (t, J= 6.45 Hz, 3H), 1.26 (m, 16H), 1.81 (tt, J= 7.36, 7.29 Hz, 2H), 2.56 (tt, J= 17.99, 7.64 Hz, 2H), 3.40 (td, J= 7.15, 4.95 Hz, 2H), 4.50 (t, J= 7.84 Hz, 2H), 5.30 (s, 1H, NH), 6.72 (d, J= 8.60 Hz, 1H) 7.61 (dd, J= 8.55, 7.84 Hz, 1H), 8.09 (d, J= 8.61 Hz, 1H), 8.45 (d, J= 8.40 Hz, 1H), 8.57 (d, J= 7.13 Hz, 1H). ¹³C-NMR (101 MHz, CDCl₃) δ 171.13, 164.39, 163.66, 149.75, 134.80, 131.33, 129.91, 126.10, 124.69, 122.74, 120.14, 109.62, 104.42, 32.29, 31.88, 29.61, 29.59, 29.55, 29.51, 29.33, 29.31, 28.96, 27.14, 22.65, 21.01, 14.16, 14.07. **ESI-MS** Calculated: 926.24, Found: 925.4 [M - H]⁻.

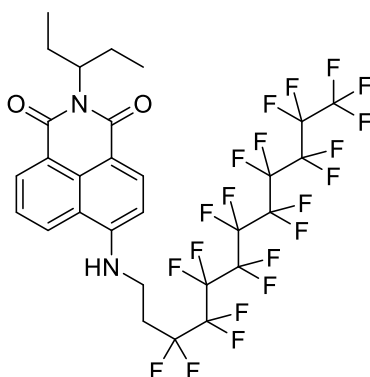
Compound 37b



The compound has been synthesized using the general procedures for the synthesis of naphthalimides. The solvent used was DMF.

¹H-NMR(400 MHz, CDCl₃): 1.03 (t, J= 7.35 Hz, 3H), 1.25 (m, 4H), 1.81 (tt, J= 7.31, 7.24 Hz, 2H), 2.59 (m, 2H), 3.42 (td, J= 6.74, 6.28 Hz, 2H), 4.51 (t, J= 7.36 Hz, 2H), 5.26 (s, 1H), 6.74 (d, J= 8.49 Hz) 7.63 (dd, J= 7.86 Hz, 1H), 8.09 (d, J= 8.40 Hz, 1H), 8.47 (d, J= 8.44 Hz, 1H), 8.59 (d, J= 7.30 Hz, 1H). **¹³C-NMR** (101 MHz, CDCl₃) δ 149.74, 131.38, 127.34, 126.07, 124.75, 104.47, 98.39, 43.44, 31.03, 20.32, 13.82, 1.00. **ESI-MS** Calculated: 814.11, Found: 813.2 [M - H]⁻.

Compound 38

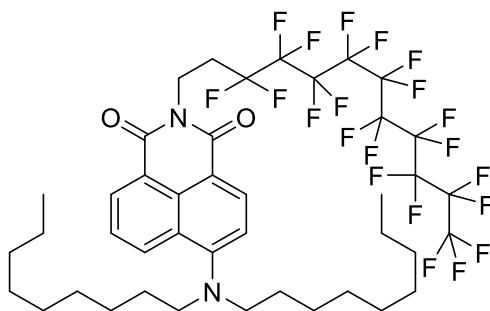


The compound has been synthesized using the general procedures for the synthesis of naphthalimides. The solvent used was DMF.

¹H-NMR(400 MHz, CDCl₃): 0.87 (t, J= 7.46 Hz, 6H), 1.88 (m, 2H), 2.24 (m, 2H), 2.59 (m, 2H), 3.85 (dt, J= 6.64, 6.63 Hz, 2H), 5.04 (tt, J= 9.65, 5.85 Hz, 1H), 5.69 (s, 1H), 6.75 (d, J= 8.42 Hz, 1H) 7.60 (dd, J= 8.44, 7.35 Hz, 1H), 8.12 (d, J= 8.63 Hz, 1H), 8.48 (d, J= 8.34 Hz,

1H), 8.56 (d, J= 7.33 Hz, 1H). ¹³C-NMR (101 MHz, CDCl₃) δ 147.98, 129.94, 125.56, 125.17, 120.43, 104.05, 57.02, 35.67, 30.27, 30.05, 29.84, 29.67, 25.06, 11.24. **ESI-MS** Calculated: 828.13, Found: 827.3 [M - H]⁻. .

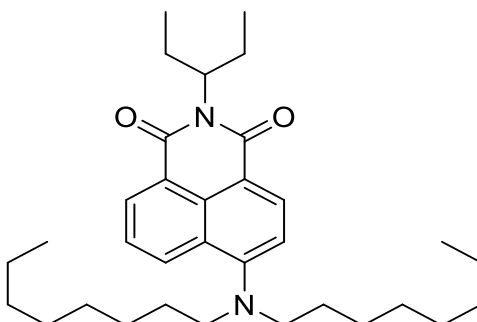
Compound 39a



The compound has been synthesized using the general procedures for the synthesis of naphthalimides. The branched amine was prepared by using the general procedures for the synthesis of substituted peryxanthene xanthenes the branched amine modification. The solvent used was DMF.

¹H-NMR(400 MHz, CDCl₃): 0.87 (m, 6H), 1.25 (m, 24H), 1.63 (m, 4H), 2.58 (m, 2H), 4.53 (t, J= 6.89 Hz, 2H), 7.08 (d, J= 16.40 Hz, 1H), 7.74 (d, J= 16.17 Hz, 1H), 7.86 (t, J= 8.52,7.32 Hz, 1H), 8.60 (d, J= 8.52 Hz, 1H), 8.67 (d, J= 7.28 Hz, 1H). **ESI-MS** Calculated: 1010.82, Found: 1012.3 [M+H]⁺, 792.0, 655.2, 360.4.

Compound 39b

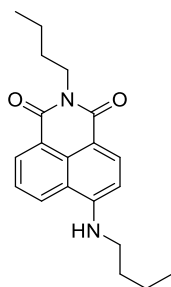


The compound has been synthesized using the general procedures for the synthesis of naphthalimides. The branched amine was prepared by using the general procedures for

the synthesis of substituted peryxanthene xanthenes the branched amine modification.
The solvent used was DMF.

¹H-NMR(400 MHz, CDCl₃): 0.86 (m, 6H), 1.23 (m, 24H), 1.61 (m, 6H), 1.89 (m, 2H), 2.23 (m, 2H), 3.34 (t, J= 7.44 Hz, 4H), 5.04 (tt, J= 9.70, 5.81 Hz, 1H), 7.20 (d, J= 7.77 Hz, 1H) 7.66 (dd, J= 8.19, 8.04 Hz, 1H), 8.45 (d, J= 8.20 Hz, 2H), 8.55 (m, 1H). **¹³C-NMR** (101 MHz, CDCl₃) δ 130.55, 85.85, 53.70, 43.74, 31.74, 29.29, 29.19, 27.13, 27.03, 25.08, 22.58, 14.04, 11.30. **ESI-MS** Calculated: 506.4 Found:507.4 [M+H]⁺, 242.2.

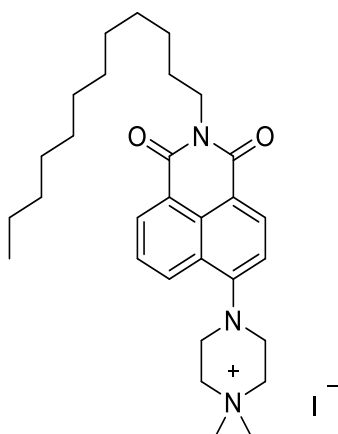
Compound 40



The compound has been synthesized using the general procedures for the synthesis of naphthalimides. The solvent used was 1-butanol.

¹H-NMR(400 MHz, CDCl₃): 0.96 (t, J= 7.36 Hz, 3H), 1.03 (t, J= 7.35 Hz, 3H), 1.43 (tt, J= 8.01, 7.07 Hz, 2H), 1.53 (tt, J= 8.01, 7.07 Hz, 2H), 1.70 (m, 2H), 1.80 (m, 2H), 3.41 (m, 2H), 4.16 (t, J= 8.01 Hz, 2H) 5.19 (s, 1H), 6.72 (d, J= 8.45 Hz, 1H), 7.61 (dd, J= 8.40, 7.33 Hz, 1H), 8.06 (d, J= 8.50 Hz, 1H), 8.46 (d, J= 8.40 Hz, 1H), 8.58 (d, J= 7.33 Hz, 1H). **¹³C-NMR** (101 MHz, CDCl₃) δ 164.68, 164.15, 149.34, 134.42, 131.03, 129.79, 125.61, 124.66, 123.27, 120.13, 110.35, 104.31, 43.41, 39.96, 31.05, 30.31, 20.43, 20.33, 13.87. **ESI-MS**: Calculated: 324.18, Found: 325.2 [M+H]⁺.

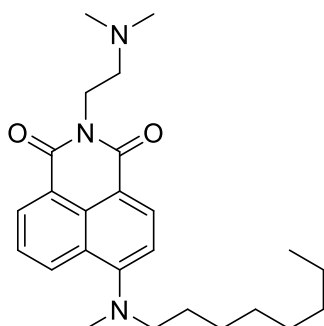
Compound 42



The compound has been synthesized using the general procedures for the synthesis of naphthalimides. The solvent used was diethylene glycol. The final methylation step was performed by adding the amine to a sealed flask with acetone (2ml) and methyl iodide (4 eq). The reaction is left for 16 hours at 56 °C. After cooling to room temperature, the reaction mixture was filtered and washed by cold acetone. The obtained yellow crude product was recrystallized with petroleum ether/chloroform to provide pure **42**.

¹H-NMR(400 MHz, CDCl₃): 0.86 (t, J= 7.08 Hz, 3H), 1.24 (m, 18H), 1.66 (m, 4H), 3.61 (m, 4H), 3.75 (s, 6H), 4.09 (t, J= 7.60 Hz, 2H), 4.16 (s, 2H), 7.41 (d, J= 8.01 Hz, 1H) 7.73 (dd, J= 8.45, 7.28 Hz, 1H), 8.41 (dd, J= 8.47 Hz, 1H), 8.44 (d, J= 7.91 Hz, 1H), 8.51 (d, J= 7.32 Hz, 1H). ¹³C-NMR (101 MHz, CDCl₃) δ 217.47, 187.62, 185.02, 152.29, 131.71, 118.73, 118.73, 100.09, 62.39, 46.81, 40.43, 31.89, 29.60, 29.39, 29.33, 28.11, 27.17, 22.66, 14.10. ESI-MS Calculated: 478.7 Found: 478.4 [M]⁺.

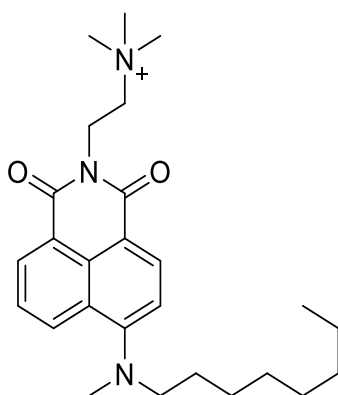
Compound 43 (non-methylated)



The compound has been synthesized using the general procedures for the synthesis of naphthalimides. The solvent used was diethylene glycol.

¹H-NMR(400 MHz, CDCl₃): 0.85 (t, J= 7.21 Hz, 3H), 1.25 (m, 12H), 1.71 (m, 2H), 2.39 (s, 6H), 2.69 (t, J= 7.21 Hz, 2H), 3.03 (s, 3H), 3.30 (t, J= 7.70 Hz, 2H), 4.33 (t, J= 7.21 Hz, 2H), 7.13 (d, J= 8.22 Hz, 1H), 7.63 (dd, J= 8.48, 7.27 Hz, 1H), 8.39 (d, J= 8.48 Hz, 1H), 8.46 (d, J= 8.20 Hz, 1H), 8.55 (d, J= 7.27 Hz, 1H). ¹³C NMR (101 MHz, CDCl₃) δ 164.66, 164.09, 157.02, 132.57, 131.08, 131.01, 130.29, 125.88, 124.90, 123.02, 114.94, 114.50, 57.10, 56.84, 45.51, 41.52, 37.67, 31.75, 29.68, 29.32, 29.19, 27.43, 26.99, 22.59, 14.06. ESI-MS Calculated: 409.27, Found: 410.3 [M+H]⁺, 365.2.

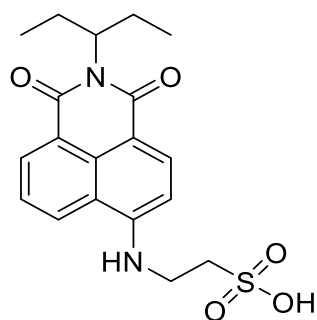
Compound 43



The compound has been synthesized using the general procedures for the synthesis of naphthalimides. The solvent used was diethylene glycol. The final methylation step was performed by adding the amine to a sealed flask with acetone (2ml) and methyl iodide (4 eq). The reaction is left for 16 hours at 56 °C. After cooling to room temperature, the reaction mixture was filtered and washed by cold acetone. The obtained yellow crude product was recrystallized with petroleum ether/chloroform to provide pure **43**.

¹H-NMR(400 MHz, CDCl₃): 0.88 (t, J= 3.55 Hz, 3H), 1.27 (m, 10H), 1.67 (m, 2H), 3.18 (s, 3H), 3.56 (s, 9H), 3.63 (t, J= 4.56 Hz, 2H), 3.85 (t, J= 6.49 Hz, 2H), 4.65 (t, J= 6.48 Hz, 2H), 7.12 (d, J= 8.38 Hz, 1H), 7.69 (dd, J= 8.53, 7.34 Hz, 1H), 8.48 (m, 1H), 8.58 (d, J= 7.35 Hz, 1H). ESI-MS: 424.29, Found: 424.30 [M]⁺.

Compound 44



The compound has been synthesized using the general procedures for the synthesis of naphthalimides. The solvent used was diethylene glycol.

¹H-NMR(400 MHz, CDCl₃): 0.88 (t, J= 7.47 Hz, 6H), 1.88 (m, 2H), 2.22 (m, 2H), 3.74 (t, J= 4.32 Hz, 2H), 3.80 (t, J= 3.67 Hz, 2H), 4.04 (t, J= 4.53 Hz, 2H), 4.42 (t, J= 4.32 Hz 2H), 5.02 (tt, J= 9.58, 5.84 Hz, 1H), 7.02 (d, J= 8.31 Hz, 1H), 7.68 (dd, J= 8.37, 7.32 Hz, 1H), 8.54 (m, 3H). **¹³C-NMR** (101 MHz, CDCl₃) δ 159.65, 129.59, 128.35, 126.02, 123.36, 105.98, 72.71, 69.32, 68.36, 61.79, 57.17, 25.05, 11.31. **ESI-MS**: Calculated: 390.12, Found: 394.0.

References

- (1) V. Balzani, G. Bergamini, P. Ceroni, *Angew. Chem.*, **2015**, 54, 11320
- (2) D. Staveness, I. Bosque Corey, R. J. Stephenson, *Acc. Chem. Res.*, **2016**, 49, 10229
- (3) T.V. Gerven, G. Mulc, J. Moulijn, A. Stankiewicz, *Chem Eng Process.*, **2007**, 46, 781
- (4) J.R. Lakowicz, (**2006**), *Principles of Fluorescence Spectroscopy*, Springer US.
- (5) D. M. Arias-Rotondo, J.K. McCusker, *Chem. Soc. Rev.*, **2016**, 45, 5803.
- (6) N.A. Romero, D.A. Nicewicz, *Chem. Rev.*, **2016**, 116, 10075–10166
- (7) B. König, (**2013**), *Chemical Photocatalysis. De Gruyter*
- (8) J. Twilton, C. C. Le, P. Zhang, M. H. Shaw, R. W. Evans, D. W. C. MacMillan, *Nature Reviews Chemistry*, **2017**, 1, 0052
- (9) J. W. Tucker, C. R. J Stephenson, *J. Org. Chem.*, **2012**, 77, 1617-1622
- (10) M. S. Lowry, J. I. Goldsmith, J. D. Slinker, R. Rohl, R. A. Jr. Pascal, G. G. Malliaras, S. Bernhard, *Chem. Mater.*, **2005**, 17, 5712-5719.
- (11) A. Joshi-Pangu, F. Lévesque, H.G. Roth, S.F. Oliver, L.C. Campeau, D. Nicewicz, D.A. DiRocco, *J. Org. Chem.*, **2016**, 81, 7244–7249
- (12) D.J.P. Kornfilt, D.W.C. MacMillan, *J. Am. Chem. Soc.*, **2019**, 141, 17, 6853–6858
- (13) R.T. Smith, X. Zhang, J.A. Rincón, J. Agejas, C. Mateos, M. Barberis, S. García-Cerrada, O. Frutos, D.W.C. MacMillan, *J. Am. Chem. Soc.*, **2018**, 140, 17433–17438
- (14) C. Li, Y. Xu, W. Tu, G. Chenb, R. Xu, *Green Chem.*, **2017**, 19, 882
- (15) S. Sharma, A. Sharma, *Org. Biomol. Chem.*, **2019**, 17, 4384.
- (16) N.A. Romero, D.A. Nicewicz, *ACS Catal.*, **2018**, 86, 4735
- (17) I. Ghosh, B. König, *Angew. Chem. Int. Ed.*, **2016**, 55, 7676 – 7679; *Angew. Chem.*, **2016**, 128, 7806– 7810
- (18) C. A. Zentner, F. Anson, S. Thayumanavan, T. M. Swager *J. Am. Chem. Soc.*, **2019**, 141, 18048–18055
- (19) L.D. Zarzar, V. Sresht, E.M. Sletten, J.A. Kalow, D. Blankschtein and T.M. Swager, *Nature*, **2015**, 518, 520–524
- (20) R. Nikhil, L.G. Jana, J.M. Catherine, *J Phys Chem*, **2001**, 105, 4065–4067
- (21) X. Wang, J. Zhuang, Q. Peng, Y.D. Li, *Nature*, **2005**, 437, 121–124
- (22) Q. Zhang, Z.N. Gao, F. Xu, S.X. Tai, X.G. Liu, S.B. Mo, F. Niu, *Langmuir*, **2012**, 28, 11979–11987

- (23) Y. Yoshimura, T. Kusano, H. Iwase, M. Shibayama, T. Ogawa, H. Kurata, *Langmuir*, **2012**, 28:9322–9331
- (24) N. Mizoshita, M. Ikai, T. Tani, S. Inagaki, *J Am Chem Soc*, **2009**, 131, 14225–14227
- (25) F. Currie, M. Andersson, K. Holmberg, *Langmuir*, **2004**, 20, 3835–3837
- (26) T. Lu, F. Han, G.R. Mao, G.F. Lin, J.B. Huang, X. Huang, Y.L. Wang, H.L. Fu, *Langmuir*, **2007**, 23, 2932–2936
- (27) J.J. Jiao, B. Dong, H.N. Zhang, Y.Y. Zhao, X.Q. Wang, R. Wang, L. Yu, *J Phys Chem B*, **2012**, 116, 958–965
- (28) B. Dong, X.Y. Zhao, L.Q. Zheng, J. Zhang, N. Li, T. Inoue, *Colloids Surf A*, **2008**, 317, 666–672
- (29) A. Zaragoza, F.J. Aranda, M.J. Espuny, J.Á. Teruel, A. Marques, A. Manresa, A. Ortiz, *Langmuir*, **2010**, 26, 8567–8572
- (30) B. Dong, Y.A. Gao, Y.J. Su, L.Q. Zheng, J.K. Xu, T. Inoue, *J Phys Chem B*, **2010**, 114, 340–348
- (31) L.J. Shi, N. Li, H. Yan, Y.A. Gao, L.Q. Zheng, **2011**, *Langmuir*, 27, 1618–1625
- (32) H.X. Wu, H.X. Wang, L. Xue, Y. Shi, X.Y. Li, *J Phys Chem B*, **2010**, 114, 14420–14425
- (33) L. Xue, Y.F. Wang, Y.L. Chen, X.Y. Li, *J Colloid Interface Sci*, **2010**, 350, 523–529
- (34) Y.J. Li, J. Reeve, Y.L. Wang, R.K. Thomas, J.B. Wang, H.K. Yan, *J Phys Chem B*, **2005**, 109, 16070–16074
- (35) X. Huang, Y.C. Han, Y.X. Wang, Y.L. Wang, *J Phys Chem B*, **2007**, 111, 12439–12446
- (36) J.H. Fendler, *Membrane Mimetic Chemistry*, Wiley, New York, **1982**
- (37) F. Mancin, L. J. Prins, P. Pengo, L. Pasquato, P. Tecilla, *Paolo Scrimin Molecules*, **2016**, 21, 1014
- (38) U. Lewandowska, W. Zajackowski, L. Chen, F. BouilliHre, D. Wang, K. Koynov, W. Pisula, K. Mellen, H. Wennemers, *Angew. Chem. Int. Ed.*, **2014**, 53, 12537–12541; *Angew. Chem.*, **2014**, 126, 12745–12749.
- (39) H. Zhylitskaya, J. Cybinska, P. Chmielewski, T. Lis, M. Stepien, *J. Am. Chem. Soc.*, **2016**, 138, 11390–11398.
- (40) J. Roncali, *Chem. Rev.*, **1997**, 97, 173–206.
- (41) J. Roncali, *Macromol. Rapid Commun.*, **2007**, 28, 1761–1775.
- (42) X. Wang, G. Sun, P. Routh, D.-H. Kim, W. Huang, P. Chen, *Chem. Soc. Rev.*, **2014**, 43, 7067–7098.
- (43) U. N. Maiti, W. J. Lee, J. M. Lee, Y. Oh, J. Y. Kim, J. E. Kim, J. Shim, T. H. Han, S. O. Kim, *Adv. Mater.*, **2014**, 26, 40–67.
- (44) X.-Y. Wang, A. Narita, X. Feng, K. Mellen, *J. Am. Chem. Soc.*, **2015**, 137, 7668–7671.

- (45) F. Wurthner, *Chem. Commun.*, **2004**, 1564–1579.
- (46) J.J.M. Halls, R.H. Friend, *Synth. Met.*, **1997**, 85, 1307–1308.
- (47) C.W. Struijk, A.B. Sieval, J.E.J. Dakhorst, M. van Dijk, P. Kimkes, R.B.M. Koehorst, H. Donker, T.J. Schaafsma, S.J. Picken, A.M. van de Craats, J.M. Warman, H. Zuilhof, E.J.R. Sudholter, *J. Am. Chem. Soc.*, **2000**, 122, 11057–11066.
- (48) C. Im, W. Tian, H. Bassler, A. Fechtenkotter, M.D. Watson, K. Mullen, *Synth. Met.*, **2003**, 139, 683–686.
- (49) R. Dabirian, V. Palermo, A. Liscio, E. Schwartz, M.B.J. Otten, C.E. Finlayson, E. Treossi, R.H. Friend, G. Calestani, K. Mullen, R.J.M. Nolte, A.E. Rowan, P. Samorì, *J. Am. Chem. Soc.*, **2009**, 131, 7055–7063.
- (50) V. Palermo, M.B.J. Otten, A. Liscio, E. Schwartz, P.A.J. de Witte, M. A. Castriciano, M.M. Wienk, F. Nolde, G. De Luca, J.J.L.M. Cornelissen, R.A.J. Janssen, K. Mullen, A.E. Rowan, R.J.M. Nolte, P. Samorì, *J. Am. Chem. Soc.*, **2008**, 130, 14605–14614.
- (51) R. Schmidt, M.M. Ling, J.H. Oh, M. Winkler, M. Konemann, Z.N. Bao, F. Wurthner, *Adv. Mater.*, **2007**, 19, 3692–3695.
- (52) A. Stabel, P. Herwig, K. Mullen, J.P. Rabe, *Angew. Chem., Int. Ed. Engl.*, **1995**, 34, 1609–1611.
- (53) P. Samorì, A. Fechtenkotter, T. Bohme, F. Jackel, K. Mullen, J. Rabe, *J. Am. Chem. Soc.*, **2001**, 123, 11462–11467.
- (54) W. Pisula, M. Kastler, D. Wasserfallen, J.W.F. Robertson, F. Nolde, C. Kohl, K. Mullen, *Angew. Chem., Int. Ed.*, **2006**, 45, 819–823.
- (55) T. Miletic, A. Fermi, I. Orfanos, A. Avramopoulos, F. De Leo, N. Demitri, G. Bergamini, P. Ceroni, M.G. Papadopoulos, S. Couris, D. Bonifazi, *Chem. Eur. J.*, **2017**, 23, 2363–2378.
- (56) a) C. Song, T.M. Swager, *Macromolecules*, **2009**, 42, 1472–1475; b) H. Li, F. Zhang, S. Qiu, N. Lv, Z. Zhao, Q. Li, Z. Cui, *Chem. Commun.*, **2013**, 49, 10492–10494.
- (57) a) R. Pummerer, E. Prell, A. Rieche, *Berichte der Dtsch. Chem. Gesellschaft*, **1926**, 59, 2159–2161; b) L.T. Rasmusson, L.J.P. Martyn, G. Chen, A. Lough, M. Oh, A. K. Yudin, *Angew. Chem. Int. Ed.*, **2008**, 47, 7009–7012; *Angew. Chem.* **2008**, 120, 7117–7120; c) N. Lv, M. Xie, W. Gu, H. Ruan, S. Qiu, C. Zhou, Z. Cui, *Org. Lett.*, **2013**, 15, 2382–2385; d) T. Kamei, M. Uryu, T. Shimada, *Org. Lett.*, **2017**, 19, 2714–2717.
- (58) a) N. Lv, M. Xie, W. Gu, H. Ruan, S. Qiu, C. Zhou, Z. Cui, *Org. Lett.*, **2013**, 15, 2382–2385; b) L. Wang, G. Duan, Y. Ji, H. Zhang, *J. Phys. Chem. C*, **2012**, 116, 22679–22686; c) N. Kobayashi, M. Sasaki, K. Nomoto, *Chem. Mater.*, **2009**, 21, 552–556.

- (59) "Semiconductor Device, Method of Manufacturing the Same, and Method of Forming Multilayer Semiconductor Thin Film": N. Kobayashi, M. Sasaki, T. Ohe, U.S. Patent 8,399,288 B2, **2013**.
- (60) "Novel Materials for Organic Electroluminescent Devices": P. Stoessel, A. Buesing, H. Heil, U.S. Patent 2010/0013381 A1, **2010**.
- (61) M. Noda, N. Kobayashi, M. Katsuhara, A. Yumoto, S.-I. Ushikura, R.-I. Yasuda, N. Hirai, G. Yukawa, I. Yagi, K. Nomoto, T. Urabe, *Dig. Tech. Pap. Soc. Inf. Disp. Int. Symp.*, **2010**, 41, 710–713.
- (62) A. Sciutto, A. Fermi, A. Folli, T. Battisti, J.M. Beames, D.M. Murphy, D. Bonifazi, *Chem. Eur. J.*, **2018**, 24, 4382 – 4389
- (63) a) L. Wang, G. Duan, Y. Ji, H. Zhang, *J. Phys. Chem. C*, **2012**, 116, 22679–22686; b) R. Al-Aqar, A.C. Benniston, A. Harriman, T. Perks, *ChemPhotoChem*, **2017**, 1, 198–205; c) N. Kobayashi, M. Sasaki, K. Nomoto, *Chem. Mater.*, **2009**, 21, 552 –556.
- (64) J.E. Bullock, M.T. Vagnini, C. Ramanan, D.T. Co, T.M. Wilson, J.W. Dicke, T.J. Marks, M.R. Wasielewski, *J. Phys. Chem. B*, **2010**, 114, 1794–1802.
- (65) a) F. Würthner, *Chem. Commun.*, **2004**, 0, 1564 – 1579; b) F. Würthner, C.R. Saha-Möller, B. Fimmel, S. Ogi, P. Leowanawat, D. Schmidt, *Chem. Rev.*, **2016**, 116, 962 – 1052.
- (66) a) N. Sakai, J. Mareda, E. Vauthey, S. Matile, *Chem. Commun.*, **2010**, 46, 4225–4237; b) S.-L. Suraru, F. Würthner, *Angew. Chem. Int. Ed.*, **2014**, 53, 7428 –7448; *Angew. Chem.*, **2014**, 126, 7558 –7578.
- (67) A.B. Wu, Y.F. Xu, X.H. Qian, J. Wang, J.W. Liu, *Eur J Med Chem*, **2009**, 44, 4674–4680
- (68) Z. Chen, X. Liang, H.Y. Zhang, H. Xie, J.W. Liu, Y.F. Xu, W.P. Zhu, Y. Wang, X. Wang, S.Y. Tan, D. Kuang, X.H. Qian, *J. Med Chem*, **2010**, 53, 2589–2600
- (69) X. Poteau, A.I. Brown, R.G. Brown, C. Holmes, D. Matthew, *Dye Pigment*, **2009**, 47, 91–105
- (70) R.W. Middleton, J. Parrick, *J. Heterocycl. Chem.*, **1985**, 22, 1567.
- (71) R.W. Middleton, J. Parrick, E.D. Clarke, P. Wardman, *J. Heterocycl. Chem.*, **1986**, 23, 849.
- (72) A. Pardo, J.M.L. Poyato, E. Martin, *J. Photochem.*, **1986**, 36, 323.
- (73) A. Pardo, E. Martin, J.M.L. Poyato, J.J. Camacho, M.F. Braiia, and J. M. Castellano, *J. Photochem. Photobiol. A*, **1987**, 41, 69.
- (74) Z.C. Xu, K.H. Baek, H.N. Kim, J.N. Cui, X.H. Qian, D.R. Spring, I.S.J. Yoon, *J Am Chem Soc*, **2010**, 132, 601–610

- (75) M.H. Lee, J.H. Han, P.S. Kwon, S. Bhuniya, J.Y. Kim, J.L. Sessler, C. Kang, J.S. Kim, *J Am Chem Soc*, **2012**, 134, 1316–1322
- (76) J. Qian, X. Qian, Y. Xu, *Chem. Eur. J.*, **2009**, 15, 319–323.
- (77) Y. Zhao, X. Li, *Sensors and Actuators B*, **2015**, 209, 258–264
- (78) D. Esteban-Gomez, L. Fabbriizzi, M. Licchelli, *J Org Chem*, **2005** 70, 5717–5720
- (79) V.F. Pais, P. Remon, D. Collado, J. Andreasson, E. Perez-Inestrosa, U. Pischel, *Org Lett*, **2011**, 13, 5572–5575
- (80) a) A. Maldotti, A. Molinari, R. Amadelli, *Chem. Rev.*, **2002**, 102, 3811–3836; b) D.G. Shchukin, D.V. Sviridov, *J. Photochem. Photobiol. C*, **2006**, 7, 23–39; c) J. Matsumoto, T. Matsumoto, Y. Senda, T. Shiragami, M. Yasuda, *J. Photochem. Photobiol. A*, **2008**, 197, 101–109;
- (81) a) D.D. Díaz, D. Kuhbeck and R. J. Koopmans, *Chem. Soc. Rev.*, **2011**, 40, 427–448; b) A. Shumburo, M.C. Biewer, *Chem. Mater.*, **2002**, 14, 3745–3750.
- (82) S. Bhat, U. Maitra, *Molecules*, **2007**, 12, 2181–2189.
- (83) a) A. Dawn, N. Fujita, S. Haraguchi, K. Sada, S. Shinkai, *Chem. Commun.*, **2009**, 2100–2102; b) A. Dawn, N. Fujita, S. Haraguchi, K. Sada, S.-i. Tamaru, S. Shinkai, *Org. Biomol. Chem.*, **2009**, 7, 4378–4385.
- (84) L. Kohler, N. Kaveevivitchai, R. Zong, R.P. Thummel, *Inorg. Chem.*, **2013**, 53, 912–921.
- (85) A. Perez-Velasco, V. Gorteau, S. Matile, *Angew. Chem., Int. Ed.*, **2008**, 47, 921–923
- (86) S. Troppmann, B. König, *Chem. Eur. J.*, **2014**, 20, 14570 – 14574
- (87) C. Lu, J. Cao, Y. Cheng, Y. Jin, Y. Qu, J. Xu, *Sensors and Actuators B*, **2017**, 255, 3102–3107
- (88) M. Giedyk, R. Narobe, S. Weiß, D. Touraud, W. Kunz, B. König, *Nat. Catal*, **2020**, 3, 40–47
- (89) S. Abbott, *Surfactant Science Principles & Practice*, *DESTech publications*, **2018**
- (90) J. A. Gladysz, D. P. Curran, I. T. Horváth, *Handbook of Fluorous Chemistry*, **2004**, 18–20, 521–561
- (91) R. G. Bedford, R. D. Dunlap, *J. Am. Chem. Soc.*, **1958**, 80, 282–285
- (92) G.D. Luca, A. Liscio, M. Melucci, T. Schnitzler, W. Pisula, C.G. Clark, L.M. Scolaro, V. Palermo, K. Müllen, P. Samorì, *J. Mater. Chem.*, **2010**, 20, 71–82
- (93) D. Andreou, M. G. Kallitsakis, E. Loukopoulos, C. Gabriel, G. E. Kostakis, I. N. Lykakis, *J. Org. Chem.*, **2018**, 83, 4, 2104–2113
- (94) W. Yang, J. Zhao, C. Sonn, D. Escudero, A. Karatay, H.G. Yaglioglu, B. Küçüköz, M. Hayvali, C. Li, D. Jacquemin, *J. Phys. Chem. C*, **2016**, 120, 19, 10162–10175

- (95)S. Rajaram, P.B. Armstrong, B.J. Kim, J.M.J. Fréchet, *Chemistry of Materials*, **2009**, 21, 1775-1777
- (96)F.S. Gaucher-Wieczorek, L.T. Maillard, B. Badet, P. Durand, *J Comb Chem.* **2010**;12(5):655-658
- (97)Y. Pellegrin, F. Odobel, *C. R. Chimie*, **2017**, 20, 283-295
- (98)Z. Zuo, D. T. Ahneman, L. Chu, J. A. Terrett, A. G. Doyle, D. W. C. MacMillan, *Science*, **2014**, 6195, 345, 437-440